THE UNIVERSITY OF CHICAGO

CELLULAR AND MOLECULAR MECHANISMS OF *CAENORHABDITIS ELEGANS* FORAGING BEHAVIOR

A DISSERTATION SUBMITTED TO
THE FACULTY OF THE DIVISION OF THE BIOLOGICAL SCIENCES
AND THE PRITZKER SCHOOL OF MEDICINE
IN CANDIDACY FOR THE DEGREE OF
DOCTOR OF PHILOSOPHY

COMMITTEE ON COMPUTATIONAL NEUROSCIENCE

BY
ADAM BROWN

CHICAGO, ILLINOIS
DECEMBER 2017

For Jamie, my partner in exploration of life's complex environment.

They say you shouldn't leave a place /

if you can eat there.

- Animal Collective, *Safer*

TABLE OF CONTENTS

LIST OF FIGURES

LIST OF TABLES

ACKNOWLEDGMENTS

In the course of my dissertation work I grew boundlessly as a scientist and person. No such growth would have been possible without the support of the exceptional people who traveled the road with me.

First, I must thank my advisor, David Biron. We first met over coffee at Bonjour Bakery on 55th Street in November 2011 when I was still months away from my graduate school interviews. Even at that very early stage I had a distinct feeling that I need look no further to find the perfect advisor. David's lucidness, curiosity, creativity, patience, and humanity were apparent then and all throughout the subsequent years. I am convinced that no other lab was doing what we were doing because no one could match David's ability to identify the most interesting questions and willingness to follow them wherever they led. To look through a microscope and see a shifting kaleidoscope of ten thousand writhing worms is to see a Rorschach upon which one's own psyche is projected. Above all, I want to thank David for the balance of freedom and guidance that allowed me to project so much of myself into the work we did together; the final product, this dissertation, is unmistakably "Adam" in its substance and style.

I also had the great fortune to share the Biron lab with several excellent scientist colleagues. In particular, I would like to thank Shachar Iwanir and Stanislav Nagy, two postdocs who were wonderful mentors to me in my first two years in the lab. I also want to thank Monika Scholz and Jarred Sanders, fellow graduate students who were always there to talk through any technical challenge, scientific puzzle, or personal struggle. Nora Tramm, Rebecca Fishman, Ilaria Merutka, Dylan Lynch, and Celia Cook were also a pleasure to work with. From my first day in the lab to my last, I felt privileged to be among such brilliant and down-to-earth people.

Beyond the lab, I would like to thank all my fellow students in the Neuroscience cluster, including some close friends I hope will remain in my life for years to come. It has been wonderful to see these fine people become scientists alongside me while we made memories

of epic bike rides, wacky musical performances, and more. I must also thank my graduate program administrators past and present for their help and my thesis committee – Janet Richmond, Dan Margoliash, Cliff Ragsdale, and Xiaoxi Zhuang – for their tremendous insights and for pushing me to do exceptional work. In particular, I want to thank Janet for the opportunity to collaborate with her lab which greatly expanded my scientific experience.

I would also like to thank the faculty for whom I TA'ed or guest lectured and the staff of the Chicago Center for Teaching for helping me discover my love of pedagogy. My experiences in the lab and classroom reinforced each other beautifully.

Lastly, I would like to thank my parents and my older brother, Jacob, who taught me from the earliest age that learning is its own reward. And finally, I thank my true love and soon-to-be wife, Jamie; that which I must thank you for should be the subject of its own dissertation.

ABSTRACT

In a spatially and temporally dynamic environment, animals must forage efficiently in order to thrive. Although foraging is studied extensively in a wide range of species both experimentally and theoretically, the biological substrates of foraging remain poorly understood. To approach a mechanistic understanding of foraging, I used continuous video recordings of *C. elegans* nematodes in patchy landscapes. Comparing quantitative behavioral phenotypes of wild-type animals and mutants, I probed the genetic basis of foraging. Using physiological imaging and optical stimulation of neurons, I also characterized cellular mediation of foraging. In this dissertation, I provide evidence that a key role of serotonergic signaling in *C. elegans* is to accelerate decision-making and promote efficient exploitation of resources in complex environments. My work primarily implicates the serotonergic neuron type NSM, the serotonin-gated chloride channel MOD-1, and the ortholog of mammalian 5-HT1 metabotropic serotonin receptors SER-4 in mediating this process. In addition, I demonstrate how different cells can use a common modulator to affect locomotion in complementary manners. I further show that, like serotonin, TGF-β pathway genes contribute to both gradual preemptive slowing as animals approach food and abrupt slowing upon encounter. My observation that double mutants of both *daf-7* and *tph-1* exhibit exaggerated defects relative to single mutants supports the hypothesis that TGF-β and serotonin function in parallel rather than in series. Finally, my work implicates both mechanosensory and chemosensory transduction in mediating responses to food encounter, with *daf-7* primarily involved in chemosensation. Taken together, the findings described above demonstrate how multiple signaling pathways play overlapping roles in regulating behavioral responses. Moreover, my work indicates that molecules implicated in mediation of developmental processes can also function on acute timescales to tune behavior.

CHAPTER 1

INTRODUCTION

1.1 Movement-based neuroethology

1.1.1 What is an animal?

The word animal comes from the Latin *animalis*, meaning having a spirit or being alive. To animate is thus to instill with spirit, to bring to life. In modern usage, animation refers to the process of assembling a series of still images such that the impression of movement is created. The impression of movement creates the impression of life; the lives of animals, by definition, are manifested in their movements. In this dissertation, I describe my efforts to understand the lives of animals by analyzing their movements as represented in series of images.

Our understanding of what an animal is has progressed considerably since the Latin word was coined. The fractal-like branching of phylogenetics has replaced categorical systems of taxonomy[1]; today we may speak of animals but more precisely of Metazoa, a group of multicellular eukaryotic organisms descended from a common ancestor that lived more than 560 million years ago (Ma)[2] [22].

Within Metazoa, we humans belong to a branch called Bilateria, which is further divided into the protostomes (including nematodes, arthropods, flatworms, mollusks, annelids, and several lesser-known groups) and the deuterostomes (including echinoderms, hemichordates, and chordates). Bilaterians are named for the roughly bilateral symmetry of their body plans,

1. In traditional taxonomy, each group contains a number of subgroups that are treated as equal. For example, within class Mammalia there are numerous orders such as primates, rodents, and bats. Phylogenetics dictates that among any three groups, one must be the outgroup relative to the others. In this example, primates, rodents, and bats are not equally related; rather, primates and rodents are more closely related to each other than to bats and thus bats are the outgroup. "Zooming in" further on one of these mammalian orders reveals not a set of equally related families but additional branching of outgroups and sister taxa.

2. Due to the poverty of the fossil record in the time preceding the Cambrian Period (beginning 541 Ma), estimates of metazoan origin vary widely with some models timing the common ancestor of metazoans as far back as 800 million years ago [196].

present in at least one life stage in each species [134]. One of the hallmarks of Bilateria is locomotion[3], the purposeful movement of the body via limbs or undulations (or both)[4]. It is hypothesized that the evolution of bilateral symmetry and the accompanying anterior-posterior organization, in which sensory organs are concentrated at one end, is closely linked to the evolution of locomotion[5]. The adaptive value of locomotion is clear: it provides a mechanism for purposeful movement in organisms too large to rely on cilia for propulsion [73]. In this thesis, quantification of locomotion serves as access point for the study of animal behavior.

As referenced above, the evolution of bilateral symmetry and the evolution of the nervous system are closely linked. Considerable evidence supports the hypothesis that complex nervous system of deuterostomes such as vertebrates (a branch within chordates) shares homology with that of protostomes like arthropods and mollusks [86]. For example, the structure of some arthropod brains resembles the tripartite organization of the vertebrate brain (hindbrain, midbrain, forebrain) and arises from homologous patterning genes [84, 85, 152]. However, not all bilaterians have complex nervous systems featuring millions or billions of neurons like those found in vertebrates, arthropods, and some others. The nervous systems of some bilaterians, such as the organism at the center of this dissertation, the nematode *Caenorhabditis elegans*, are composed of only a few hundred neurons[6].

3. Some definitions of locomotion include so-called passive locomotion such as "sailing" in jellyfish; however, in this dissertation "locomotion" refers to non-ciliary active locomotion and is thus specific to bilaterians. Among bilaterians, some species exhibit active locomotion only during certain life stages and are otherwise non-motile (e.g., barnacles).

4. Animals that move on land and in water often exhibit different modes of locomotion in the two environments. For example, salamanders use limb movement to locomote on land and body undulations while swimming [93].

5. Another explanation for the evolution of bilaterianism is the facilitation of internal transport [56].

6. See footnote 8 of this chapter.

1.1.2 Why move?

In general, animals move for two reasons: to get closer to an attractive stimulus (e.g., a food source, a potential mate, or a suitable place to lay eggs) or to get away from a noxious stimulus (e.g., a predator, a pathogen, or harmful atmospheric conditions) [73]. Both reasons for movement often depend upon the ability to detect and track environmental gradients, such as temperature or the concentration of a volatile or soluble chemical [11, 95]. Foraging behavior, the subject of this dissertation, depends on tracking a chemical gradient (either via directional locomotion or a "biased random walk"[7] [29]) to arrive at a food source and then responding appropriately upon encounter.

1.1.3 Is behavior synonymous with movement?

Ethology is the study of animal behavior in a naturalistic setting. Nikolaas Tinbergen, considered the father of ethology, defined animal behavior as "the total movements made by the intact animal" [191]. The act of observation lies at the heart of ethology; through observation it is possible to infer an animal's needs and understand the adaptations that allow it to respond appropriately to its environment. To analyze a given behavior, Tinbergen theorized, one must address four questions. The first two concern "how" a behavior is executed: (1) what *mechanism* underlies the behavior? and (2) how does the behavior change during *ontogenesis* (i.e., the development or lifespan of the animal)? The final questions concern "why" a behavior is performed [191]: (3) what selective forces shaped the *evolution* of the behavior? and (4) what are the *fitness* consequences of the behavior in its present form? Together, these four levels of analysis provide a comprehensive understanding of naturalistic behavior.

To claim that behavior and movement are synonymous may be an oversimplification,

7. Unlike a purely random walk, in which any movement direction is equally likely, a biased random walk is characterized by a nonuniform probability distribution of movement directions. In the case of biased random walk for chemotaxis, the probability of movement is highest in the direction of chemical gradient ascent.

but it is not an unreasonable one. After all, behavior depends upon muscle contraction and muscle contraction is movement. Moreover, the behavior-as-movement generalization is useful. Movement, especially locomotion, can be easily captured and quantified through video recordings and subsequent analysis. Combining quantifications of behavior with measurements of neuronal activity, stimulation of neurons, and genetic tools (see below) forms the basis of behavioral neuroscience. Performing behavioral neuroscience research with an emphasis on ecological relevance (in a relative sense; see Introduction of Chapter 4) and Tinbergen's four levels of analysis constitutes neuroethology. With the quantification of locomotion at the center of the studies reported in this dissertation, an appropriate descriptor for the work as a whole might be "movement-based neuroethology".

Characterization of behavior and elucidation of underlying mechanisms requires the right model system. The nematode *Caenorhabditis elegans*, a small animal that possesses a simple nervous system but exhibits an array of interesting behaviors, is suitable for neuroethological studies. This dissertation reports on my investigations of foraging, an ancient and fundamental animal behavior, in *C. elegans*.

1.2 The nematode *Caenorhabditis elegans*

1.2.1 General description

Caenorhabditis elegans is a 1 mm, free-living, unsegmented nematode (roundworm) that feeds on bacteria and other microbes in rotting vegetation. The animal passes through four larval stages (denoted L1, L2, L3, and L4) separated by molts before reaching sexual maturity (see Fig. 1.2). In conditions of abundant food and ambient temperature of 20 °C the generation time of *C. elegans* is about 3.5 days. Generation time scales inversely with temperature within a viable range.

Two sexes exist in *C. elegans*: self-fertilizing hermaphrodites (XX) and males (X0). Males arise via spontaneous non-disjunction during gametogenesis in the hermaphrodite. Under

standard laboratory conditions non-disjunction is rare and males comprise only 1 in 1000 individuals. Environmental stressors such as high temperature increase the probability of non-disjunction. Upon reaching maturity hermaphrodites self-fertilize and lay about 300 eggs over the period of four days. If mated with males, hermaphrodites can lay over 1000 eggs and half of the eggs fertilized by male sperm will be male [171].

Like all nematodes, *C. elegans* is anatomically simple. The body *C. elegans* consists of an "outer tube" and an "inner tube" separated by a pseudocoelomic space. The cuticle, hypodermis, excretory system, longitudinal muscles, and neurons comprise the outer tube, or body wall. The inner tube consists of the pharynx, intestine, and gonad. Hydrostatic pressure in the pseudocoelomic space maintains the animals body shape and, in conjunction with the musculature, allows for the generation of the undulatory body bends that characterize *C. elegans* locomotion.

The entire body of the adult hermaphrodite consists of only 959 somatic cells; a few dozen additional cells are found in the mature male, primarily in the mating organ at the end of its tail [171].

1.2.2 Nervous system

Of the 959 somatic cells that comprise the *C. elegans* adult hermaphrodite, 302 are neurons. These fall into 118 classes, mostly bilateral pairs or quartets. Meticulous reconstruction of serial electron micrographs yielded a complete synaptic connectivity map (i.e., a "connectome") of the adult hermaphrodite *C. elegans* nervous system [205]. The connectome reveals a roughly four-layer organization: (1) sensory neurons, (2) interneurons that receive sensory information, (3) command interneurons that integrate information from the two preceding layers, and (4) motor neurons. A complex of sensory neurons, interneurons, and support cells constitutes the nerve ring in the head of the animal. An additional ganglion is found near the tail. Longitudinal nerve cords innervate the muscles that line the body wall. The pharynx has a separate nervous system connected to the somatic nervous system by a single synapse;

the duality of the *C. elegans* somatic/pharyngeal nervous system is likely homologous to the somatic/visceral nervous system duality in vertebrates [17].

How useful are synaptic connectivity maps such as the *C. elegans* connectome? A neural "wiring diagram" is perhaps best thought of as an advantageous starting point for the elucidation of the cellular basis of behavior. Evidence from *C. elegans*, arthropods, and vertebrates reveals that functional and anatomical connectivity are distinct. For example, neuromodulators such as neuropeptides and bioamines modify synaptic efficiency, excitability, and neuronal dynamics and can be released extrasynaptically, affecting local or distant targets [12]. Thus, knowledge of anatomical connections helps to generate hypotheses but cannot itself explain behavior.

Despite the simplicity of its nervous system[8], *C. elegans* exhibits an array of sensory modalities including sensitivity to numerous chemicals, light, temperature, harsh and gentle touch, vibration, magnetic fields, and other stimuli [11, 71, 95, 200, 201]. A considerable behavioral repertoire is also displayed by *C. elegans* including food-seeking and feeding, mating, egg-laying, and avoidance of noxious stimuli [11, 71, 117].

1.2.3 Genetics

Easy to maintain and biologically simple, *C. elegans* is suitable for genetic analysis. Hermaphrodites have five pairs of autosomes (I-V) and two sex chromosomes (X/X). Males have five pairs of autosomes (I-V) and a single sex chromosome (X/0). Mutant strains can be easily isolated and propagated because hermaphrodites self-fertilize and males are rare under standard conditions.

C. elegans was the first animal to have its genome completely sequenced. The genomes of both humans and *C. elegans* contain about 20,000 genes, yet the total number of base pairs in the human genome is about 30 times greater than in the *C. elegans* genome. Because tens

8. The limitedness of the *C. elegans* nervous system may be due to secondary simplification rather than primitiveness; see Chapter 5.

of thousands of nematodes can be cultivated in a single petri dish, screening for mutations is highly efficient. Chemical mutagenesis and screening has yielded numerous mutants now stored at and readily available from the *Caenorhabditis* Genetics Center.

When injected into the gonad of young adult hermaphrodites, DNA is readily taken up as extrachromosomal arrays. Through the use of tissue- or cell-specific gene promoters, expression of certain proteins can be targeted to single cells or sets of cells. One application of this technique, used throughout this dissertation and in neuroscience in general, is the expression of genetically-encoded calcium indicators (GECIs) in subsets of neurons [189]. When depolarized, neurons undergo rapid and robust influx of calcium ions across the membrane of the cell body. Binding of calcium-sensing domains precipitates a conformational change in GECIs such that the fluorescence intensity of fluorescent proteins increases. Thus, time series measurements of physiological activity in one or more neurons of a freely behaving animal are obtained through fluorescence microscopy.

1.2.4 Foraging in C. elegans

The spatial distribution of resources in natural environments can be non-uniform. For example, non-linear interactions between multiple species and inhomogeneous environmental conditions can cause the formation of locally dense concentrations of food, termed patches. [9, 49, 124]. As a result, foraging behavior in patchy environments is extensively studied both theoretically and experimentally in diverse species and habitats [19, 40, 44, 48, 170, 174, 211].

Studies of patch foraging often center on the "leave-versus-stay" problem, i.e., the necessity of deciding whether to stay and continuing exploiting the current patch or to leave and find a new patch to exploit [180]. Frameworks based on the marginal value theorem state that an animal should leave approximately when the density of food in the current patch falls below the average density of the environment as a whole, with the exact threshold determined by the travel time between patches [33, 101]. The work reported in this dissertation addresses a related but simplified question, essentially the "leave-versus-stay"

problem taken to an extreme: when an animal encounters a patch of food, does it stop to exploit the patch or simply pass through it? Using genetic tools, we identified cellular and molecular mechanisms that enable wild-type animals to abruptly slow their locomotion upon encountering food, in contrast to mutants that slow down gradually or, if the patch is sufficiently small, pass through without stopping to feed. In this way, we gained insight into the fitness consequences and neural basis of foraging behavior.

What types of foraging environments must *C. elegans* contend with in its natural habitat? *C. elegans* is a filter-feeder, encountering colonies of bacteria suspended in liquid. Through the action of a muscular pump (the pharnyx) the nematode separates the liquid and ingests only the bacteria. *C. elegans* therefore lives primarily in microbe-rich environments such as rotting plant matter and can be found in abundance in human-made compost heaps, for example. [53]. In such environments, microbial food is concentrated in patches. However, to understand the true context in which *C. elegans* foraging occurs, one must consider the rather complex life cycle of the animal. In a given substrate sample, *C. elegans* may often be found primarily in the dauer stage, a facultative diapause state that can occur during development in adverse conditions. Dauer larvae can survive for months without food and sometimes disperse to new environments when carried by larger invertebrates [27, 53] (see below for a detailed description of dauer larvae). Thus, *C. elegans* is specialized for "boom-and-bust" cycles, i.e., long stretches of arrested development and dispersal punctuated by brief periods of explosive proliferation upon finding favorable conditions. Appropriate exploitation of a patch of food is a crucial component of the *C. elegans* life cycle.

1.3 Approaches to quantifying foraging behavior

Laboratory investigations of *C. elegans* foraging behavior have implicated the neuropeptide receptor NPR-1 in regulating rates of food-leaving as a large patch of bacteria becomes depleted [45, 66, 125]. Other studies identified the neuromodulator serotonin (5-hydroxytryptophan; 5-HT) as the mediator of "enhanced slowing", the exaggerated attenua-

tion of locomotion exhibited by *C. elegans* upon being transferred to a bacterial lawn after a period of deprivation [77, 164] (see Chapter 2 for a detailed discussion of this phenomenon). However, the dynamics of *C. elegans* locomotion during an encounter with newly discovered food have not been previously characterized.

Studying foraging behavior in *C. elegans* begins with creating a suitable environment in which foraging can take place. In the laboratory, *C. elegans* are normally grown on agar plates seeded with a thick lawn of bacteria that covers nearly the entire surface of the plate [21]. For foraging assays, we simply replaced the bacterial lawn with either one large patch of bacteria or a grid of very small patches. Thus, animals were sometimes on the bacteria and sometimes not. This enabled us to study the transition between "off" and "on" (i.e., the encounter with a patch of food) which was the focus of our study of foraging. Our patch experiments are discussed in detail throughout this dissertation.

After establishing an experimental setup in which animals can perform behaviors of interest, we formulated ways to record animals' movements. Efforts to study animal movement through analysis of captured images date to the earliest days of photography [176]. In 1878 Eadweard Muybridge sought to determine whether a horse becomes fully airborne while galloping; the motion is too fast for the human eye to perceive [129]. The series of photographic images Muybridge captured clearly showed a galloping horse with all four legs off the ground simultaneously (Fig. 1.1).

Analyzing foraging behavior in *C. elegans* requires only minor modification of Muybridge's method. One modification, due to the small size of the subject, is the use of a microscope in conjunction with a camera. A second modification is the use of digital rather than analog photography, enabling automated analysis of images through patterns or changes in pixel brightness. Our imaging setups are described in detail in the Methods sections of Chapters 2, 3, and 4. In general, we used two primary recording paradigms: single-worm and multi-worm. In the single-worm setup, we used a high resolution analysis tool to quantify the posture and motion of an individual animal (the only animal in the field of view). This

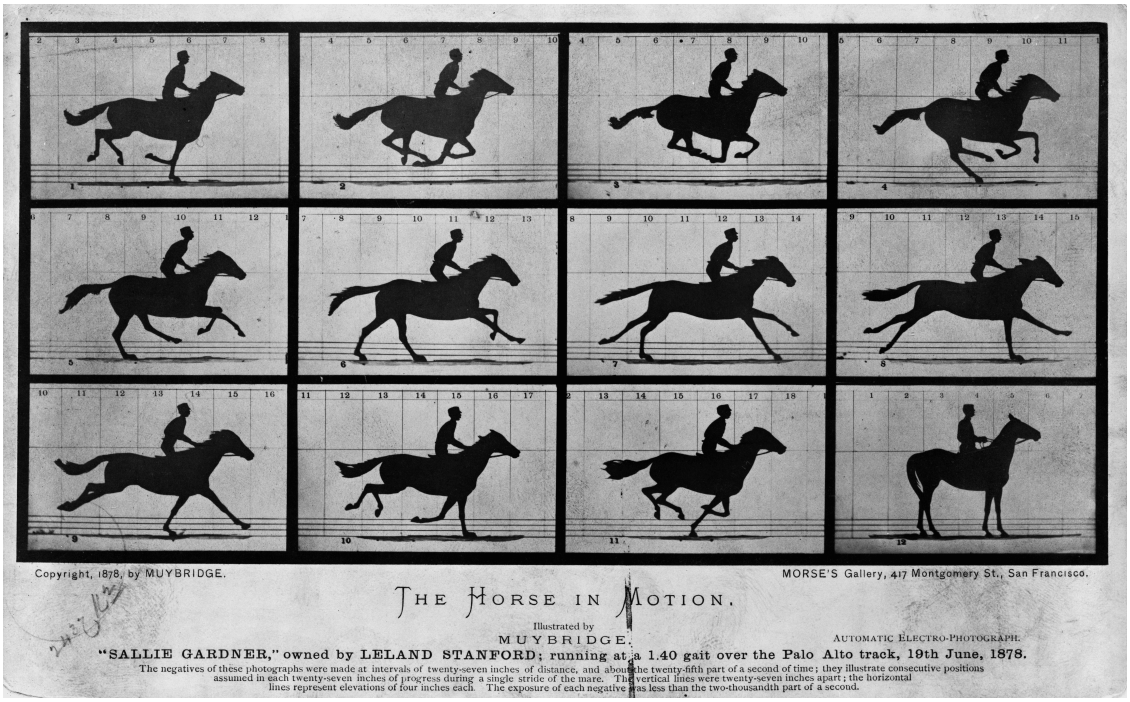

Figure 1.1: **Early use of photography to analyze animal motion.** Eadweard Muybridge's 1878 experiment provided conclusive evidence that a galloping horse becomes fully airborne. Reproduced from [130].

paradigm was especially useful for studies that required detailed analysis of body shapes and locomotion patterns. For the multi-worm setup, we tracked the motion of many animals simultaneously, treating each as a cluster of pixels without analysis of posture. We thus faced a fundamental trade-off between resolution and throughput. However, we were able to select the appropriate method for addressing our research questions in each experiment.

Our study of foraging centered on quantification of locomotion through video recording, but we complemented these methods with two others: (1) calcium imaging, in which the intensity of a fluorescent particle is measured to correlate physiological activity of individual neurons with observed behaviors, and (2) optogenetics, in which individual neurons or classes of neurons are stimulated to demonstrate that activation of certain cells is sufficient to evoke specific behavioral responses. Beyond characterizing the behavior of wild-type animals, we elucidated biological mechanisms underlying foraging by performing our experiments with genetic variants in which the function of specific cells or proteins was altered.

1.4 Dauer formation in *C. elegans*

Interacting biochemical pathways regulate behavioral, physiological, and developmental responses to food [67, 80, 99, 187]. In nematodes such as *C. elegans*, these responses can be quite dramatic. Under harsh environmental conditions including high ambient temperature and high population density relative to food supply, young *C. elegans* larvae can undergo a developmental change termed dauer arrest [27] (see Fig. 1.2). Dauer larvae are morphologically and behaviorally distinct from larvae that develop in favorable environments; they do not feed and are shielded from the external world by a specialized cuticle [27, 157]. Dauer arrest is a diapause state in which animals can survive for months until conditions improve and normal development resumes [104]. With respect to underyling biochemical pathways, dauer arrest in free-living nematodes such as *C. elegans* shares homology with obligate infective developmental stages of parasitic nematodes and is thus a general feature of the complex lifestyles of animals of this phylum [137].

Genes involved in regulation of dauer arrest are classified as dauer-constitutive (Daf-c; mutants undergo irreversible dauer arrest under favorable conditions) or dauer-defective (Daf-d; mutants fail to undergo dauer arrest under adverse conditions) [62, 157]. Several well-characterized biochemical pathways regulate dauer arrest. Among these is the transforming growth factor beta (TGF-β) pathway, defined by a set of Daf-c and Daf-d genes [143] (see Fig. 3.1). TGF-β family ligands bind to and activate cell surface receptors, resulting in the activation of transcription factors involved in metabolic and developmental processes [172].

Chapter 3 reports on our rather unexpected observation that TGF-β contributes to foraging behavior in a manner similar to 5-HT. Yet, perhaps this finding is not so surprising given that dauer formation occurs in the absence of food [27]. Dauer formation can be thought of as part of the same set of behaviors to which slowing responses upon encounter with food belong: an array of behavioral or physiological responses that result from changes in food availability. In that sense, it is logical that molecules involved in acute sensation of food, such as 5-HT, interact with pathways involved in responses to food on longer timescales,

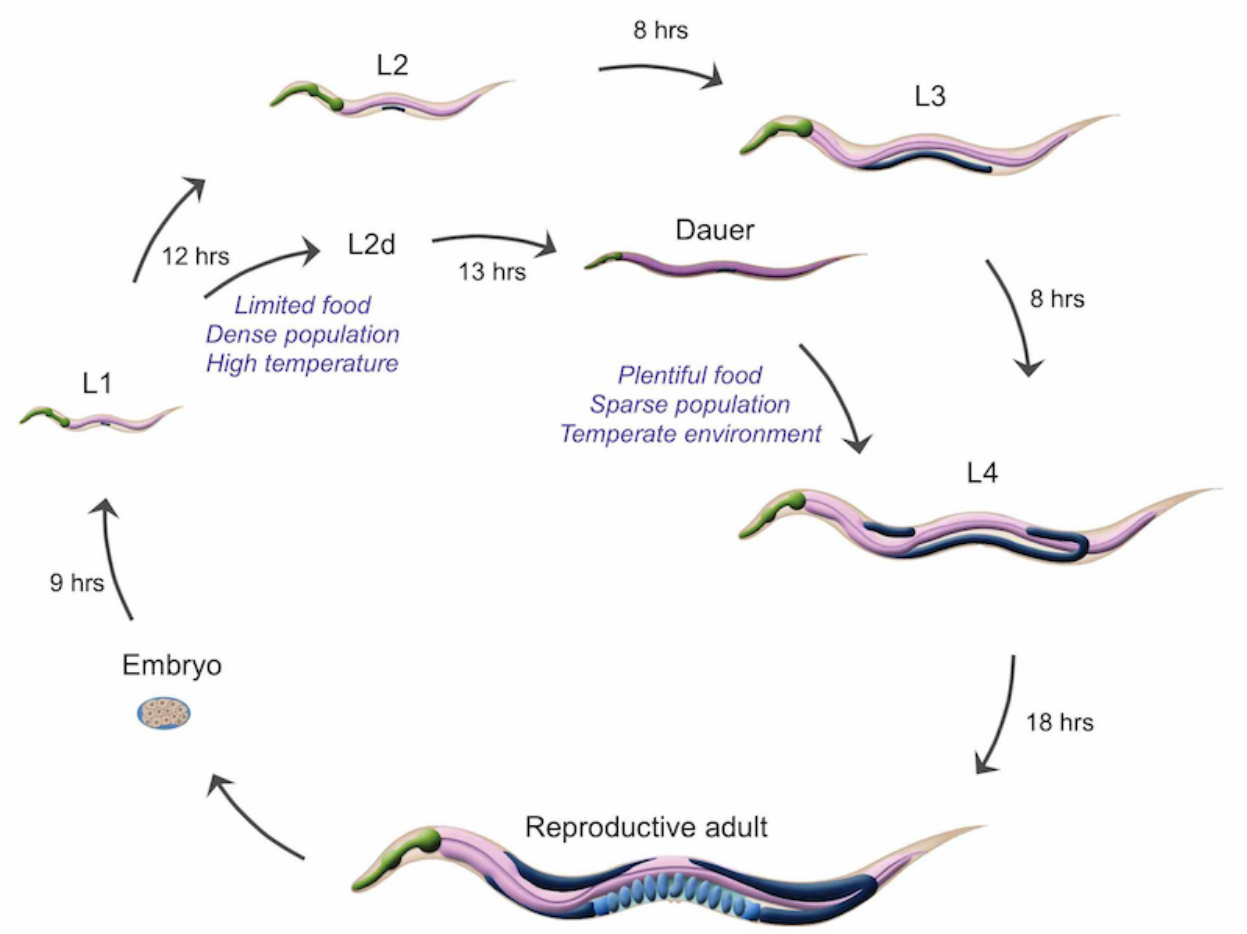

Figure 1.2: ***C. elegans* life cycle with dauer branch.** *C. elegans* larval development proceeds through 4 larval stages (L1 through L4). L4 larvae molt into young adults which then develop into reproductive adults that survive for approximately 3 weeks under normal laboratory conditions. If L1s are starved, crowded and experience elevated temperatures, they may select an alternative developmental pathway developing into L2d and then dauer larvae. Dauer larvae are adapted for survival in the absence of food by dispersing into new environments. When suitable environmental conditions return, dauers may reenter reproductive development by molting into L4 larvae. Reproduced from [206].

such as TGF-β.

1.5 About this dissertation

In the following chapters I present a group of studies that use quantitative behavioral observations to understand foraging in *C. elegans*. In Chapter 2, I present novel foraging assays and characterize wild-type foraging behavior. I also show how serotonergic signaling accelerates the response to encounter with food and contributes to efficient foraging in a complex environment. Chapter 3 describes the contribution of TGF-β signaling to foraging behavior, probes the sensory basis of responses to encounter with food, and explores the relationship between TGF-β and 5-HT pathways. In Chapter 4 I describe in greater detail experimental and computational methodologies referenced in the preceding chapters. I also present an additional application of these methods toward the study of synaptic vesicle release regulation and related effects on locomotion. In Chapter 5, I discuss future experiments that could help elucidate further the mechanisms that underlie foraging. I also discuss the relationship between *C. elegans* and other animals and speculate about the future of comparative genetic neuroethology.

CHAPTER 2

SEROTONIN PROMOTES EXPLOITATION IN COMPLEX ENVIRONMENTS BY ACCELERATING DECISION-MAKING

Adam Brown[*1], Shachar Iwanir[*2], Stanislav Nagy[2], Dana Najjar[3], Alexander Kazakov[4], Kyung Suk Lee[5], Alon Zaslaver[4], Erel Levine[5], and David Biron[2,3]

This chapter is adapted from Iwanir et al., BMC Biology 2016 [97]. AB contributed to the conception and design of the study, performed, analyzed, and interpreted behavioral and physiological assays, and contributed analysis tools. SI contributed to the conception and design of the study, generated transgenic animals, performed, analyzed, and interpreted behavioral and physiological assays, and contributed analysis tools. SN contributed to the conception and design of the study, performed, analyzed, and interpreted behavioral assays, and contributed analysis tools. DN performed, analyzed, and interpreted behavioral and physiological assays. AK performed, analyzed, and interpreted behavioral and physiological assays. KSL contributed reagents/materials. AZ contributed to the conception and design of the study. EL contributed to the conception and design of the study. DB contributed to the conception and design of the study and helped analyze and interpret the data. All authors contributed to writing and editing of drafts, and approved the final manuscript. An asterisk (*) denotes equal contribution.

1. Committee on Computational Neuroscience, The University of Chicago, Chicago, IL 60637, USA.

2. The Institute of Biophysical Dynamics, The University of Chicago, Chicago, IL 60637, USA.

3. Department of Physics and the James Franck Institute, The University of Chicago, Chicago, IL 60637, USA.

4. Department of Genetics, The Alexander Silberman Institute of Life Sciences, The Hebrew University of Jerusalem, Jerusalem, Israel.

5. Department of Physics and Center for Systems Biology, Harvard Univeristy, Cambridge, United States

2.1 Abstract

Fast responses can provide a competitive advantage when resources are inhomogeneously distributed. The nematode *C. elegans* was shown to modulate locomotion on a lawn of bacterial food in serotonin (5-HT) dependent manners. However, potential roles for serotonergic signaling in responding to food discovery are poorly understood. We found that 5-HT signaling in *C. elegans* facilitates efficient exploitation in complex environments by mediating a rapid response upon encountering food. Genetic or cellular manipulations leading to deficient serotonergic signaling resulted in gradual responses and defective exploitation of a patchy foraging landscape. Physiological imaging revealed that the NSM serotonergic neurons responded acutely upon encounter with newly discovered food and were key to rapid responses. In contrast, the onset of responses of ADF serotonergic neurons preceded the physical encounter with the food. The serotonin-gated chloride channel MOD-1 and the ortholog of mammalian 5-HT1 metabotropic serotonin receptors SER-4 acted in synergy to accelerate decision-making. The relevance of responding rapidly was demonstrated in patchy environments, where the absence of 5-HT signaling was detrimental to exploitation. Our results implicate 5-HT in a novel form of decision-making, demonstrate its fitness consequences, suggest that NSM and ADF act in concert to modulate locomotion in complex environments, and identify the synergistic action of a channel and a metabotropic receptor in accelerating *C. elegans* decision making.

2.2 Introduction

The spatial distribution of resources in natural environments can be non-uniform. Patches of food sources generically result from non-linear interactions between multiple species and inhomogeneous environmental conditions [9, 49, 124]. As a result, foraging behavior in patchy environments is extensively studied both theoretically and experimentally in diverse species and habitats [19, 40, 44, 48, 170, 174, 211]. Yet, key questions such as the fitness

consequences of efficient foraging and the neural basis of these behaviors are not sufficiently understood [83, 108, 110, 182, 197].

Food availability can affect locomotion patterns [6, 74, 140, 164]. In the absence of food, *C. elegans* predominantly roams, a behavioral state characterized by fast, directional locomotion. In contrast, on a standard bacterial lawn *C. elegans* exhibits mostly non-directional dwelling and mean velocities are an order of magnitude lower than off food [6, 57, 58, 140]. In addition, several minutes after being placed on food, starved *C. elegans* exhibits slower motion than well-fed animals. This was termed "enhanced slowdown". The biogenic amine serotonin (5-hydroxytryptamine; 5-HT) modulates behaviors of *C. elegans* including locomotion, feeding, and egg laying [34, 79, 88, 168, 177, 179] as well as the enhanced slowdown [77, 140, 164].

The dynamics of *C. elegans* locomotion during an encounter with newly discovered food have not been previously characterized. Under standard laboratory conditions, *C. elegans* typically forages on a large and homogeneously food-covered landscape. In such an environment responses to newly discovered food are not easily assayed and potential deficiencies may not incur a significant impact. In contrast, on a patchy foraging landscape responding quickly to a newly discovered patch of food may be crucial to efficient exploitation. Delayed reactions could potentially prove as detrimental as a deficiency in navigating to a patch in the first place.

Three neuronal cell types display robust serotonin biosynthesis in the hermaphrodite: the amphid sensory neuron ADF, the pharyngeal neurosecretory motor neuron NSM and the hermaphrodite specific neuron HSN [98]. NSM was implicated in mediating an enhanced slowdown of locomotion on food after a period of starvation [164, 77, 81] and in decision-making during steady-state transitions between roaming and dwelling on food [57, 207]. The sensory neuron ADF has been primarily associated with navigation [13, 30, 91, 147, 178] and pharyngeal pumping [41, 178]. However, the specific roles of serotonergic neurons in mediating responses to newly encountered food are not well understood.

Here we show that serotonergic signaling accelerated the slowdown of animals upon encountering food, such that they could abruptly pause at the edge of a bacterial lawn. To address the biological relevance of an abrupt slowdown, we assayed exploration and resource exploitation of animals in patchy environments. Under these conditions, serotonergic signaling afforded a substantial advantage in exploitation. The pharyngeal neurosecretory motor neuron NSM responded physiologically to the actual encounter and was the primary driver of the abrupt slowdown. In contrast, the onset of activity in the chemosensory serotonergic neuron ADF occurred prior to the encounter with food. Correspondingly, ADF affected locomotion during this time. Finally, we found that a 5-HT gated chloride channel (MOD-1) and a 5-HT metabotropic receptor (SER-4) act together to accelerate *C. elegans* decision-making.

2.3 Results

2.3.1 The slowdown of C. elegans *upon encountering food is abrupt.*

Behavioral and physiological responses of *C. elegans* during encounters with newly found food were not previously characterized [164]. Under standard laboratory conditions, successful foraging does not depend on acute responses. However, on more complex terrain responding to discovery in a timely fashion may prove as important as the ability to navigate towards the food source. To address this, we used continuous video recordings to resolve the dynamics of locomotion upon re-feeding after a period off food with a high temporal resolution (Fig. 2.1A).

The most striking feature of the observed dynamics was an abrupt slowdown upon encountering the edge of the bacterial lawn: a nearly complete halt reached within 3 sec ($\tau = 1.73 \pm 0.12$ sec, Fig. 2.1B), where the timescale τ was obtained from a fit to a single exponential decay. After a brief pause, wild-type animals typically advanced about one body-length into the large bacterial lawn during a one-minute period. During the following 10-15 minutes, animals predominantly dwelled before reaching steady-state transition rates between roam-

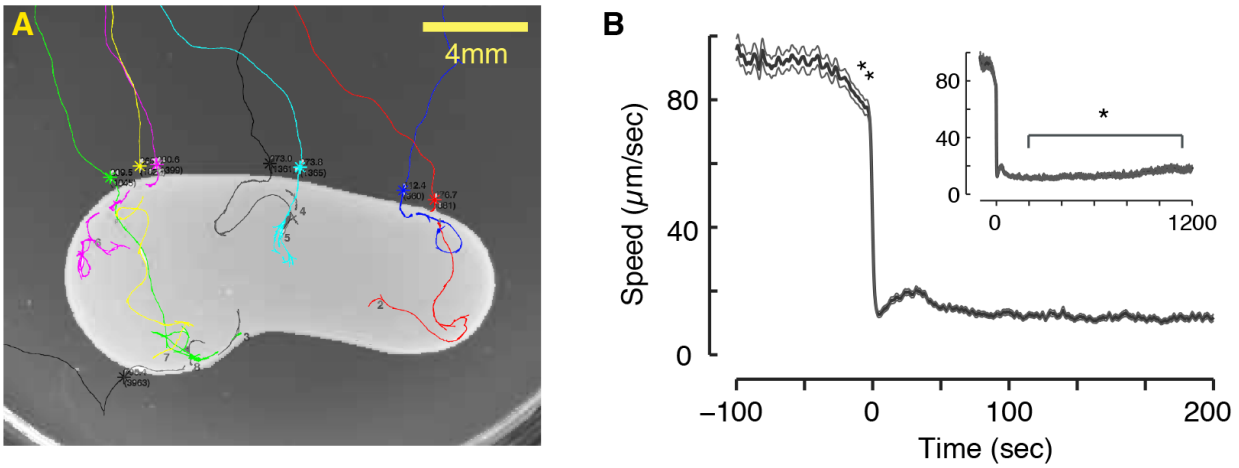

Figure 2.1: **The slowdown of *C. elegans* upon encountering novel food is abrupt. A** Typical trajectories of multiple tracked animals approaching a large bacterial lawn (light grey area). **B** The center of mass speed of tracked animals aligned to the time of encountering the edge of the bacterial lawn, t = 0 (mean ± s.e.m., N = 288 animals). The mean deceleration during the 30 sec period that immediately preceded the encounter was 0.66 ± 0.04 μm/sec^2 (double asterisks denote that it was significantly different from zero as determined by a t-test, $p<0.01$) with the edge of the bacterial lawn. Inset: The center of mass speed on food during intermediate and long times post encounter. The mean speed at t = 1100-1200 was significantly higher than at t = 100-200 in agreement with previous reports (as determined by a t-test, asterisk denotes $p<0.05$).

ing (fast, mostly forward locomotion) and dwelling [57, 173]. The transiently augmented dwelling behavior was consistent with previous reports of enhanced slowing [164, 6].

Immediately preceding the encounter with the edge of the bacterial lawn, the roaming animals exhibited a mild but significant deceleration. During the 30 sec period preceding the encounter, the mean deceleration was 0.66 $\pm$ 0.04 μm/sec^2, p<0.01 (Fig. 2.1B). Despite being small in magnitude, this mild preemptive slowdown was observed in >70% of the individual wild-type encounters (Fig. 2.2D). The overall structure of the response to encountering food was conserved across a range of experimental conditions. In particular, characteristics of motion during the encounter and the following 15 minutes were only weakly affected by or independent of the time the animals spent off food prior to the assay (Fig. 2.2). Thus, a robust and eminent feature of the response to newly discovered food was a rapid slowdown upon encounter with the edge of the lawn.

2.3.2 Serotonergic signaling accelerates slowdown upon re-feeding.

We next asked whether serotonin might affect the timescale of slowdown upon encountering an edge of a bacterial lawn [6, 74, 140, 164]. To test this, we assayed mutants in which the synthesis of 5-HT was abolished due to the loss of function of the tryptophan hydroxylase TPH-1 [187]. Upon re-feeding, *tph-1* mutants exhibited a significant increase of the timescale of slowdown: τ = 14.49 $\pm$ 0.39 sec and τ = 30.80 $\pm$ 1.72 sec for *tph-1(mg280)* and *tph-1(n4622)*, respectively. In our hands, this was the most prominent phenotype resulting from loss of 5-HT synthesis and center of mass speeds of *tph-1* mutants were not higher than wild-type 20 minutes after the encounter (see Figs 2.3 and 2.4). Expressing the functional *tph-1* gene under its innate promoter successfully rescued the defect, i.e., restored wild-type like rapid responses (τ = 2.89 $\pm$ 0.17 sec, Fig. 2.3A-B).

Animals in which vesicle exocytosis was blocked by the tetanus toxin light chain gene [167, 116] in all of the serotonergic neurons (*Ptph-1::TeTx*) were phenotypically similar to *tph-1* mutants (τ = 24.90 $\pm$ 0.56 sec, Figs 2.3 and 2.4). Mutants in the *mod-5* gene, encoding

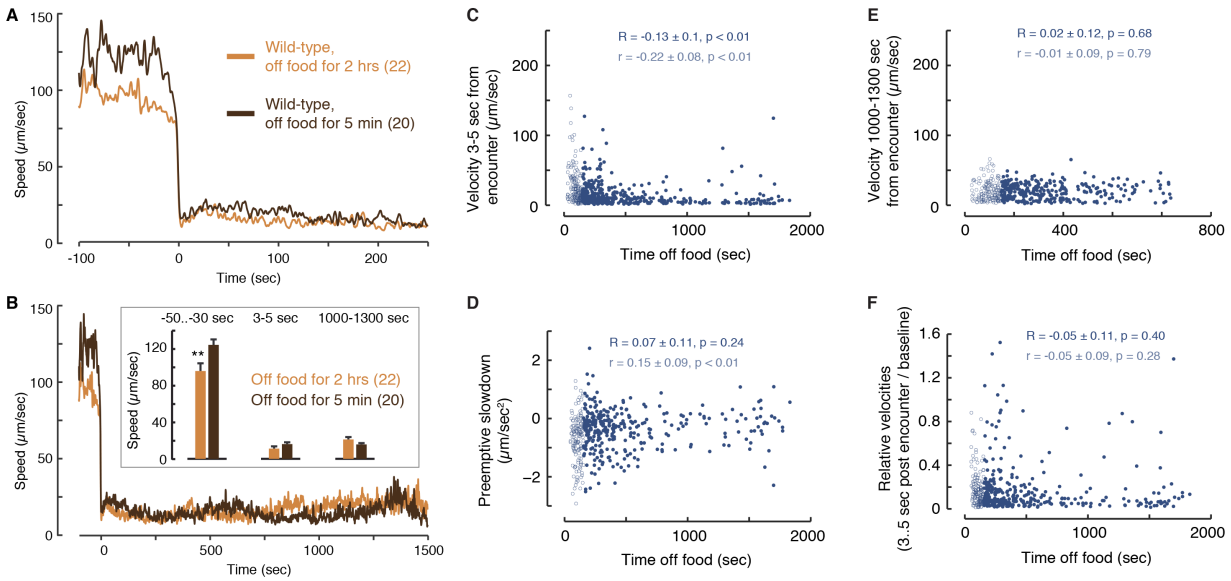

Figure 2.2: **Invariance of wild-type responses to food encounter. A-B** The center of mass velocities of wild-type animals that were kept off food for two hours or 5 minutes prior to the assay. In our hands, the different starvation conditions did not strongly affect the abrupt slowdown upon encountering food or locomotion thereafter. A small but significant difference was observed in baseline velocities (as determined using a t-test, $p<0.01$). **C-F** Scatter plots of wild-type behavior: velocities at t = 3..5 seconds post encounter, velocities 1000-1300 seconds post encounter, the preemptive slowdown during the 50 seconds prior to the encounter, and the relative velocities post encounter. Filled/dark circles represent all animals that arrived at the edge of the bacterial lawn at least 150 sec after being transferred to the assay plate. All four aspects of locomotion are weakly or not significantly correlated with the duration of prior food deprivation (denoted by R). Empty/light circles denote animals that arrived at the edge of the lawn less than 150 sec after being transferred to the assay plate. When these data are added to the analysis, correlations (denoted by r) with the duration of prior food deprivation remain weak or insignificant.

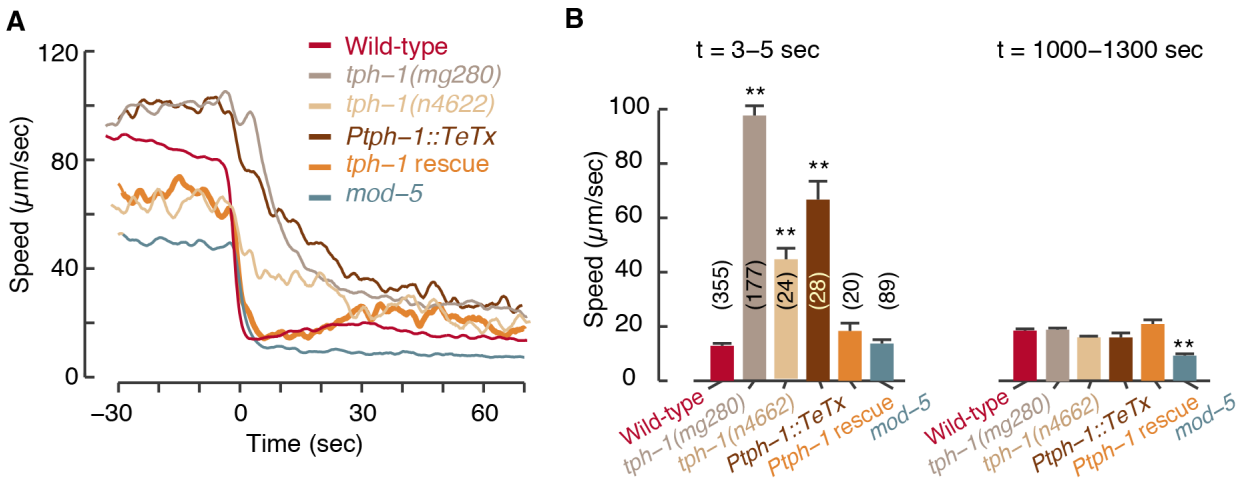

Figure 2.3: **Serotonergic signaling accelerates slowdown upon re-feeding.** **A** The mean speeds of wild-type and 5-HT deficient strains around the time of encounter with the edge of a large bacterial lawn (shown without standard errors as a guide to the eye; see summary statistics in next panel). **B** The speeds of the strains shown in panel (**A**) shortly after the encounter and 20 minutes later. Twenty minutes after the encounter, wild-type and *tph-1* center of mass speeds were similar. Bars depict mean ± s.e.m and the number of animals assayed for each strain is noted in parentheses. Mean velocities were compared to wild-type using an ANOVA test and corrected post hoc for multiple comparisons using Tukey's honest significant difference (HSD) test. Double asterisks denote a significant difference from wild-type ($p<0.01$). For *Ptph-1::TeTx* and *Ptph-1::tph-1*, three independent transgenic lines were assayed and one representative dataset is shown.

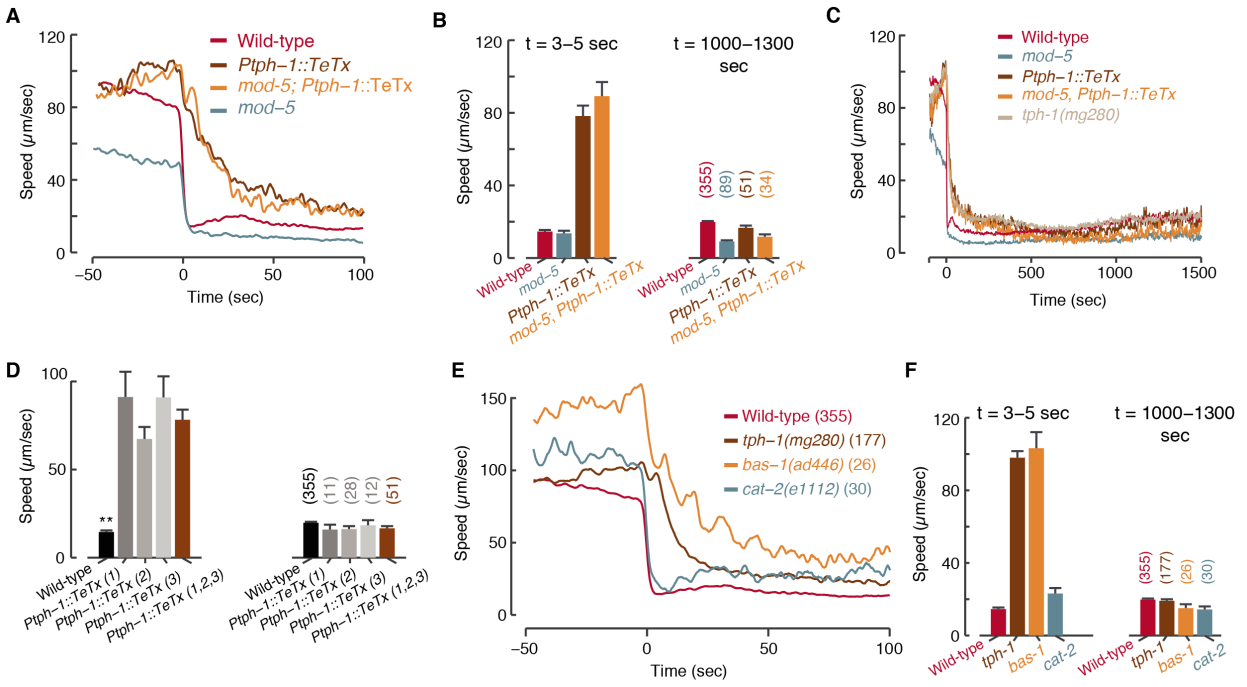

Figure 2.4: **Contributions of other bioamines and bioamine-related proteins to slowdown dynamics. A-B** The same assays and analysis as described in **Fig. 2.3A-B** were also performed on a *mod-5* mutant background. **C** The velocity of wild-type animals, *tph-1* mutants, *mod-5* mutants, and transgenics in which the serotonergic neurons have been genetically silenced as measured up to 1500 sec after the encounter with food. **D** The same assays and analysis as described in **Fig. 2.3A-B** are shown for the three independent transgenic lines. **E-F** The same assays and analysis as described in **Fig. 2.3A-B** were also performed on *bas-1* mutants, lacking serotonin and dopamine, and *cat-2* mutants, lacking dopamine. Dopamine in and of itself was not required for rapid decision-making upon encountering food. Comparisons were performed using an ANOVA test corrected post hoc for multiple comparisons using Tukey's HSD test. Single and double asterisks denote significant differences ($p<0.05$ and $p<0.01$).

a transporter required for 5-HT re-uptake, exhibited a lower mean speed both off and on food (see also [151, 164]) and an abrupt slowdown upon encounter ($\tau = 3.24 \pm 0.14$ sec, Figs 2.3 and 2.4). To test the impact of differences in baseline locomotion, we confirmed that the changes in relative velocity maintain the phenotypic trends observed in the wild-type, mutant, functional ablation, and rescue strains assayed (Fig. 2.10). Taken together, these results indicate that 5-HT signaling accelerates slowdown upon encountering food and acts on a timescale of 2-3 seconds.

2.3.3 An abrupt slowdown supports exploitation of a small patch of food.

Under what circumstances could an abrupt slowdown be advantageous? A gradual modulation of locomotion can suffice when the spatial scale of the feeding area is much greater than the length scale associated with the slowdown. In contrast, in environments where food is spatially confined to small patches, an abrupt slowdown may increase exploitation [1, 9, 83]. The ratio between the typical speed of a roaming animal and the timescale of slowdown determined the relevant length scale, which was comparable to one body length.

To test the utility of abrupt slowdown, we placed animals on plates with patches of bacterial food that were 0.5-1 mm in diameter, termed micro-patches. This assay was repeated using different concentrations of food and various patch arrangements (see Methods). We measured the fraction of time spent on a patch of food during the 5 minutes following the first encounter with this patch. Responses were scored visually and divided to four categories, where the first two resulted in favorable exploitation of the food patch (see Methods).

We assayed *tph-1* mutants and *Ptph-1::TeTx* transgenics in the presence of micro-patches. In both cases the animals spent significantly less time on a patch of food during the 5 minutes following the first encounter with this patch, as compared to wild-type (Fig. 2.6A). The chances of exploitation increased with the concentration of food on the patch in a dose-dependent manner in wild-type animals, *tph-1* mutants, and *Ptph-1::TeTx* transgenics. Serotonin deficient animals were completely unable to stop at patches of low food concentrations and performed poorly as compared to wild-type under all of the conditions tested. Thus, a deficiency in either the synthesis or the release of 5-HT reduced the efficiency of translating an encounter with a small patch of food to successful exploitation in a concentration dependent manner.

2.3.4 Serotonergic signaling promotes exploitation in a complex environment.

Exploitation on a patchy landscape can be affected not only by first encounters, but also by various (possibly compensatory) factors including feeding behavior once on food or differences in foraging patterns. Thus, a first encounter phenotype may not translate in a straightforward manner to a competitive advantage. To test this, we placed the animals in an arena where 49 micro-patches were positioned in a square lattice arrangement and monitored their behavior for 5-10 hours. Although fast locomotion does not entirely preclude feeding, small deposits of food are more efficiently exploited when the animals move very slowly on the patch. Therefore, in these assays, detectable exploitation events were defined when two conditions were met concurrently: the mouth of the animal was on a patch of food and its velocity during the encounter was below an experimentally determined threshold (see Fig. 2.5A and Methods).

To examine the role of 5-HT signaling in exploiting a complex environment, we assayed wild-type animals, *tph-1* mutants, and quintuple mutants lacking the function of the five serotonin-binding receptors that have been identified in *C. elegans* [34, 79]. Two simple measures of the efficiency of food exploitation are: (i) comparing the numbers of patches that were exploited with those merely encountered; and (ii) comparing the overall fraction of time spent at patch locations to the time spent exploiting. Both measures were quantified during the first two hours of the experiment, when the environment was mostly intact, and throughout the experiment, as patches were progressively consumed (Figs 2.5B-C and 2.6B-D). While wild-type animals exploited as many patches as they encountered, *tph-1* mutants were unable to exploit the vast majority of encountered patches. Moreover, these mutants spent significantly less time than wild-type at patch locations, whether they were regarded as exploiting or not. Thus, even if animals fed efficiently without slowing, e.g., by frequent turns resulting in multiple passes through a patch, serotonergic signaling remained advantageous.

Next, we measured the fractions of the area of a food patch that was encountered or

exploited (Figs 2.5D and 2.6C). When all encountered patches (throughout the experiment) were considered, wild-type animals covered a significantly larger fraction per patch than *tph-1* mutants (Fig. 2.5Di). When we limited the analysis to exploited patches, the difference between wild-type and *tph-1* mutants was smaller but remained significant (Fig. 2.5Dii), indicating that *tph-1* mutants were capable of exploiting patches once exploitation was initiated.

Possible contributors to deficient exploitation could have been a smaller coverage of the patch per event due to enhanced patch leaving [15], an exploration defect resulting in fewer encounters, or the defect in initiating exploitation upon encounter demonstrated above. As depicted in the Fig. 2.5Diii, *tph-1* mutants exploited a similar area per event, suggesting that elevated patch leaving did not appreciably contribute to reduced exploitation. The time spent between encountering patches was also similar between *tph-1* and wild-type animals (Fig. 2.5Div), indicating that the mutants did not exhibit an exploration/navigation defects. Combined, our various assays suggested that a major contributor to the *tph-1* exploitation defect was their inability to slow down abruptly, and that this defect was not sensitive to experimental details. Moreover, mutants lacking the function of all five *C. elegans* serotonin receptors were significantly defective as compared to wild-type and similar to *tph-1* mutants (Fig. 2.5B-D). Thus, serotonergic signaling conferred an exploitation advantage in a complex environment by accelerating decision-making.

2.3.5 The serotonergic neurons ADF and NSM respond prior to and upon encountering food, respectively.

Spontaneous physiological activity of NSM on food is sporadic [57] and chemical cues can evoke slow changes in NSM cytosolic calcium [111]. In ADF, familiar food and salt can evoke calcium transients [177, 188]. However, the activity of serotonergic neurons was not examined during encounters with newly discovered food. To characterize the physiological activity that promotes the rapid responses we observed, we monitored calcium levels in freely behaving

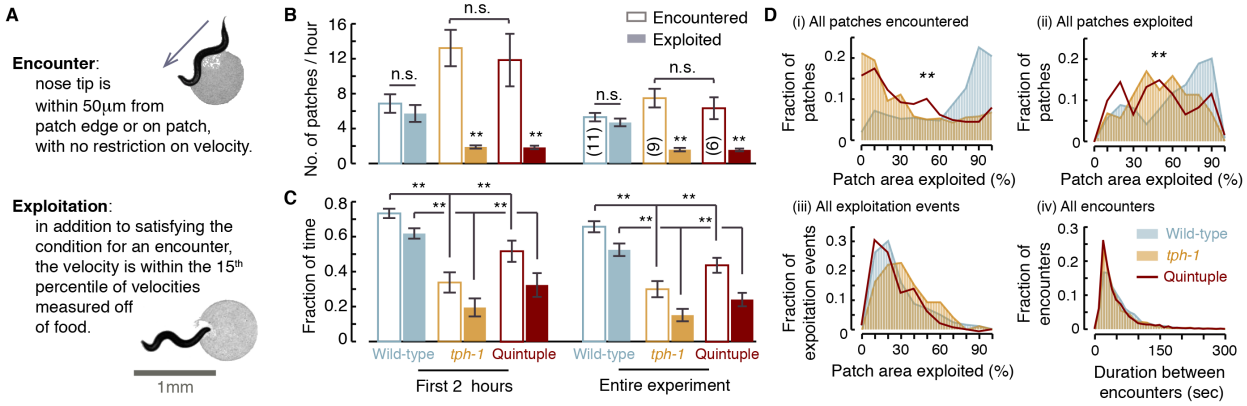

Figure 2.5: **Serotonergic signaling promotes exploitation in a complex environment.** Wild-type animals and *tph-1* mutants were assayed on a square lattice arrangement of 49 micro-patches (see also Figs. 2.5, 2.2). **A** Frames in which the nose of the animal was on a patch were labeled "encountered". Frames were labeled "exploited" once, in addition, sub-threshold speed was measured (see Methods). Top: a *tph-1* mutant encountering a patch. Bottom: a wild-type animal exploiting a patch. **B** The mean number of micro-patches encountered and exploited during the first two hours or the entire duration of each assay. **C** The mean fraction of time spent on encounters or exploitation during the first two hours or the entire duration of each assay. When animals were not encountering or exploiting they were moving (predominantly roaming) off food between the patches. In panels (**B-C**), the number of animals assayed for each strain is noted in parentheses, error bars depict s.e.m, means were compared using an ANOVA test corrected post hoc for multiple comparisons using Tukey's HSD test, and double asterisks denote a significant difference ($p<0.01$). By both measures, *tph-1* mutants were deficient as compared with wild-type. **D** The percentage of the area exploited during the assay was calculated for each micro-patch that was encountered at least once. (i) A histogram of exploited percentages for all encountered patches. (ii) A histogram of exploited percentages for all exploited patches (excluding patches that were only encountered). (iii) A histogram of exploited percentages for single continuous periods of exploitation (termed "events"). (iv) A histogram of the durations between consecutive encounters. The mutants encountered as many patches as wild-type and did not exploit a smaller area of the patch during a single event. However, once they veer off of the patch or fully consume it, *tph-1* mutants are deficient in initiating the next exploitation event and thus exhibit lower cumulative exploitation. The distributions were compared to wild-type using the k-sample Anderson-Darling test and double asterisks denote a significant difference ($p<0.01$).

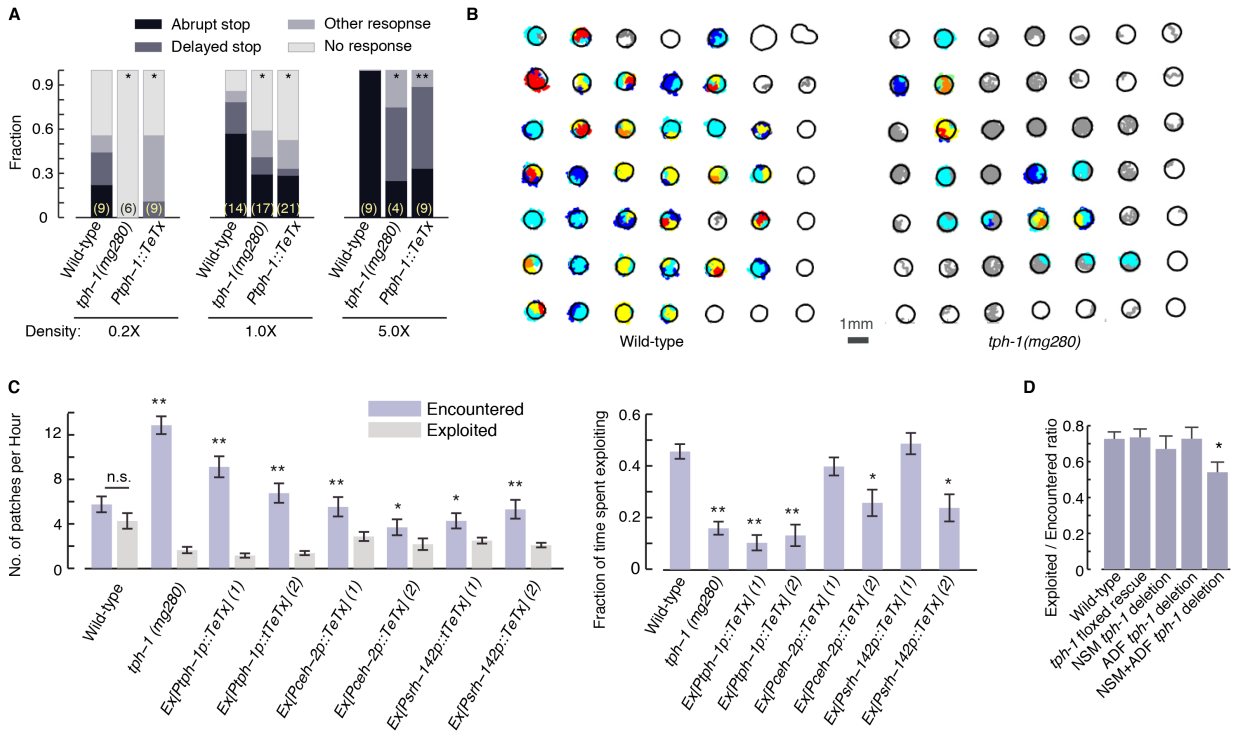

Figure 2.6: **Details of micro-patch assay behavior of wild-type and 5-HT deficient strains. A** Responses of wild-type and 5-HT deficient strains upon encounter with a micro-patch (see Methods). The number of animals assayed for each strain is noted in parentheses. Comparisons were performed by assigning the four types of responses numerical values (0-3) and using an ANOVA test corrected post hoc for multiple comparisons using Tukey's HSD test. Single and double asterisks denote a significant difference from wild-type ($p<0.05$ and $p<0.01$). Here, a single *Ptph-1::TeTx* line was assayed. **B** Sample maps of two patchy environments on which a single wild-type animal (left) and a single *tph-1* mutant (right) were assayed. Each outlined circle depicts a single patch of bacterial food. Cyan, blue, red, and yellow colors depict the positions of the nose of the animal during single exploitation events. Grey depicts events in which the animal encountered the patch but did not slow down sufficiently to be considered "exploiting" for the purpose of the analysis. **C-D** The efficiency of exploitation in the small patch assay of TeTx transgenics and Cre mediated *tph-1* deletion strains. Functional ablations of individual neurons resulted in partial phenotypes. Deletion of *tph-1* in NSM and ADF resulted in a mild partial defect.

animals using the genetically encoded indicator GCaMP3.0 [190]. Our behavioral assays indicated that *egl-1* mutants, lacking the HSN serotonergic neuron type [160, 193], were indistinguishable from wild-type (data not shown). Therefore, to study cellular mechanisms, we focused on the physiological activity in NSM and ADF prior to, during, and after refeeding encounters.

NSM neurons of food-deprived animals were strongly activated at the time of the encounter with the edge of a bacterial lawn (t = 0, Fig. 2.7). Calcium levels peaked 15-20 sec after the encounter and remained above baseline for >100 sec. In contrast, ADF neurons responded up to 25 sec prior to the arrival of the animals at edge of the lawn (see Fig. 2.7) and returned to baseline calcium levels after 50 sec. The early activation of ADF was likely due to its known role as a chemosensory neuron [13, 30, 147, 178]. To further address the activation of ADF, we assayed its physiological activity in *osm-6* mutants. The *osm-6* gene encodes an intraflagellar transport component. Its absence results in defects to the ultrastructure of sensory celia and, as a result, in chemosensory and mechanosensory defects. Expression of *osm-6* was reported in many ciliated neurons, including ADF, but not in NSM [39, 145]. In these assays, we observed a prominent activation of ADF prior to the encounter in control animals and no activation of ADF at any time in *osm-6* mutants. Correspondingly, the preemptive slowdown was significant in the control group and absent in the mutants (Fig. 2.7B). In contrast, NSM responses were not prominently affected by the loss of OSM-6 function (Fig. 2.7C). Thus, chemosensation by ADF contributes to the preemptive slowdown.

Physiological responses of ADF to bacteria supernatant were detected in a microfluidic device [208]. To demonstrate ADF responses to diffusible chemicals from food in freely behaving animals on a standard assay plate, we recorded from animals placed on the face of an agar pad opposing the side supporting the bacterial lawn (see Methods). The minimal possible distance between animals thus placed and the bacterial lawn was 2-3 mm, as determined by the thickness of the pad. Although this assay does not reproduce the geometry

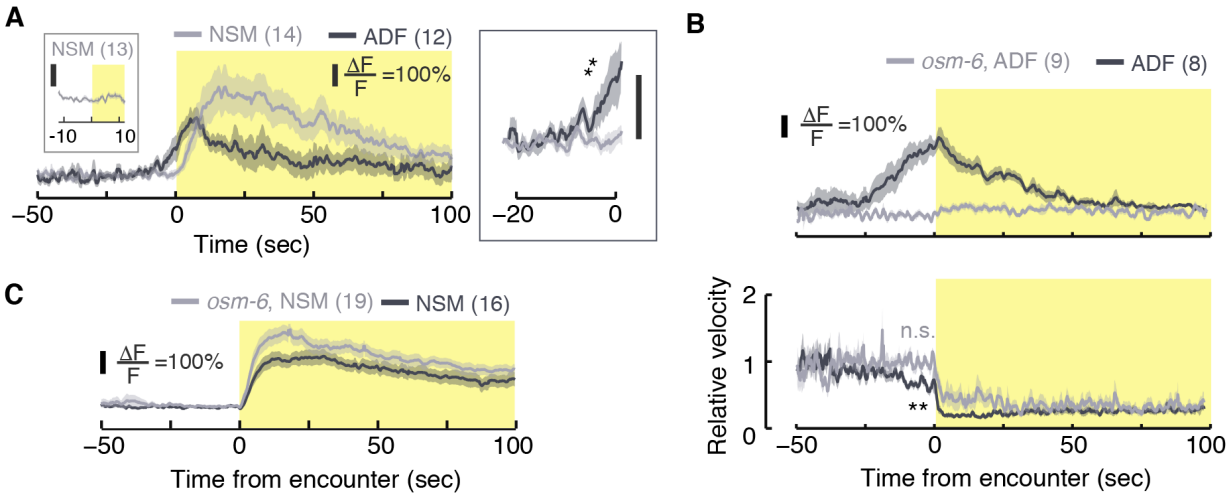

Figure 2.7: **The serotonergic neurons ADF and NSM respond physiologically during re-feeding.** **A** Left: traces of fluorescence from NSM::GCaMP (grey) and ADF::GCaMP (black) transgenics re-feeding on a large bacterial lawn. The time of encountering the edge of the lawn was defined as t = 0. Plots depict mean ± s.e.m and the number of animals assayed for each strain is noted in parentheses. Inset: NSM was not activated when the animals abruptly paused due to gently colliding with an obstacle. The yellow shading denotes the time following the encounter (t > 0). Right: a zoomed view of the calcium transients shortly prior to the encounter. Fluorescence in ADF but not NSM neurons was significantly higher than baseline during the 5 seconds preceding the encounter (mean intensities were compared to their respective baselines using a t-test, $p<0.01$). **B-C** GCaMP fluorescence in ADF and NSM in *osm-6* mutant backgrounds and their respective wild-type background control groups using an improved imaging system (see Methods). The velocity of the tracked ADF neurons was reduced prior to the encounter in the control group but not in *osm-6* mutants (panel (**B**) bottom, t-test, $p<0.01$). NSM activity was not abolished by the mutation.

of a gradient near the edge of a lawn, it effectively serves to isolate the diffusible chemicals from the bacteria that produce them. A mock encounter was defined as the time when the position of the animal was directly above the edge of the lawn, and activity during the 20 seconds surrounding the mock encounter was compared to baseline (Fig. 2.8A). Consistent with chemosensation, we observed activation of ADF, but not of NSM, in the vicinity of the mock encounter in the reverse patch assay.

The abrupt slowdown is completed in 2-3 sec while the calcium transients in NSM and ADF last for 10s of seconds. However, *tph-1* mutants and *Ptph-1::TeTx* transgenics slow down over >30 sec (Fig. 2.8B). Moreover, NSM calcium transients predict dwelling states for several minutes on bacterial lawns [57] and the average time spent by a wild-type animal on a small patch is similarly long (see Fig. 2.5B-C). Taken together, our measurements demonstrated that ADF and NSM responded physiologically to the proximity and encounter with bacterial food, respectively, and continue to affect locomotion for tens of seconds after the encounter.

Is NSM required for exploiting food resources or for generic motor control? To address this we monitored the activity of NSM when the animal paused for a reason other than food encounters, i.e., in order to avoid an obstacle. We positioned a standard platinum pick near the anterior of a forward moving animal, such that the animal gently touched it due to its own motion. These collisions typically evoked abrupt pauses followed by brief reversals. In this case, NSM neurons were not detectably activated (Fig. 2.7A, left inset). Thus, NSM is not part of a general motor circuit that controls slowing down. Rather, it underlies a specific subset of behaviors including responses that facilitate exploitation of localized food resources.

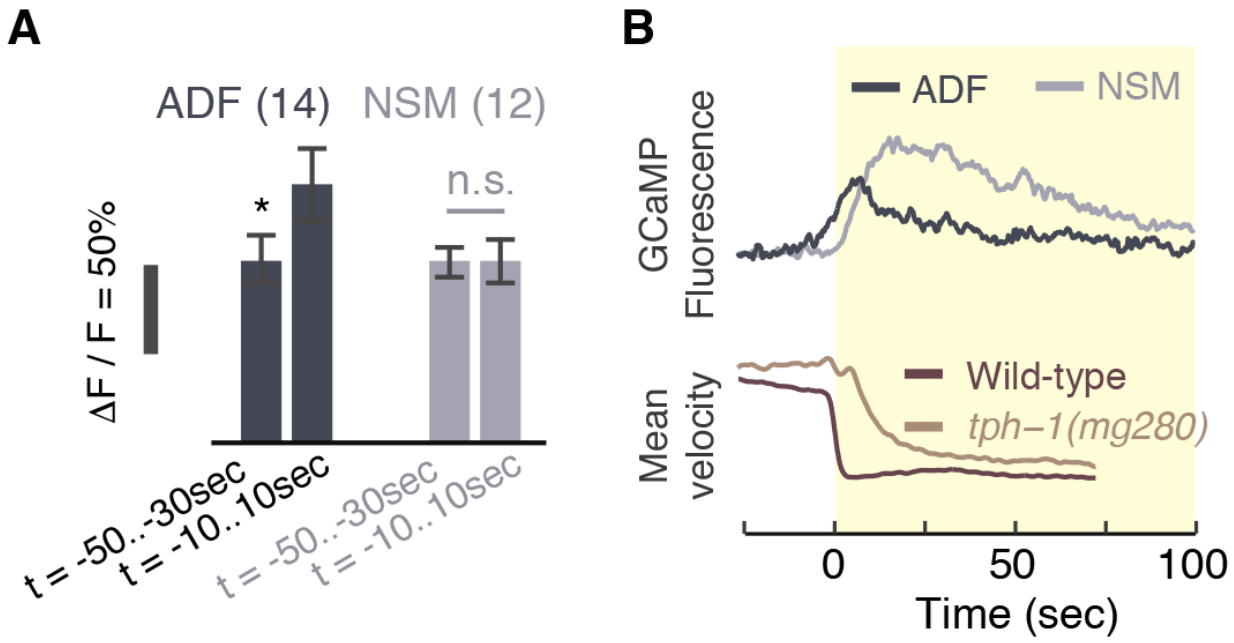

Figure 2.8: **Details of calcium imaging experiments. A** Mean values of NSM::GCaMP (grey) and ADF::GCaMP (black) fluorescence from animals assayed on a reversed patch (see Methods). The time in which the animal crawled directly above the edge of the bacterial lawn was defined as t = 0. Mean fluorescence was measured during 20 sec periods, before and around the mock encounter. Baseline activity was measured was measured in the same neurons 30..50 seconds prior to the mock encounter. The change in fluorescence observed in ADF mirrored the change observed several seconds prior to the encounter. Bars depict mean ± s.e.m, the number of animals assayed for each strain is noted in parentheses, pairwise comparisons were performed using a t-test, and the asterisk denotes a statistically significant difference between the two periods ($p<0.05$). **B** The mean kinetics of the GCaMP fluorescence data from **Fig. 2.7A** and the mean velocities from **Fig. 2.3A**. The yellow shaded area denotes post-encounter times (see Discussion).

2.3.6 ADF and NSM play complementary roles in mediating the dynamics of slowdown.

We observed that ADF, but not NSM, was activated before the animal reached the edge of the bacterial lawn. The timing of ADF activation resembled the timing of the mild preemptive slowdown prior to the encounter (Figs. 2.1B and 2.7). Both the abrupt slowdown upon encounter and the mild preemptive slowdown were affected by changes in 5-HT signaling (Figs. 2.3 and 2.11), suggesting that 5-HT may regulate distinct aspects of the overall response. To explore the individual contributions of different serotonergic neurons, we assayed transgenics expressing TeTx in either NSM or ADF.

Animals expressing TeTx in NSM but not in ADF slowed down gradually upon encounter ($\tau = 25.65 \pm 1.18$ sec), similarly to *Ptph-1::TeTx* animals and *tph-1* mutants, but retained the mild preemptive slowdown. In contrast, the preemptive slowdown was abolished in animals expressing TeTx in ADF but not in NSM while their abrupt slowdown upon encounter was more mildly defective ($\tau = 7.62 \pm 0.39$ sec, Figs. 2.9A-B and 2.10). These trends were maintained on a background of the loss of function of the 5-HT transporter MOD-5 (Figs. 2.9C-D and 2.10). In addition, functional ablation of either NSM or ADF resulted in partial phenotypes with respect to foraging in a complex environment (Fig. 2.6C). Thus, ADF and NSM may play complementary roles in mediating locomotion during foraging.

To assay the sufficiency of ADF and NSM, we expressed *tph-1* specifically in NSM or ADF on a *tph-1(mg280)* mutant background. Rescuing the function of TPH-1 in NSM mostly restored the abrupt slowdown upon encounter ($\tau = 2.49 \pm 0.16$ sec) but not the preemptive slowdown. ADF specific rescues resulted in an opposite phenotype (Figs. 2.9E-F and 2.11). High expression levels typical of such experiments may have contributed to the observed phenotypes by allowing one neuronal type to partially compensate for the absence of the other. Cell specific *tph-1* deletion transgenics [57] exhibited similar, albeit weaker, phenotypes (Figs. 2.9G-H, 2.10, 2.6D and 2.11). Incomplete penetrance of Cre expression or inactivation of the floxed *tph-1* gene could not be ruled out as a possible contributor to

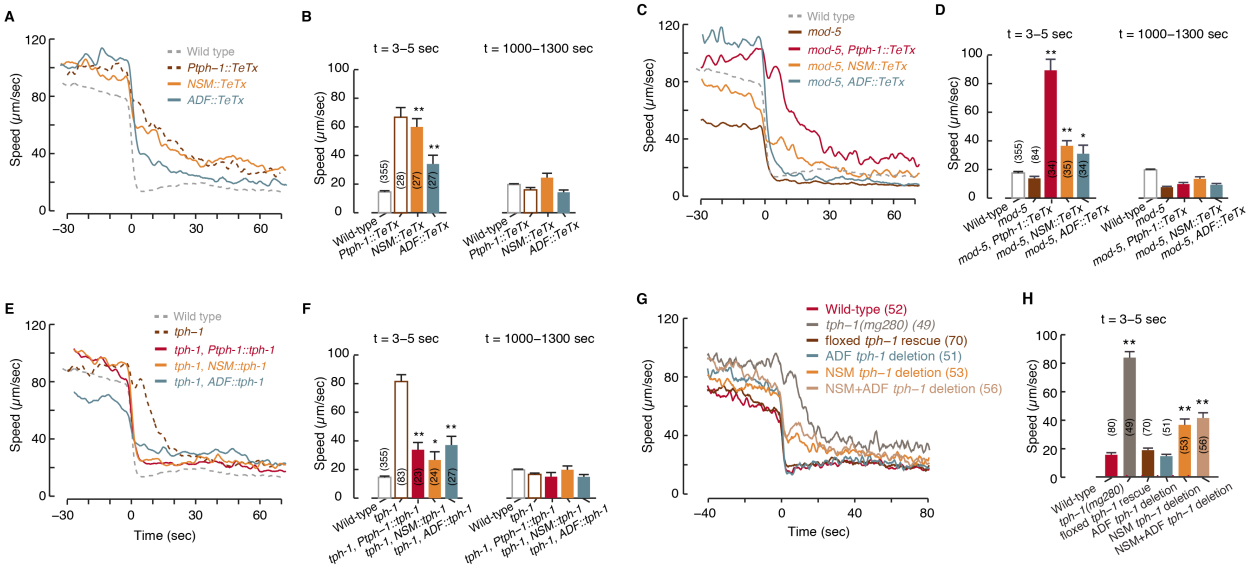

Figure 2.9: **Both ADF and NSM serotonergic neuron types affect the dynamics of slowdown. A** The mean speeds of transgenics in which NSM or ADF have been genetically silenced. The time of encounter with a large bacterial lawn was defined as t = 0. Traces are shown without standard errors as a guide to the eye; see summary statistics in next panel. **B** The speeds of the strains shown in panel (**A**) shortly after the encounter and their baseline speeds on food 20 minutes later. Bars depict mean ± s.e.m and the number of animals assayed for each strain is noted in parentheses. Double asterisks denote a significant difference from wild-type, p<0.01. Data from wild-type and *Ptph-1::TeTx* strains was reproduced from Fig. 2.3 and shown as dashed lines and empty bars for comparison. **C-D** Same as panels (**A-B**), except that the genetic silencing was performed on a *mod-5* mutant background. **E-F** Same as panels (**A-B**) for transgenics in which the intact *tph-1* gene was rescued in NSM, in ADF, or in both. Combined, genetic silencing and rescue assays implicate both neuronal types in mediating the observed behavior. **G-H** Same as panels (**A-B**) for Cre-mediated deletions of the *tph-1* genes (see [57]). In all bar plots, mean velocities were compared to wild-type using an ANOVA test and corrected post hoc for multiple comparisons using Tukey's HSD test. Single and double asterisks denote a significant difference from wild-type (p<0.05 and p<0.01). Three independent transgenic lines were assayed in the cases of *NSM::TeTx*, *ADF::TeTx*, *NSM::tph-1*, and *ADF::tph-1*. One of each of the TeTx lines (*Ptph-1::TeTx*, *NSM::TeTx*, and *ADF::TeTx*) was crossed to a *mod-5(n3314)* mutant background and similarly assayed. One line was assayed for each floxed *tph-1* deletion strain [57].

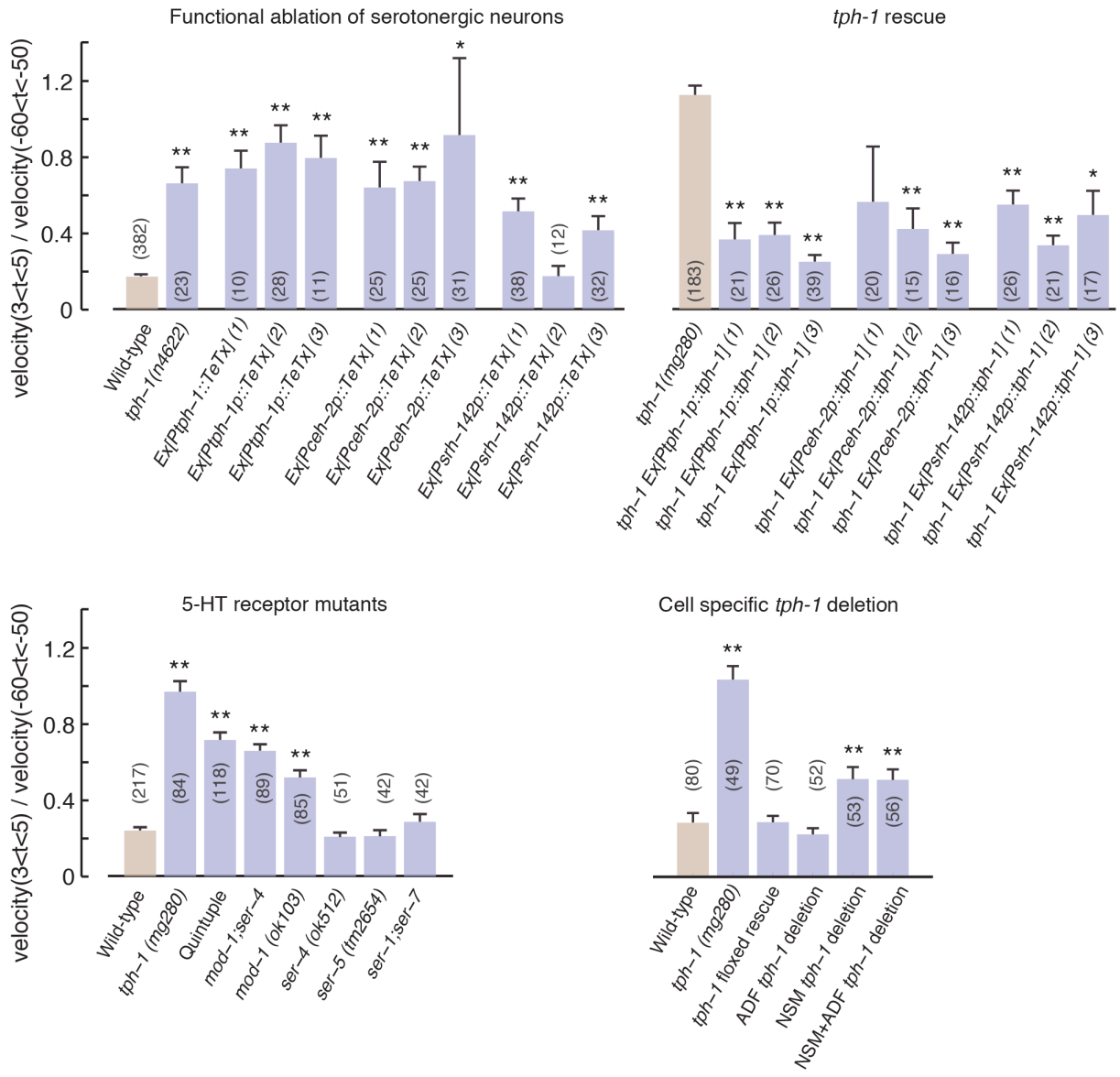

Figure 2.10: **Relative velocities of key mutants and transgenics assayed in this work.** Relative velocities were calculated as the ratio of the mean velocities at t = 3..5 sec and t = -60..-50 sec, where the encounter was defined as t = 0. Comparisons were performed using an ANOVA test corrected post hoc for multiple comparisons using Tukey's HSD test. Single and double asterisks denote significant differences ($p<0.05$ and $p<0.01$).

these weaker phenotypes. Taken together, these results indicate that NSM and ADF act through 5-HT signaling to mediate slowdown prior to and during encounters.

2.3.7 Optogenetic activation of serotonergic neurons induces a rapid slowdown off food.

Optogenetic activation of serotonergic neurons was previously shown to affect locomotion on food [57] and off food [77]. To assess the sufficiency of 5-HT signaling in mediating abrupt slowdown, we optogenetically activated the serotonergic neurons of freely moving starved animals using the light-activated cation channel Channelrhodopsin (ChR2). Innate responses of *C. elegans* to blue light were avoided by performing the assays on a light-insensitive (*lite-1*) mutant background [50, 201].

Upon exposure to a pulse of blue light, the locomotor activity of *lite-1; Ex[Ptph-1::Chr2]* animals declined by 35% as measured by the frame difference method [132], and remained low for the duration of the pulse (Fig. 2.12). The timescales of the decline were 3.6 $\pm$ 0.5 and 5.2 $\pm$ 0.9 sec in the two lines that were assayed. After the blue light was turned off, locomotor activity returned to baseline levels on timescales of τ = 5.4 $\pm$ 0.6 sec and τ = 10.1 $\pm$ 0.6 sec, respectively (Fig. 2.12, inset). Animals not expressing ChR2 assayed in the presence of the co-factor all trans retinal (ATR) did not detectibly respond to blue light. Importantly, activating the serotonergic neurons on a *tph-1* mutant background (*tph-1; lite-1; Ex[Ptph-1::ChR2]*) did not evoke a detectable slowdown response (Fig. 2.12). This indicated that 5-HT signaling was required for the observed responses.

To further investigate the role of 5-HT, we assayed *mod-5* mutants. Exposure to blue light reduced the locomotor activity of *mod-5; lite-1; Ex[Ptph-1::ChR2]* animals by 70%. Locomotion of *mod-5* mutants declined throughout the 30 sec light stimulus (τ = 5.1 $\pm$ 1.1 sec) and returned to baseline post stimulation slower than wild-type (τ = 37.3 $\pm$ 2.1 sec, p $<$ 0.01, see Fig. 2.12). This suggested that the uptake of endogenous 5-HT also contributed to shaping the modulation of locomotion on short timescales. Combined with our earlier

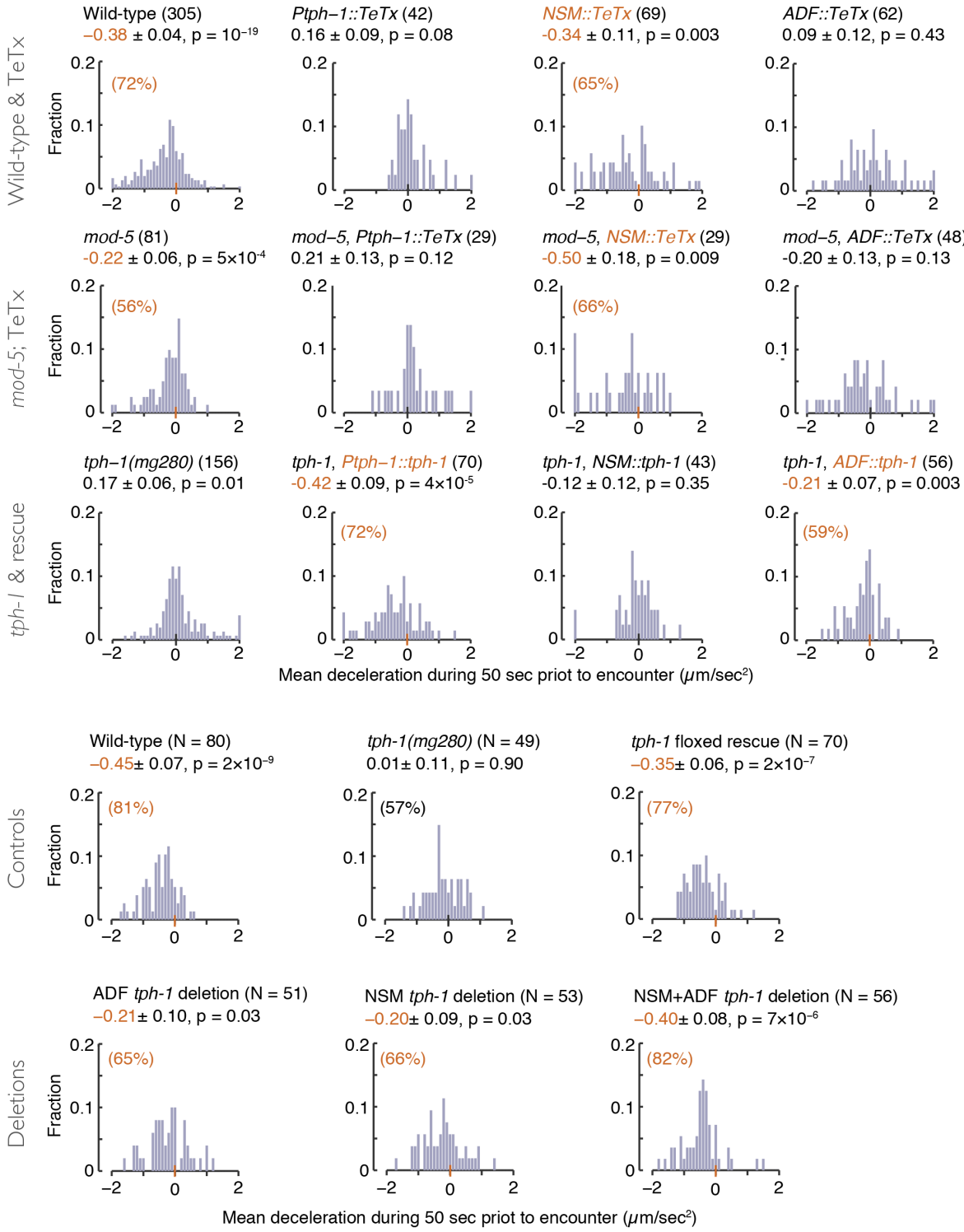

Figure 2.11: **Histograms of preemptive slopes measured in individual animals during the 50 sec prior to encountering a large patch of food.** Negative slopes are emphasized in red. Errors denote ± s.e.m and p values denote the probability that the measured distribution of slopes was obtained from a distribution with zero mean, as determined by a t-test.

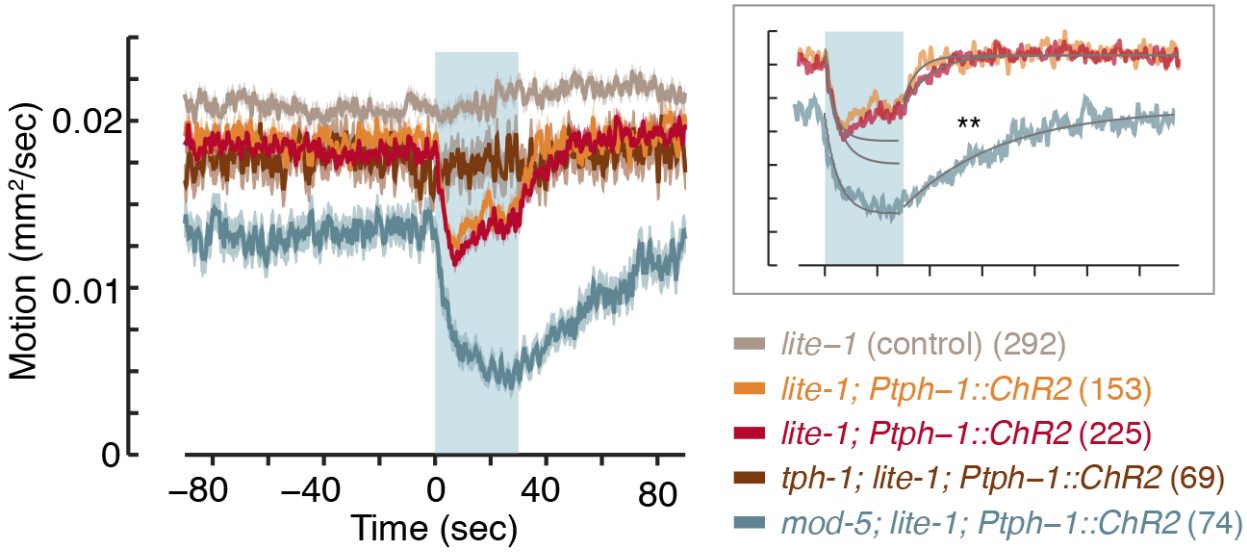

Figure 2.12: **Optogenetic activation of serotonergic neurons induces a rapid slow-down off food.** The temporal dynamics of motion were assayed using the frame difference method (i.e., the number of pixels that changed their value between consecutive frames of a movie of single animal; see Methods). Three independent lines (two *lite-1* backgrounds and one *lite-1; mod-5* background) expressing ChR2 in both NSM and ADF serotonergic neurons (*Ptph-1::ChR2*) were assayed. Control animals (*lite-1*) lacked ChR2 or TPH-1. The shaded area depicts the period in which the blue light was on. Inset: single exponential fits to each dataset (see Methods). Plots depict mea n± s.e.m, the number of stimuli assayed is noted in parentheses for each condition, the recovery timescale of *lite-1; mod-5* double mutants was compared to that of *lite-1* mutants using an ANOVA test corrected post hoc for multiple comparisons using Tukey's HSD test, and double asterisks denote significant differences ($p<0.01$).

results, these observations associate the dynamics of 5-HT signaling and of slowdown.

2.3.8 Efficient exploitation on a patchy landscape is mediated through the synergistic action of the 5-HT gated channel MOD-1 and the 5-HT metabotropic receptor SER-4.

Five serotonin-binding receptors have been identified in *C. elegans* [34, 79]. Of these, the G_o-protein coupled receptor SER-4 (an ortholog of mammalian 5-HT1 receptors) and the serotonin-gated chloride channel MOD-1 have been implicated in slowing locomotion in response to exogenous 5-HT [77]. However, endogenous 5-HT acted appreciably only through MOD-1 to increase steady-state dwelling at the expense of exploration on bacterial food [57].

To test which receptors may mediate rapid decision-making upon newly encountering food we assayed 5-HT receptor mutants. In all cases, encounters were compared to same day wild-type and *tph-1* controls. On standard large lawns, quintuple mutants carrying null mutations of all five 5-HT receptors [79] were deficient in abrupt slowdown despite a slight but detectable initial response (Fig. 2.13A). As discussed above, the residual responsiveness of the quintuple mutants was insufficient for efficient exploitation of a complex environment (see Fig. 2.5). The encounter dynamics of *mod-1; ser-4* double mutants were identical to those of the quintuple mutants (Fig. 2.13A), while *ser-5* mutants and *ser-1; ser-7* double mutants exhibited wild-type like abrupt slowdowns (Fig. 2.13B). In this assay, *mod-1* mutants exhibited a defect that was similar but not identical to that of *mod-1; ser-4*, and *ser-4* mutants resembled wild-type (Figs. 2.13 and 2.14).

To test the efficiency of foraging of these mutants in a complex environment we assayed them for 1.5-2.5 hours on a 5 by 5 patch arena. In this assay, the quintuple receptor mutants and *ser-4; mod-1* double mutants exhibited severe defects in the number of exploited patches (as compared to the number of patches encountered) and in the total time spent on exploitation during the assay. The phenotypes of these two strains were identical and re-

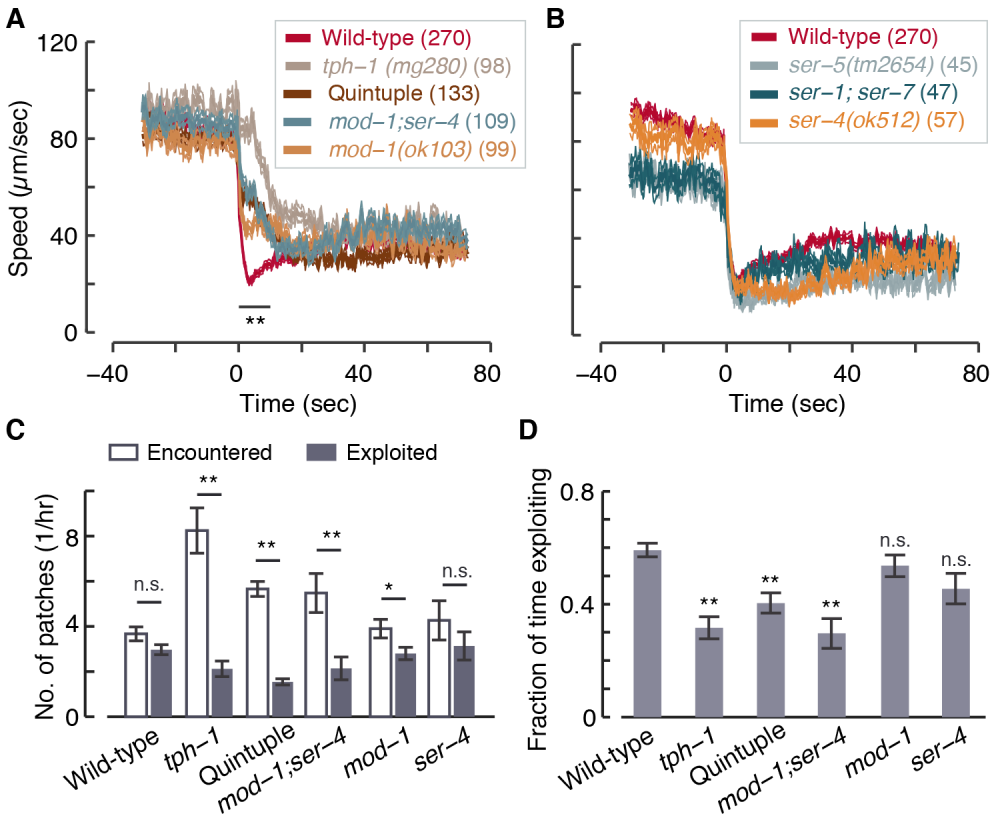

Figure 2.13: **The MOD-1 5-HT gated chloride channel is the primary mediator of abrupt slowdown upon encountering food. A** The mean speeds of 5-HT receptor mutants deficient in 5-HT signaling encountering the edge of a bacterial lawn. Wild-type and *tph-1* same day controls are shown for comparison. **B** Same as panel (**A**) for 5-HT receptor mutants that did not negatively affect the abrupt slowdown upon encounter. **C** The number of patches encountered and exploited during 2.5 hours of foraging on a 5x5 hexagonal lattice of food patches. Mutants lacking all five serotonin receptors (quintuple) and *mod-1; ser-4* double mutants exhibited a strong defect that resembled *tph-1* mutants. Single receptor mutants exhibited a mild (*mod-1*) or no (*ser-4*) defect. **D** The overall fraction of time spent exploiting food resources in the experiments described in panel (**C**). Likewise, this criterion suggests that *tph-1*, the quintuple mutant, and *mod-1; ser-4* mutants are similarly deficient while *mod-1* and *ser-4* mutants are similar to wild-type. Thick and thin lines or bars and error bars depict mean ± s.e.m, respectively. In panels (**A-B**), the number of animals assayed is noted in parentheses for each strain, mean velocities at t = 3..5 sec were compared to wild-type using an ANOVA test corrected post hoc for multiple comparisons using Tukey's HSD test, and double asterisks denote a significant difference ($p<0.01$). Pairwise comparisons in panel (**C**) were performed using t-tests and the means in panel (**D**) were compared to wild-type using an ANOVA test corrected post hoc for multiple comparisons using Tukey's HSD test. Single and double asterisks denote significant differences ($p<0.05$ and $p<0.01$). N(wild-type)=19, N(*tph-1*)=9, N(quintuple)=7, N(*mod-1; ser-4*)=8, N(*mod-1*)=8, and N(*ser-4*)=8.

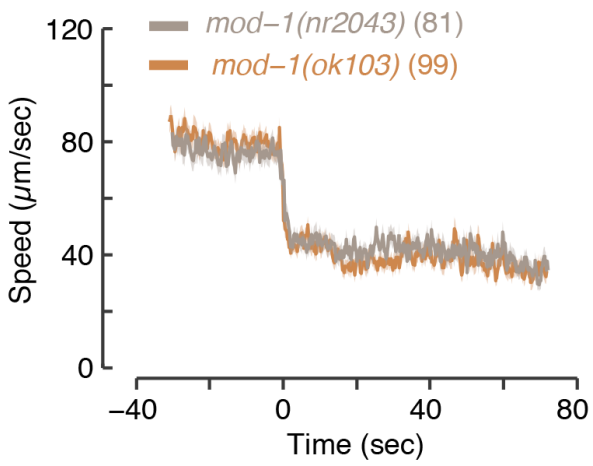

Figure 2.14: **The mean speeds of animals carrying two independent *mod-1* alleles, assayed for encountering the edge of a bacterial lawn.** The two mutants exhibited identical locomotion dynamics around the time of the encounter. The number of animals assayed is noted in parentheses for each strain.

sembled that of *tph-1* mutants (Fig. 2.13C-D). In contrast, *mod-1* and *ser-4* single mutants exhibited a milder defect and no significant defect, respectively. Combined, these results implicate MOD-1 and SER-4 in acting synergistically to mediate rapid decision-making.

2.4 Discussion

Foraging and exploitation in patchy environments is a well-studied neuroethological paradigm for the enhancement of fitness afforded by decision-making circuits. Similarities in the challenges facing different species yield repeated algorithmic aspects of their solutions and conserved underlying mechanisms. As a result, decision-making is associated with fundamental functions of nervous systems [1, 144, 207]. Recently, the activity of dorsal raphe neurons was recorded in behaving mice that predicted and responded to rewards and punishment. The results indicated that serotonergic neurons signal about reward and punishment on short (hundreds of milliseconds) and long (minutes) timescales [36].

We have shown that in *C. elegans* 5-HT signaling accelerates the attenuation of locomotion upon encountering newly discovered food. We address the importance of this accelera-

tion by showing that deficiencies in serotonergic signaling reduced the efficiency of foraging in a patchy environment. Previously, NSM was the major neuron implicated in affecting locomotion on food. It was shown to release serotonin extrasynaptically to diffuse in the vicinity of the nerve ring and activate a distributed circuit of target cells (as opposed to post synaptic partners) [57]. Here, the serotonergic neuron types NSM and ADF were found to play complementary roles, where one neuron could partially compensate for a deficiency in another. The combined action of the 5-HT activated chloride channel MOD-1 and the 5-HT receptor SER-4 was required for the accelerated response to discovering food.

Serotonergic modulation of locomotion has been examined under various sets of conditions [6, 46, 57, 77, 78, 81, 82, 88, 98, 150, 164, 168]. In contrast, fitness consequences of these effects on locomotion have not been studied in detail [173, 207]. Exogenous 5-HT robustly attenuates locomotion [88, 168] and stimulation of endogenous 5-HT release can cause slowdown [57, 77]. In addition, serotonergic signaling accelerates food-dependent aversive responses [78, 81, 82].

Prior to the isolation of *tph-1* mutants, Sawin et al. assayed locomotion by manually scoring body bends five minutes after placing animals on a bacterial lawn. Under these conditions, they showed that the slowdown of locomotion on food is enhanced in starved nematodes as compared to well-fed controls [164]. Enhanced slowdown was more severe on a *mod-5* mutant background and required the action of the MOD-1 receptor [46, 77, 150]. The same assay was used to show that SER-4 contributed to post-starvation slowing on food [77] and to assay *tph-1* mutants [77, 141]. Both studies found that the slowdown of *tph-1* mutants was only mildly reduced as compared to wild-type and Gurel et al. did not report on the basal slowing of well-fed animals in their hands. These assays resulted in highly active well-fed animals on food (compare basal slowing in [140, 141, 164] to steady state locomotion on food in [57, 58]) suggesting that the transfer to the assay lawn may have been a factor in determining behavioral outcomes (as noted in [141]).

Unless specified otherwise, animals in the current study were deprived of food prior

to the assay. However, in our hands starvation did not appreciably alter the preemptive slowdown, the abrupt slowdown upon encounter, nor the velocity 15 minutes post encounter (Fig. 2.2). Moreover, 5-HT signaling deficiencies affected the approach to the edge of a lawn and the abruptness of responding to the encounter, but not center of mass motion 10-20 minutes thereafter. Figs. 2.2 and 2.4 demonstrate that the five-minute interval used in [46, 77, 141, 150, 151] is intermediate between the abrupt response to the encounter and the relaxation time to steady state locomotion on food. Since the transient adaptation of locomotion upon encounter is not completed within 5 minutes, we suggest a different interpretation of the existing collective body of data: upon encountering food, rather than determining the target locomotion activity on food, serotonergic signaling accelerates the response to the sudden change in the external environment. The resulting abrupt response contributes to the efficiency of foraging in complex landscapes.

Flavell et al. assayed well-fed animals for 90 minutes on food, where wild-type animals predominantly dwell (as opposed to predominantly roaming off food). They found that the serotonergic NSM neurons are active during dwelling periods and inhibit roaming through 5-HT secretion. Moreover, they found that *tph-1* mutants roamed 3-5 fold more than wild type on a bacterial lawn. Thus, serotonergic signaling can affect steady-state transitions between dwelling and roaming [57]. We did not observe large differences between the center of mass velocities of wild-type animals and *tph-1* mutants 5-20 minutes post encounter (Fig. 2.4). However, since the focus of this work was on the encounter with food, the duration of our assays was limited as compared to the 90-minute recordings with no prior starvation described in [57].

The NSM neuron is physically separated from the locomotor circuit by the basal membrane [205]. Based on its location and structure, NSM was hypothesized to play a role in reporting the availability of resources [8]. Nevertheless, it was implicated in modulating locomotion in [57, 77] and in the current study. Moreover, our data reveals prominent activation of NSM upon encountering bacteria. This raises the question of whether food signals onto

NSM to drive locomotion through sensory neurons or whether NSM may directly monitor the state of the pharynx. Indirect activation of NSM was demonstrated in [111]. However, a detailed anatomical dissection of NSM identified a putative sensory process that may monitor pharyngeal activity [8]. We observed NSM activation in *osm-6* mutants, where cilium structure (and hence chemosensory function) is severely disrupted (Fig. 2.7C). Although our data cannot support a definitive answer, it is consistent with the notion that NSM monitors the state of the pharynx.

Significant physiological activity in ADF was detectable prior to the encounter with the food while NSM responded detectably upon encounter. Thus, ADF may act to refine the dynamics of the slowdown response. This can conceivably occur in several, not mutually exclusive, manners: (i) early release of 5-HT may prime the downstream neural circuit such that an abrupt slowdown can take place before NSM is fully activated; (ii) the mild ADF-dependent early slowdown may positively affect detection (e.g., by affecting the angle of attack or providing more time for sampling the environment in the vicinity of food); (iii) responses to potentially competing stimuli may be suppressed in the vicinity of a patch of food. In addition, 5-HT released by ADF may contribute to the robustness of the response if it can be scavenged and used by *mod-5* expressing neurons (NSM and/or others [98]).

Rather than identifying distinctive roles of individual serotonergic neuronal types, our combined physiological and behavioral data suggest partial functional redundancy. The phenotypes of wild-type animals, *tph-1* mutants, and *Ptph-1::TeTx* transgenics were consistent across conditions. Disrupting the function of ADF or NSM resulted in partial defects as compared to *tph-1* mutants. These findings suggest that different neurons capable of synthesis and/or uptake of 5-HT may act redundantly to modulate locomotion upon encountering food. Jafari et al., using the assays described in [164], reported that synaptic release of 5-HT from uptake neurons (that do not synthesize 5-HT themselves) was not required for locomotor responses to food deprivation. Rather, these neurons prevent exaggerated responses by scavenging extrasynaptic 5-HT [98]. A detailed analysis of neurons that promote

exploitation in complex environments would require the dissection of 5-HT uptake, storage, and synaptic release in subsets of serotonergic and 5-HT uptake cells.

The SER-4 receptor and the MOD-1 chloride channel were shown to affect locomotion through GOA-1 activation in target cells or hyperpolarizing them, respectively [57, 77, 114, 139]. Head sensory- and inter-neurons were implicated as sites of action of GOA-1 and MOD-1 for inhibiting locomotion [57, 77]. It was further proposed that additional identified effectors act to facilitate the MOD-1 or SER-4 signaling pathways [77] or to oppose them [57]. While our data implicate SER-4 and MOD-1 in the abrupt response, the phenotypes of the *mod-1; ser-4* double and the quintuple receptor mutants fall short of recapitulating in full the deficits of *tph-1* mutants and *Ptph-1::TeTx* transgenics. Thus, our data suggests that an effect of a serotonin non-canonical receptor, metabolite, or precursor is yet to be accounted for.

When *C. elegans* navigates on shallow chemical or thermal gradients, typical responses to external cues include gradual changes in the curvature of their trajectories [92, 115] or modulation of the rate of infrequent sharp turns [74, 146, 161]. As a result, sensory stimuli can be integrated over timescales of tens of seconds, allowing the animal to filter out perceived abrupt (noisy) stimuli. In contrast, in a patchy environment an abrupt change in the availability of food is information of the utmost importance [35]. Correspondingly, behavioral responses must be rapid - analogous to a filter with a high cut-off frequency. The typical scales of the problem are expected to determine the required abruptness.

Typical roaming velocities off food are in the 100-200 μm/sec range. In our hands, patches as small as 400-500 μm in diameter merited exploitation. An order of magnitude estimate yields a timescale of slowdown of 2-3 sec, in agreement with our experimental observations and with the 2 Hz frequency of exploratory head motion [3]. Additional factors, such as concentration and quality, can affect the detailed responses to discovering food. However, abruptness remains advantageous under a range of conditions. Taken together, the robust activation of serotonergic neurons, the contribution of 5-HT re-uptake to proper locomotion

dynamics, and the importance of this pathway to efficient foraging suggest that responding to newly discovered food is a key role of serotonergic signaling in *C. elegans*.

2.5 Conclusions

This study suggests that a key role of serotonergic signaling in *C. elegans* is to accelerate decision-making and promote efficient exploitation of resources in complex environments. It primarily implicates the serotonergic neuron type NSM, the serotonin-gated chloride channel MOD-1, and the ortholog of mammalian 5-HT1 metabotropic serotonin receptors SER-4 in mediating this process. In addition, it demonstrates how different cells can use a common modulator to affect locomotion in complementary manners.

2.6 Methods

2.6.1 Strains

C. elegans strains were maintained and grown according to standard protocols [21]. The following strains were used: wild type strain N2, MT15434 *tph-1(mg280)*, FQ77 *tph-1(n4622)*, MT7988 *bas-1(ad446)*, CB1112 *cat-2(e1112)*, MT9668 *mod-1 (ok103)*, MT9667 *mod-1(nr2043)*, AQ866 *ser-4(ok512)*, RB2277 *ser-5(ok3087)*, RWK213 *ser-5(tm2654)*, OT179 *ser-4(ok512); mod-1(ok103)*, DA2109 *ser-7(tm1325); ser-1(ok345)*, RWK3 *mod-1; ser-1; ser-4; ser-5; ser-7* quintuple mutant, MT1082 *egl-1(n487)*, MT2060 *egl-1(n987)*, MT2251 *egl-1(n1084)*, INV80003 *mod-5(n3314)*, INV90001 *mod-1 (ok103); ser-4(ok512)*, INV33006/INV33009/INV33010 *Ex[ptph-1::TeTx-mCherry punc122::GFP]*, INV30003/INV30004/INV30008 *Ex[pceh-2::TeTx-mCherry punc122::GFP]*, INV30001/INV30002/INV30010 *Ex[psrh-142::TeTx-mCherry punc122::GFP]*, INV63006 *mod-5(n3314); Ex[ptph-1::TeTx-mCherry punc122::GFP]*, INV60008 *mod-5(n3314); Ex[pceh-2::TeTx-mCherry punc122::GFP]*, INV60001/INV60009/INV60010 *mod-5(n3314); Ex[psrh-142::TeTx-mCherry punc122::GFP]*, INV70001/INV70002 *tph-*

1(mg280); Ex[ptph-1::tph-1::SL2::mCherry punc122::GFP], INV70004 *tph-1(mg280); Ex[ptph-1::tph-1::SL2::GFP punc122::RFP]*, INV70005/INV70006/INV70007 *tph-1(mg280); Ex[pceh-2::tph-1::SL2::GFP punc122::RFP]*, INV70008/INV70009,INV70010 *tph-1(mg280); Ex[psrh-142::tph-1::SL2::GFP punc122::RFP]*; INV50001 *lite-1(ce314); Ex[Ptph-1::mcherry::SL2::GCaMP3 punc122::RFP]*, INV50002 *lite-1(ce314); Ex[Psrh-142::mcherry::SL2::GCaMP3 punc122::RFP]*, AZ200 *osm-6(p811); lite-1(ce314); Ex[ceh-2::mcherry::SL2::GCaMP3 punc122::RFP]*, AZ201 *osm-6(p811); lite-1(ce314); Ex[Psrh-142::mcherry::SL2::GCaMP3 punc122::RFP]*, INV60005/INV60006 *lite-1 (ce314); Ex[ptph-1:::Chr2-mCherry punc-122::GFP]*, INV60012 *mod-5(n3314); lite-1 (ce314); Ex[ptph-1::Chr2-mCherry punc-122::GFP]*, CX13228 *tph1(mg280); kySi56*[floxed tph1 genomic rescue], CX13572 *tph1(mg280); kySi56 IV; kyEx4057[ceh2::nCre]*, CX13571 *tph1(mg280); kySi56 IV; kyEx4077[srh-142::nCre]*, CX13576 *tph1(mg280); kySi56 IV; kyEx4107[egl6::nCre]*, CX15658 *tph1(mg280); kySi56 IV; kyEx5262[ceh-2::nCre, egl6::nCre]*, ERL78 *tph1(mg280); kySi56 IV; opyEx18[ceh2::nCre, srh142::nCre, myo-3::mCherry].* The RWK213, OT179, DA2109, and RWK3 strains were a gift from Richard Komuniecki's laboratory (University of Toledo). The CX13228, CX13572, CX13571, CX13576, and CX15658 strains were a gift from Cornelia Bargmann's laboratory (Rockefeller University).

2.6.2 Behavioral assays: large bacterial lawn

To assay re-feeding on a large bacterial lawn, 72-96 hour old adults were washed twice in a drop of M9 buffer and transferred to unseeded NGM plates for 1-2 hours. Animals were assayed on 35 mm or 60 mm NGM plates seeded with a 25 μl drop of 3X concentrated overnight culture of OP50 bacteria. The bacteria were spread in an oval shape of area 100-150 mm^2 on one side of the plate and assay plates were kept at 4 °C prior to the assay. In each assay, 8-10 animals were transferred to M9 droplets on the empty side of the assay plate and started to crawl once the droplets were absorbed. Unless stated otherwise, animals that reached the bacterial lawn in less than 150 sec (<20% of the total number of

animals) were not scored in order to minimize the effect of the transfer on the data. Images were captured using a cooled CCD camera (Photometrics Cool- SNAP HQ2, Tucson, AZ), an Olympus SZX16 stereo- microscope equipped with an SDF PLAPO 1XPF objective (Olympus America Inc., Center Valley, PA), and the Micro-manager open source software. Imaging was performed at 5 frames per sec, using a magnification of 0.7X and 4x4 binning. Under these conditions, the area of a single animal was 40-45 pixels. The centers of mass of the animal bodies were tracked using custom Matlab scripts. Center of mass velocities were computed using a temporal resolution of 1 sec. Each genotype was assayed at least on 3 different days and control animals were recorded each day. In our hands, day to day variability was typically small. To assess whether the preemptive slowdown was statistically significant, a linear function was fitted to the speeds of individual animals during the 50 sec prior to encountering food using the Matlab curve fitting toolbox. Post-encounter decay constants (τ) were based on a single exponential fit of the 0-150 sec data. The goodness of fit (R^2) was higher than 0.9 in all cases. Experiments were performed on at least three independent days and day-to-day inconsistencies were not identified.

2.6.3 Behavioral assays: micro-patches

For Fig. 2.6A, the 1X concentration was defined as $OD_{600} = 1.5$. Patches were arranged in concentric rings, 20 animals were placed on the assay plate, and only first encounters with a single patch were scored. Four ordinal categories were scored by visual inspection: (i) a full stop at the edge of the patch; (ii) a noticeable slowdown of locomotion at the edge without a full stop; (iii) a delayed slowdown of locomotion; (iv) the absence of a noticeable response. The former two response types resulted in feeding on the patch of food and the latter two did not. For long-term assays in a complex environment, patches contained OP50 bacteria at a concentration of $OD_{600} = 2.5$. Assay plates were freshly seeded prior to the experiment. Individual food patches were seeded by gently touching preloaded thin gel loading tips to a standard agar plate, typically resulting in a patch diameter of 0.8-1 mm.

Unless stated otherwise, the bacteria mix was supplemented with 10X kanamycin to prevent growth. Prolonged experiments (5-10 hours, Fig. 2.5) were performed on a 7x7 square lattice. Shorter experiments (2.5 hours, Fig. 2.13) were performed on a 5x5 hexagonal lattice. In both cases the distance between nearest neighbors was 2 mm. Food deprivation was performed as described above.

A single animal per plate was imaged at 5 frames per second using a 5MP scientific CCD camera (Prosilica GC2450, Allied Vision Technologies, Stadtroda, Germany) at magnifications of 0.33-0.65X. A 3D printed square frame (18 mm inner and 24 mm outer diameter) lined with copper tape was used to contain the animal in the field of view. Custom LabView (National Instruments Inc., Austin TX) and Matlab (Mathworks Inc., Natick, MA) scripts were used for image acquisition and data analysis.

Images were analyzed using the posture-based method as described previously [133]. Patch outlines were traced manually for each experiment, and frames where the nose-tip of the worm was within 5% of the body-length from a patch were labeled "encounter". If, during an encounter, the mean velocity of the animal was at the lowest 15th percentile of measured roaming velocities then the frames of the encounter were labeled "exploitation". Brief (exploratory or accidental) excursions out of the patch, in which the distance between the edge and the nose-tip was no greater than 20% of the body-length, were consolidated. Thus, motion on the order of 100 μm beyond the patch edge did not fractionate a continuous event. Patch coverage was quantified by determining the area occupied during each exploitation event. Experiments were performed on at least three independent days and day-to-day inconsistencies were not identified.

2.6.4 Calcium imaging

Calcium imaging was performed on freely behaving animals on large bacterial lawn, 60 mm diameter, assay plates. Here, 50 μl overnight bacterial culture was seeded in a ring and incubated overnight at 37 °C. The transgenic strains assayed expressed the calcium

indicator GCaMP3 in the target neuron on a *lite-1* mutant background [50, 201] (see strain list). Food deprivation was performed as described above, several animals were initially placed at the center of the ring, and a single animal approaching the inner diameter of the ring was continuously imaged. To image NSM during evoked pauses (Fig. 2.7, left inset), a standard platinum pick was manually placed near the anterior of a forward moving animal such that it gently touched it due to its own motion.

The analysis of neuronal calcium transients was performed similarly to the previously described procedure in [163]. Data shown in Figs. 2.7A and 2.8 was acquired using the setup described above for large bacterial lawn assays. Imaging was performed at 5 frames per second at a magnification of 10X for up to 25 minutes. In our hands, bacterial lawns had clearly visible sharp edges. First-day adults were transferred to assay plate and allowed several minutes to equilibrate. Animals were tracked manually until they were approximately 15 body lengths from the edge of the food patch, at which point the assay plate remained in place. For reverse patch imaging (Fig. 2.8A), assay plates were prepared with 2 ml agar; the resulting thickness was 2-3 mm. Prior to the assay, the agar was carefully flipped such that the animals crawled on the agar surface opposite to the lawn. The minimal possible distance of the animal from the bacteria was thus 2-3 mm.

Data shown in Fig. 2.7B-C, imaging was acquired at a frame rate of 11 frames per second. Images were captured using a cooled EMCCD camera (Evolve 512, Photometrics, Tucson AZ), an Olympus 83X inverted microscope equipped with a UPLSAPO 10X objective (Olympus America Inc., Center Valley, PA), and the Micro-Manager open source microscopy software. Animals were tracked automatically using a custom worm tracker (coded in Matlab).

Image analysis was performed using custom MATLAB scripts (Mathworks, Inc. Natick, MA) which identified the fluorescent neuron (the only bright particle in the head), measured the background fluorescence in its vicinity, and calculated the background subtracted mean fluorescence intensity of the identified particle. Velocities in Fig. 2.7B were calculated based

on the displacement of the imaged cell. Experiments were performed on three independent days and day-to-day inconsistencies were not identified.

2.6.5 Optogenetics

Optogenetic assays were performed in 1.1x1.1 mm microfluidic chambers in which the animals could move freely. Blue light illumination ($\lambda = 475\pm15$ nm) was supplied by a Luxeon Star 7-LED assembly with a diffused optic array driven by a 700 mA FlexBlock driver. The LED assembly was mounted to the scopes approximately 7 cm from the sample location. Light intensity at the location of the animals was set to 0.8 mW/mm^2. Transgenic animals expressing the light-gated ion channel channelrhodopsin (ChR2) in all serotonergic neurons on a *lite-1* mutant background (see strain list) were illuminated for 30 sec in the presence of 1 mM ATR. Control animals were assayed in the absence of ChR2 and presence of ATR (Fig. 2.12). The level of activity of the animals was assayed using the frame subtraction method as previously described [132]. In order to obtain the timescales of slowdown and recovery, as described in the text, a single exponential function was fitted to each dataset using the Matlab curve fitting toolbox. The goodness of fit (R^2) was higher than 0.9 in all cases except for the recovery of the faster recovering *lite-1; Ex[Ptph-1::ChR2]* line (shown in orange), where $R^2 = 0.73$. Experiments were performed on three independent days and day-to-day inconsistencies were not identified.

2.6.6 Statistical analysis

Data analysis was performed using custom Matlab (Mathworks Inc., Natick, MA) scripts. Individual statistical tests are detailed in the corresponding figure legends.

CHAPTER 3

TRANSFORMING GROWTH FACTOR BETA CONTRIBUTES TO FORAGING BEHAVIOR

Adam Brown[1] and David Biron[2,3]

AB contributed to the conception and design of the study, performed, analyzed, and interpreted behavioral and physiological assays, and contributed analysis tools. DB contributed to the conception and design of the study and helped analyze and interpret the data.

3.1 Abstract

Effective foraging requires appropriate behavioral responses upon encounter with food. The nematode *C. elegans* was shown to stop abruptly upon reaching the edge of a bacterial lawn in a serotonin (5-HT) dependent manner. However, interactions between 5-HT signaling and other pathways in the context of foraging are poorly understood. We found that transforming growth factor beta (TGF-β) signaling in *C. elegans* contributes to slowing responses prior to and upon encounter with food. Genetic manipulations leading to deficient TGF-β signaling resulted in defective locomotion patterns as animals approached food and gradual responses upon encounter. Double mutants of the TGF-β ligand-encoding gene *daf-7* and the 5-HT synthesis gene *tph-1* exhibited exaggerated defects relative to single mutants, indicating that TGF-β and 5-HT function in parallel rather than in series. Physiological imaging revealed that the *daf-7*-expressing ASI chemosensory neurons exhibit suppressed activity in the proximity of food, suggesting that ASI contributes to behavioral priming in advance of food encounter. Experiments with inedible food-like substances implicate chemosensation

1. Committee on Computational Neuroscience, The University of Chicago, Chicago, IL 60637, USA.

2. The Institute of Biophysical Dynamics, The University of Chicago, Chicago, IL 60637, USA.

3. Department of Physics and the James Franck Institute, The University of Chicago, Chicago, IL 60637, USA.

rather than mechanosensation as the primary mediator of slowing responses and suggest that *daf-7* functions in chemosensation. Our results illustrate the contribution of developmental signaling pathways to acute responses to environmental changes.

3.2 Introduction

In natural environments resources are not uniformly distributed. Food, for example, is often found in locally dense concentrations termed patches [33, 181]. Foraging in a patchy environment is therefore a fundamental feature of animal behavior across a wide range of habitats and taxa [42, 107, 169]. However, the neural basis of foraging remains poorly understood [1, 83, 125].

Locomotion patterns underlie foraging strategies [158, 164, 202]. When food is absent, *C. elegans* exhibits fast, directional locomotion. In contrast, *C. elegans* exhibits slow locomotion and local dwelling behavior on a lawn of bacterial food [6, 57, 58, 140].

We recently characterized *C. elegans* behavioral responses to encounter with a patch of food after a period of deprivation [97]. We showed that serotonin (5-hydroxytryptamine; 5-HT) signaling mediates a dramatic locomotor slowdown upon encountering food, such that animals could abruptly pause at the edge of a bacterial lawn. When patches were sufficiently small, 5-HT-dependent abrupt stopping was essential for successful foraging; 5-HT-deficient animals often passed through patches, missing opportunities to feed. We also elucidated the relative contributions to abrupt stopping of serotonergic neuron types and 5-HT receptor types.

Interacting biochemical pathways regulate behavioral, physiological, and developmental responses to food [67, 80, 99, 187]. In nematodes such as *C. elegans*, these responses can be quite dramatic. Under harsh environmental conditions including high ambient temperature and high population density relative to food supply, young *C. elegans* larvae can undergo a developmental change termed dauer arrest [27]. Dauer larvae are morphologically and behaviorally distinct from larvae that develop in favorable environments; they do not feed

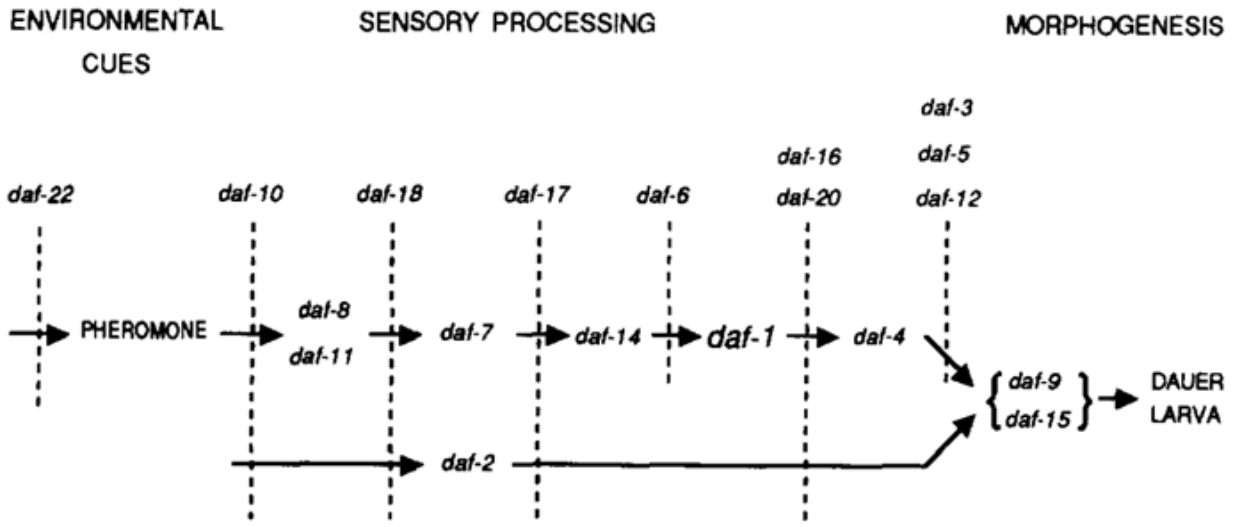

Figure 3.1: **A genetic pathway for dauer larva development.** Genes are ordered based on epistatic relationships between dauer-constitutive mutations (drawn in the pathway) and dauer-defective mutations (represented as blocking the pathway). Reproduced from [61].

and are shielded from the external world by a specialized cuticle [27, 157]. Dauer arrest is a diapause state in which animals can survive for months until conditions improve and normal development resumes [104]. With respect to underyling biochemical pathways, dauer arrest in free-living nematodes such as *C. elegans* shares homology with obligate infective developmental stages of parasitic nematodes and is thus a general feature of the complex lifestyles of animals of this phylum [137].

Genes involved in regulation of dauer arrest are classified as dauer-constitutive (Daf-c; mutants undergo irreversible dauer arrest under favorable conditions) or dauer-defective (Daf-d; mutants fail to undergo dauer arrest under adverse conditions) [62, 157]. Several well-characterized biochemical pathways regulate dauer arrest. Among these is the transforming growth factor beta (TGF-β) pathway, defined by the Daf-c genes *daf-1, 4, 7, 8,* and *14* and the Daf-d genes *daf-3* and *daf-5* [143] (see Fig. 3.1). TGF-β family ligands bind to and activate cell surface receptors, resulting in the activation of transcription factors involved in metabolic and developmental processes [172].

As the TGF-β signaling pathway regulates responses to food on relatively long timescales

(i.e., the availability of food during developmental processes on the order of tens of hours), we speculated that TGF-β-related genes might also affect acute responses to encounters with food. Furthermore, the gene that encodes the TGF-β ligand, *daf-7* was shown to interact with the serotonin synthesis gene *tph-1* such that expression levels of the two genes encode information about food availability [47, 51]. For example, compared to single mutants, *tph-1*; *daf-7* double mutants showed an exaggerated increase in the expression of *tph-1* in NSM neurons at higher food densities (see Fig. 5 of [51]).

Here we show that TGF-β pathway genes contribute to both gradual preemptive slowing as animals approach a food source and abrupt slowing upon encounter with food. Double mutants of both *daf-7* and *tph-1* exhibited exaggerated defects relative to single mutants, indicating that the two genes function in parallel. We partially characterized contributions of neurons that express *daf-7* including chemosensory ASI neurons which likely contribute to pre-encounter priming of respones. Finally, we showed that both mechanosensory and chemosensory transduction play a role in responses to food encounter, with *daf-7* primarily involved in chemosensation.

3.3 Results

3.3.1 Mutants of dauer-constitutive TGF-β pathway genes exhibit defective responses to food encounter.

We previously characterized behavioral and physiological responses of *C. elegans* during encounters with newly found food [97]. In brief, we described the abrupt slowdown of locomotion upon encounter and the underlying 5-HT signaling. However, we conjectured that other genes, not just those directly involved in 5-HT signaling, contribute to this behavior as well. To address this, we considered biochemical pathways known to regulate aspects of feeding and development in *C. elegans*. Among these is the TGF-β signaling pathway involved in food availability-dependent regulation of dauer formation (see Fig. 3.1).

As in our previous study [97], we used continuous video recordings to resolve the dynamics of locomotion upon encounter with food. We identified mutants of all Daf-c TGF-β pathway genes that exhibited gradual, rather than abrupt, responses to food encounter.

Two features of the wild-type response to food encounter were absent in several TGF-β pathway mutants. Firstly, whereas wild-type animals exhibited an abrupt slowdown upon encountering the edge of the bacterial lawn with a nearly complete halt reached within 3 sec, TGF-β pathway mutants *daf-1* (three alleles), *daf-7* (three alleles), *daf-8* (one allele), and *daf-14* (two alleles) slowed down gradually (Fig. 3.2. Even the least defective (with respect to response to encounter) among these strains, *daf-7(ok3125)*, crawled at more than double the speed of wild-type animals in the period immediately after reaching the edge of the lawn. Secondly, whereas wild-type animals exhibited a mild but significant deceleration during the 50 sec period preceding the encounter (mean deceleration = 0.48 ± 0.04 μm/sec^2, $p<0.01$), TGF-β pathway mutants exhibited steady velocities or significant accelerations during this period (Fig. 3.3. In all *daf-7* and *daf-14* mutants and in *daf-1(m213)* mutants, the magnitude of preemptive acceleration was greater than the magnitude of wild-type animals' deceleration during the same period.

Both the pre-encounter and post-encounter features of the defective phenotype exhibited by TGF-β pathway mutants were also present 5-HT deficient *tph-1* mutants (except that *tph-1(n4622)* mutants retained a very mild pre-encounter deceleration).

Phenotypes of key mutants and transgenics assayed in this study are summarized in Table 3.1.

We also assayed mutants of several TGF-β pathway genes, mutants of genes related to the expression profile of *daf-7* (see below), and mutants of other genes implicated in dauer formation that did not exhibit defective responses to food encounter (see Fig. 3.11 and Table 3.2 near end of this chapter).

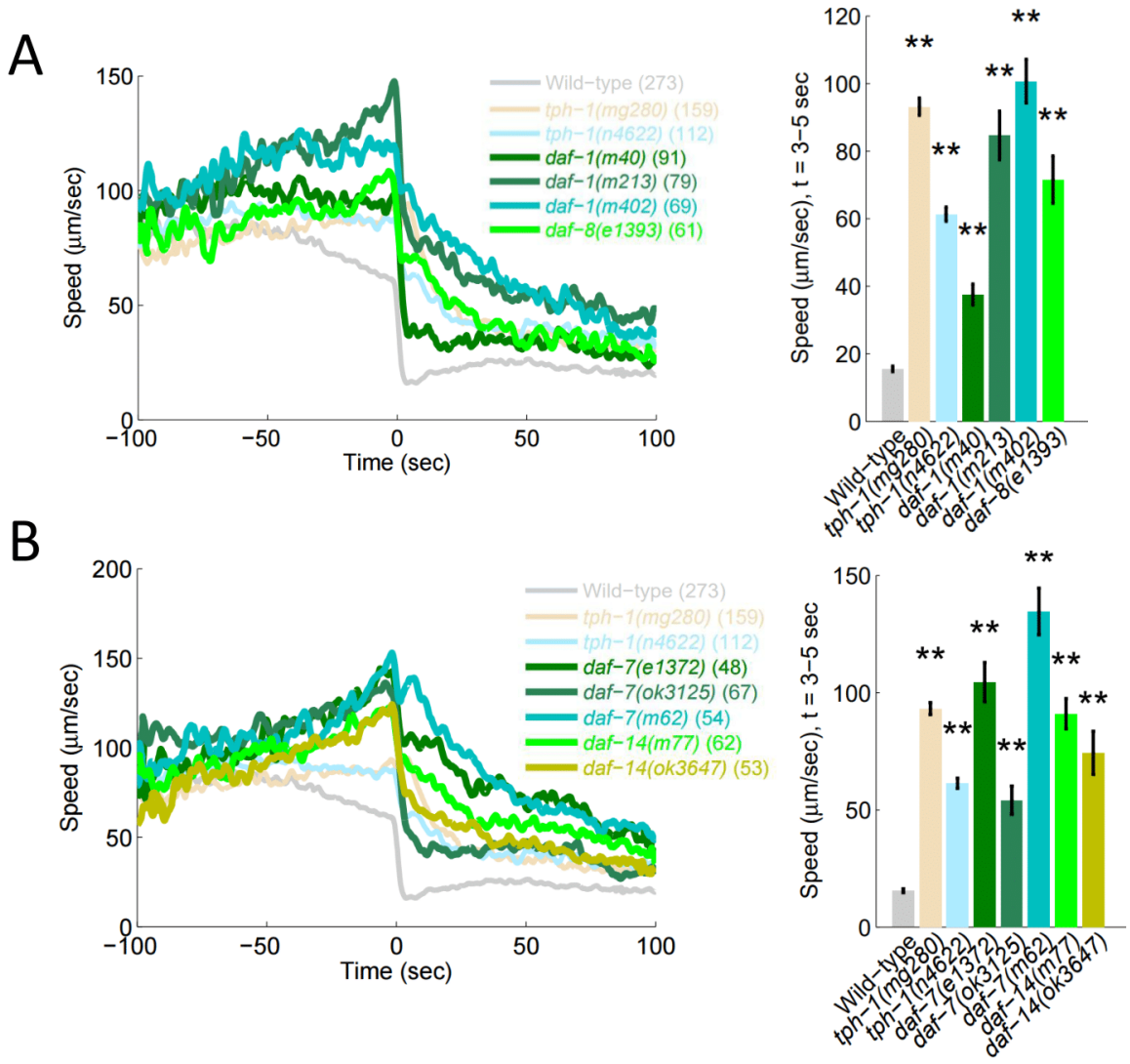

Figure 3.2: **Mutants of several TGF-β pathway genes exhibit defective responses to encounter with food.** Note: in this figure, the responses of TGF-β pathway mutants to food encounter are split into two panels for clarity. In each panel, the responses of wild-type animals and two *tph-1* mutants are also shown for comparison. **A** Left: the mean speeds of *daf-1* and *daf-8* mutants around the time of encounter with the edge of a large bacterial lawn (shown without standard errors as a guide to the eye; see summary statistics in adjacent plot). Right: The speeds of the strains shown to the left shortly after the encounter. **B** The same comparisons in panel (**A**) for *daf-7* and *daf-14* mutants. Bars and error bars (right side) depict mean ± s.e.m and the number of animals assayed for each strain is noted in parentheses (left side). Mean velocities were compared to wild-type using a t-test and corrected post hoc for multiple comparisons with a Bonferroni correction. Double asterisks denote a significant difference from wild-type ($p<0.01$).

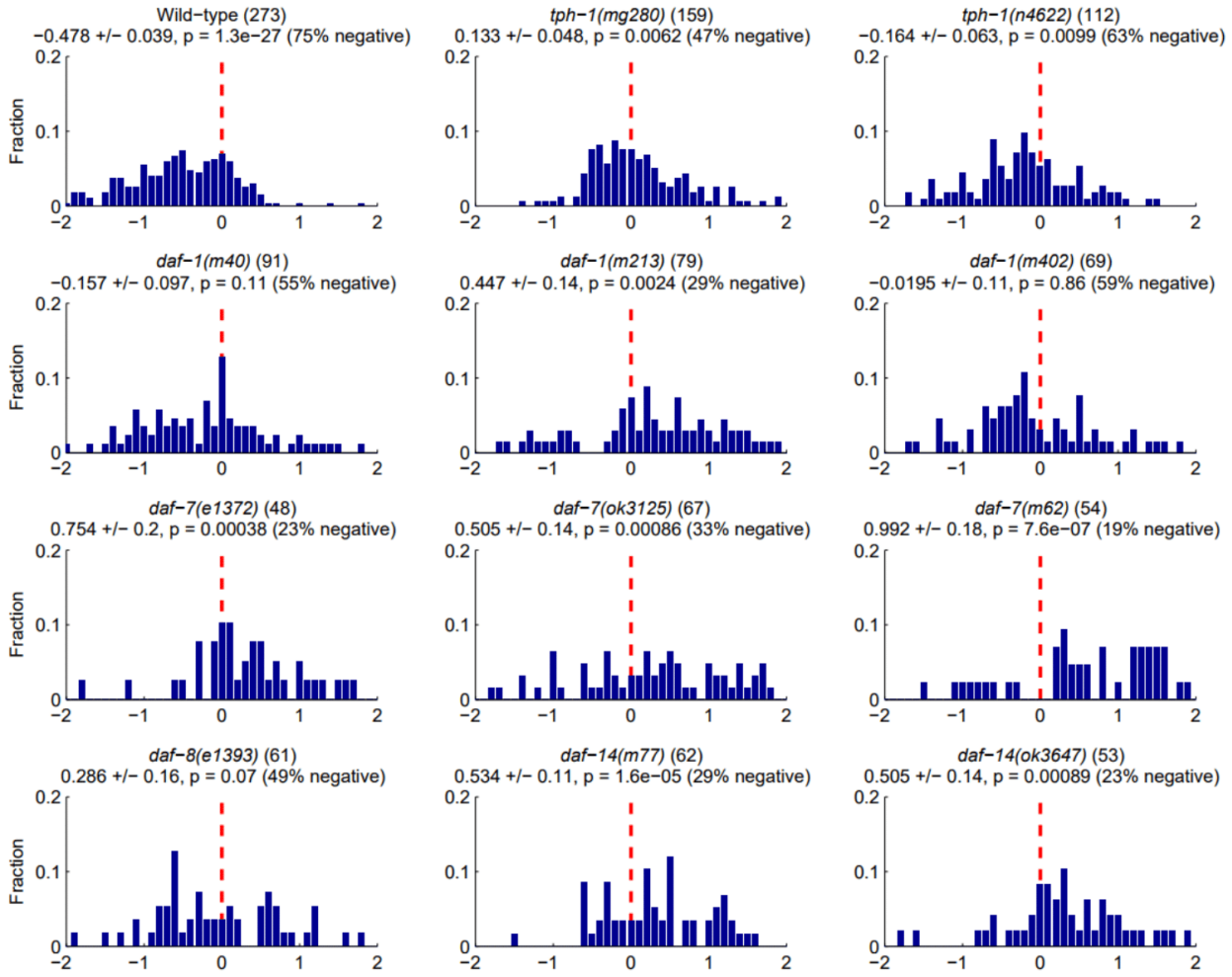

Figure 3.3: **Preemptive responses to encounters a large patch of bacterial food.** For wild-type animals, *tph-1* mutants, and several TGFβ pathway mutants, histograms of preemptive slopes measured in individual animals during the 50 sec prior to encountering a large patch of food. The number of animals assayed is noted in parentheses for each strain. Errors denote ± s.e.m and p values denote the probability that the measured distribution of slopes was obtained from a distribution with zero mean (red dashed line), as determined by a t-test.

3.3.2 Defective responses to food encounter persist in the absence of dauer formation.

Under adverse conditions, *C. elegans* larvae can enter a developmental diapause state termed dauer arrest [61, 68, 69, 89]. Because TGF-β pathway signaling regulates dauer formation, mutants of some TGF-β pathway genes form dauers at high rates under favorable (i.e., standard laboratory) conditions while mutants of other genes fail to form dauers under adverse conditions (see Fig. 3.1). High temperature is one of several adverse environmental cues that precipitate dauer formation in *C. elegans* [2, 69, 127]. In some TGF-β pathway mutants that form dauers under standard conditions, raising the animals at a slightly lower temperature (e.g., 15 °C instead of 20 °C) greatly reduces the rate of dauer formation [127]. We asked whether raising mutants at 15 °C (see Methods) would eliminate defective responses to food encounter.

Under standard conditions (20 °C), more than 90% of *daf-1(m213)* mutants constitutively became dauers; only the fraction that did reach adulthood were assayed for responses to food encounter. Raising animals of this strain at 15 °C reduced the rate of dauer formation to near zero. We found that raising *daf-1(m213)* animals in 15 °C until just prior to adulthood preserved both the preemptive acceleration and gradual slowdown exhibited by this strain in the re-feeding assay (Fig. 3.4). Raising wild-type animals at 15 °C did not alter their responses to encounter with food. Other mutants continued to form dauers when raised at 15 °C and thus were not assayed under those conditions. Thus, for at least one TGF-β pathway mutant we were able to decouple the dauer-formation phenotype from the behavioral re-feeding phenotype.

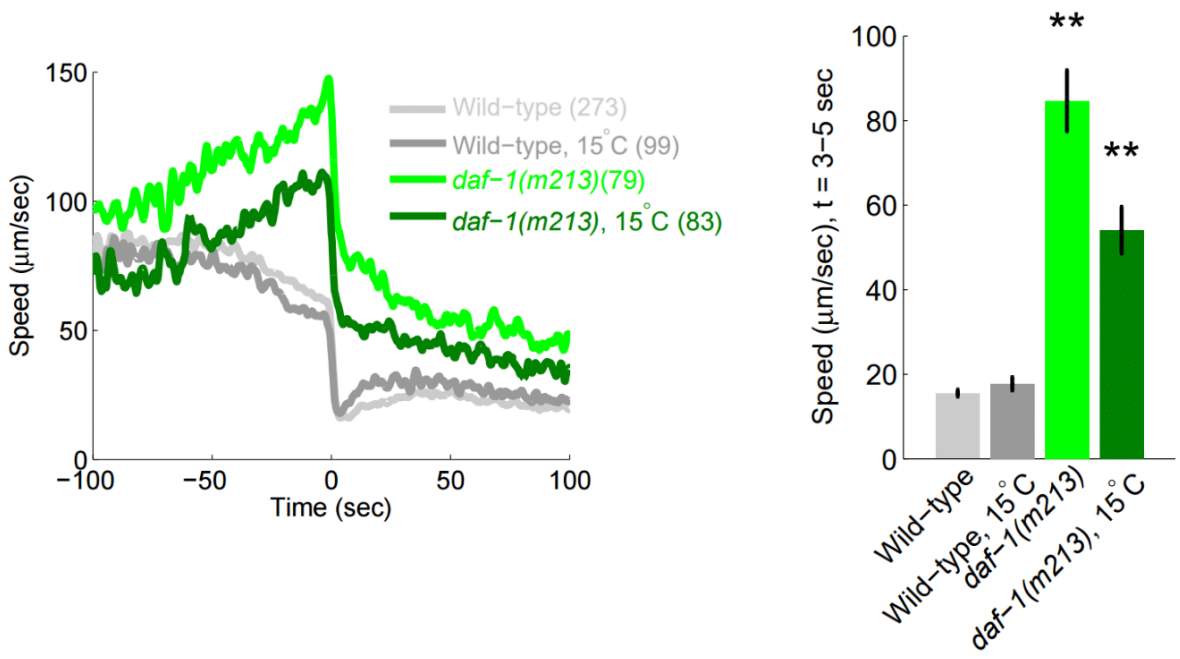

Figure 3.4: **Slowdown defects persist in the absence of dauer formation.** Growing *daf-1(m213)* mutants at 15 °C until just prior to adulthood (see Methods) eliminated the strain's tendency to form dauer larva but did not abolish the slowdown defect. Left: the mean speeds of wild-type and *daf-1(m213)* mutants grown at 15 °C (as noted) or at 20 °C around the time of encounter with the edge of a large bacterial lawn (shown without standard errors as a guide to the eye; see summary statistics in adjacent plot). Right: The speeds of the strains shown to the left shortly after the encounter. Bars and error bars (right side) depict mean ± s.e.m and the number of animals assayed for each strain is noted in parentheses (left side). Mean velocities were compared to wild-type using a t-test and corrected post hoc for multiple comparisons with a Bonferroni correction. Double asterisks denote a significant difference from wild-type ($p<0.01$).

3.3.3 Double mutants of both daf-7 *and* tph-1 *exhibit hyper-defective responses to food encounter.*

Of the TGF-β pathway genes we investigated, *daf-7* merited further exploration for three reasons: (1) *daf-7* encodes the TGF-β ligand itself, (2) *daf-7* has a limited expression profile (see next section within Results), and (3) recent work demonstrated a relationship between *daf-7* and the 5-HT synthesis gene *tph-1* [47, 51]. Regarding point (2): crosstalk and self-regulation of *tph-1* and *daf-7* was shown to shape the pattern, range, and variability of food-induced gene-expression responses. For example, compared to single mutants, *tph-1*; *daf-7* double mutants showed an exaggerated increase in the expression of *tph-1* in NSM neurons at higher food densities (see Fig. 5 of [51]). The non-redundant phenotypes of *daf-7* and *tph-1* indicated that the two genes act in parallel pathways; that is, 5-HT and TGF-β likely signal in parallel rather than in sequence.

To further clarify the epistatic relationship between the two genes, we assayed the re-feeding responses of *tph-1(n4622)*; *daf-7(ok3125)* double mutants. Double mutants exhibited hyper-defective responses to food encounter relative to either single mutant, with high post-encounter speed (Fig. 3.5) and exaggerated pre-encounter acceleration (Fig. 3.10, left column). Thus, we found no evidence of epistasis between *daf-7* and *tph-1*: in agreement with [51], our data suggest the two genes act in parallel rather than in series because the double mutant is more defective than either single mutant.

3.3.4 ASI and ADE neuron types may contribute to slowdown but are not strictly required.

In *C. elegans daf-7* is expressed in only three neuron types, all located in the head: ASI, a pair of peptidergic chemosensory/thermosensory neurons [13, 18, 76]; ADE, a pair of dopaminergic/peptidergic mechanosensory neurons [71, 78]; and OLQ, a quartet of glutamatergic/peptidergic mechanosensory neurons [102, 120]. We therefore considered transgenic

Genotype	Description	Pre-encounter	Encounter	Ref.
Wild-type	n/a	Mild deceleration	Abrupt stop	[21]
tph-1(mg280)	5-HT synthesis enzyme	Mild acceleration	Gradual slowing	[187]
tph-1(n4622)	See above	Very mild deceleration	Gradual slowing	[51]
daf-1(m40)	TGF-β receptor	Constant speed	Incomplete abrupt stop	[61]
daf-1(m213)	See above	Acceleration	Gradual slowing	[61]
daf-1(m402)	See above	Constant speed	Gradual slowing	[61]
daf-7(e1372)	TGF-β ligand	Acceleration	Gradual slowing	[153]
daf-7(ok3125)	See above	Acceleration	Incomplete abrupt stop	[51]
daf-7(m62)	See above	Acceleration	Gradual slowing	[153]
daf-8(e1393)	Intracellular TGF-β transducer	Constant speed	Gradual slowing	[157]
daf-14(m77)	Intracellular TGF-β transducer	Acceleration	Gradual slowing	[70]
daf-14(ok3647)	See above	Acceleration	Gradual slowing	[70]
tph-1(n4622); daf-7(ok3125)	See above	Acceleration	Gradual slowing	[51]
mec-10::deg-3	Degeneration of body wall mechanosensory neurons	Mild deceleration	Abrupt stop	[90]
ASI::TeTx	Silencing of ASI neurons	Mild deceleration	Mildly incomplete abrupt stop	[24]
dat-1p::TeTx	Silencing of dopaminergic neurons	Constant speed	Incomplete abrupt stop	[163]

Table 3.1: Phenotypes of key mutants and transgenics assayed in this study. For mutant strains, description refers to the affected gene (presumed to be a null mutation in each case). For transgenic stains, description refers to the effect of the transgene.

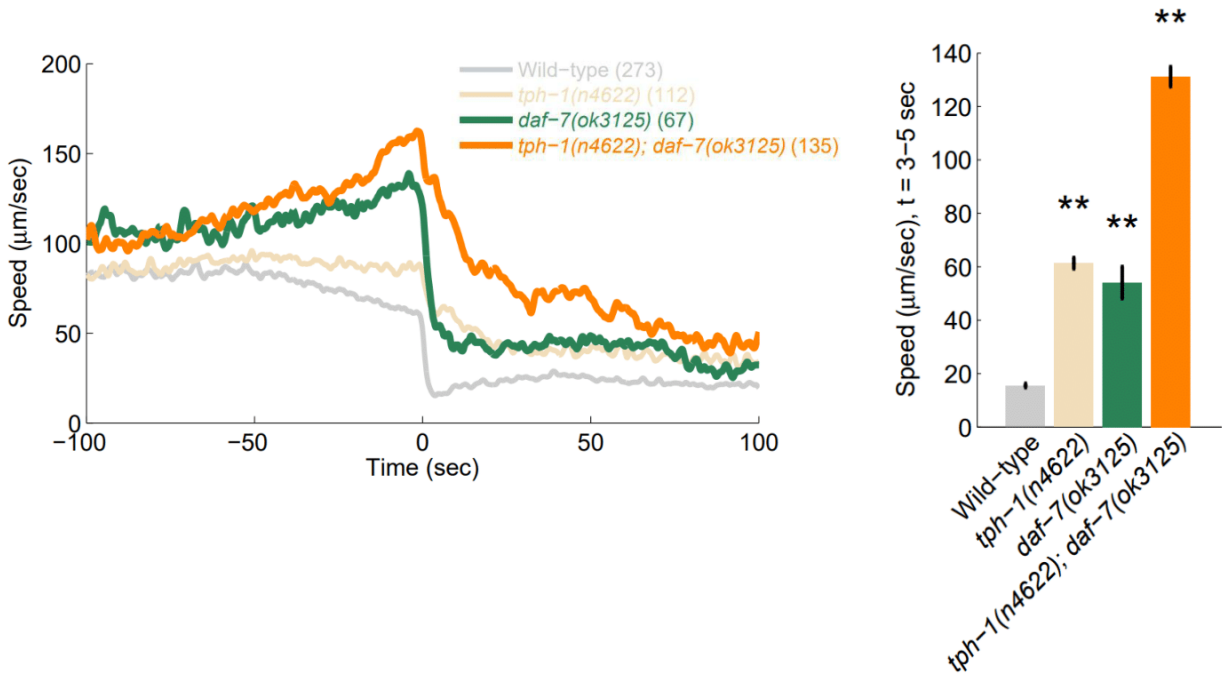

Figure 3.5: **Double mutants of both *daf-7* and *tph-1* exhibit hyper-defective responses to food encounter.** Left: the mean speeds of wild-type animals, *tph-1(n4622)* mutants, *daf-7(ok3125)* mutants, and double mutants around the time of encounter with the edge of a large bacterial lawn (shown without standard errors as a guide to the eye; see summary statistics in adjacent plot). Right: The speeds of the strains shown to the left shortly after the encounter. Bars and error bars (right side) depict mean ± s.e.m and the number of animals assayed for each strain is noted in parentheses (left side). Mean velocities were compared to wild-type using a t-test and corrected post hoc for multiple comparisons with a Bonferroni correction. Double asterisks denote a significant difference from wild-type ($p<0.01$).

animals in which one of these neuron types was genetically silenced by expression of tetanus toxin. Animals in which ASI neurons were genetically silenced displayed a mild but significant deficit in the magnitude of slowdown upon encounter with food (Fig. 3.6A). Animals in which all dopaminergic neurons, including ADE neurons, were silenced (*dat-1p::TeTx*) exhibited a moderate slowdown defect; however, because neurons other than ADE were silenced in this strain it is unclear whether the defect was related to disruption of *daf-7* signaling. Importantly, neither tetanus toxin-expressing strain exhibited the pre-encounter acceleration observed in *daf-7* mutants (Fig. 3.6B). Therefore, although ASI and ADE neurons may partially contribute to slowdown, it is unlikely that *daf-7* acts primarily in either of these neuron types to regulate responses to food encounter; as we were not able to assay a strain in which OLQ neurons were silenced, we cannot rule out the possibility that *daf-7* acts primarily in OLQ neurons (see Discussion).

3.3.5 Physiological activity of ASI neurons is suppressed with proximity to food encounter.

We previously showed that serotonergic neuron types ADF and NSM respond physiologically around the time of re-feeding [97]. In light of the phenotypic similarity between *tph-1* and *daf-7* mutants upon food encounter, we asked whether neurons that express *daf-7* would exhibit patterns of activity similar to ADF or NSM neurons. To characterize the physiological activity of *daf-7*-expressing neurons around the time of refeeding, we monitored calcium levels in freely behaving animals using the genetically encoded indicator GCaMP3.0 [190].

Calcium levels levels in ASI neurons of food-deprived animals were elevated during the period 120-60 sec prior to the time of encounter with the edge of a bacterial lawn (t = 0, Fig. 3.7) but suppressed thereafter. In contrast, ADE neurons showed no changes in physiological activity throughout the assay. Transgenic animals expressing GCaMP in OLQ neurons were assayed but the intensity of fluorescence in these cells was too dim to be reliably measured with our setup (see Discussion).

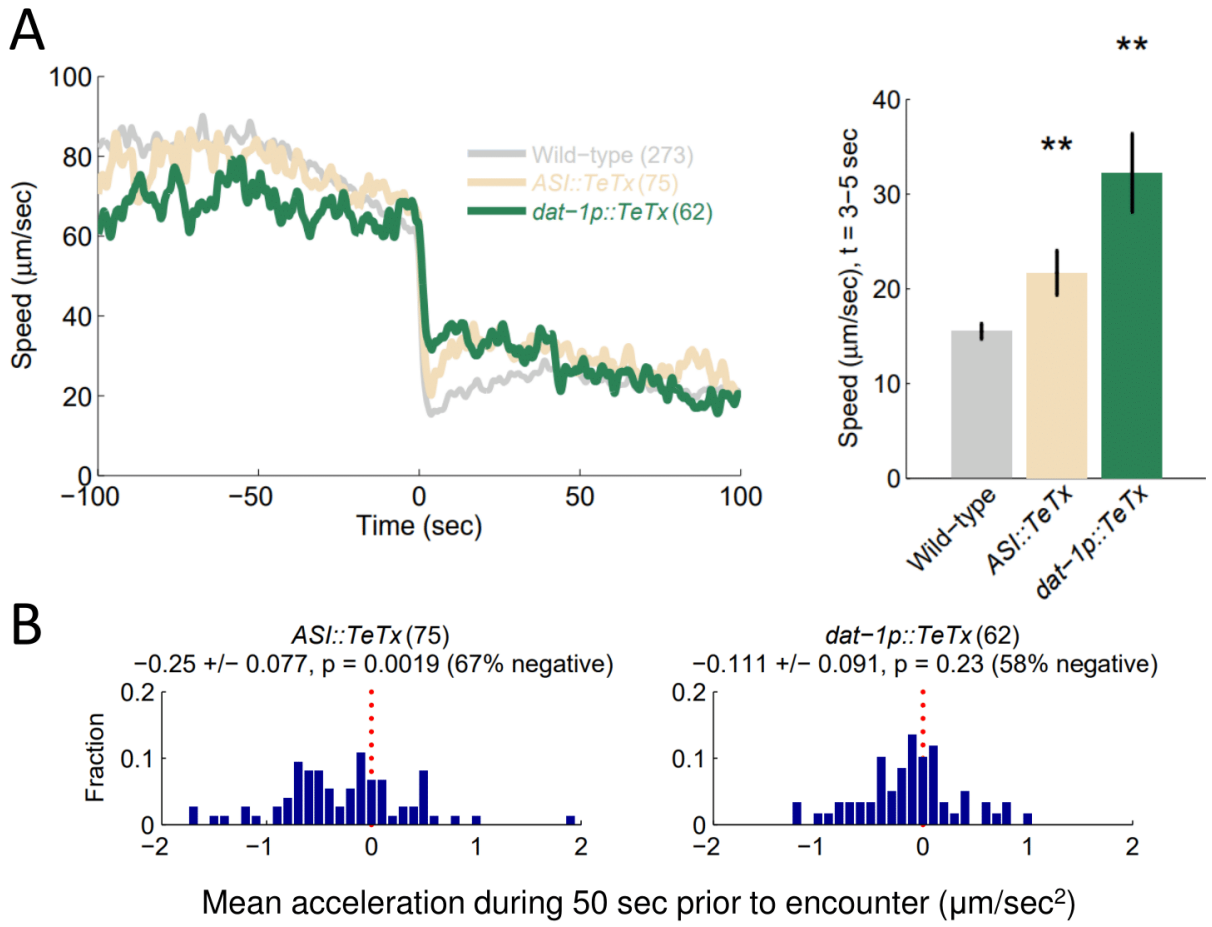

Figure 3.6: **ASI and ADE neuron types contribute to slowdown. A** Left: the mean speeds of wild-type animals and transgenics in which a *daf-7*-expressing neuron type was genetically silenced around the time of encounter with the edge of a large bacterial lawn (shown without standard errors as a guide to the eye; see summary statistics in adjacent plot). Right: The speeds of the strains shown to the left shortly after the encounter. Bars and error bars (right side) depict mean ± s.e.m and the number of animals assayed for each strain is noted in parentheses (left side). Mean velocities were compared to wild-type using a t-test and corrected post hoc for multiple comparisons with a Bonferroni correction. Double asterisks denote a significant difference from wild-type ($p<0.01$). **B** For *ASI::TeTx* and *dat-1p::TeTx* transgenics, histograms of preemptive slopes measured in individual animals during the 50 sec prior to encountering a large patch of food. The number of animals assayed is noted in parentheses for each strain. Errors denote ± s.e.m and p values denote the probability that the measured distribution of slopes was obtained from a distribution with zero mean (red dotted line), as determined by a t-test. Note that in *dat-1p::TeTx* animals all dopaminergic neurons are silenced rather than just the subset that express *daf-7*, ADE neurons.

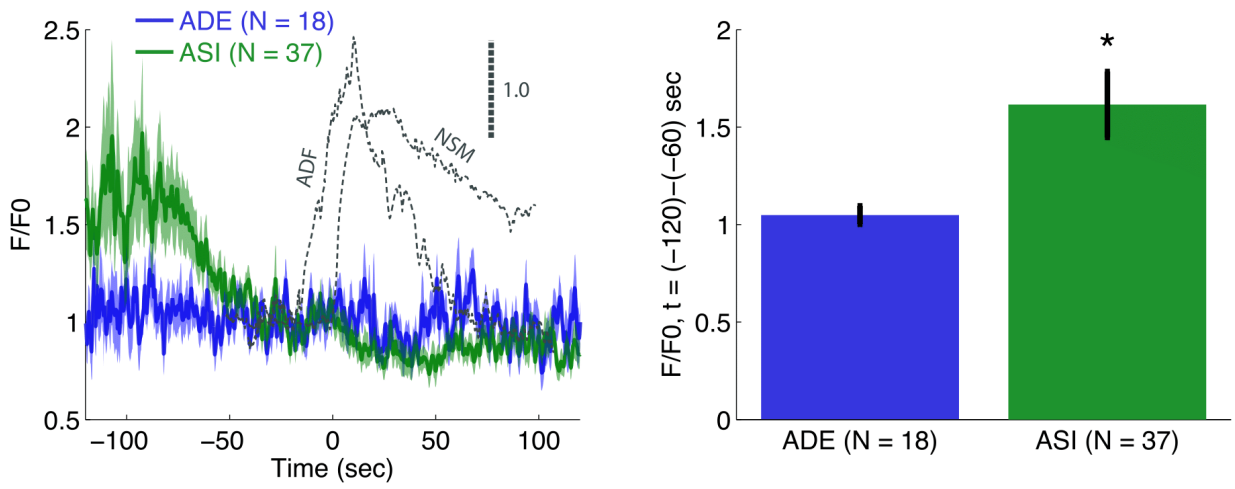

Figure 3.7: **Physiological activity of ASI neurons is suppressed with proximity to food encounter.** Left: traces of fluorescence from ADE::GCaMP (blue) and ASI::GCaMP (green) transgenics re-feeding on a large bacterial lawn. The time of encountering the edge of the lawn was defined as t = 0. The number of animals assayed for each strain is noted in parentheses and the lightly shaded area surrounding the traces depicts s. e.m. Fluorescence in ASI but not ADE neurons was significantly elevated during the period of 120 sec to 60 sec preceding the encounter (mean intensities were compared to their respective baselines, defined as the period just prior to encounter, using a t-test, $p<0.05$). Dotted lines depict fluorescence traces from ADF and NSM neurons in the same assay as reported in Fig. 4 of [97]. Scale bar (upper right) denotes 100% fold change in fluorescence intensity for superimposed ADF and NSM data. Right: bar plots depict mean ± s.e.m of intensities during the period of interest.

The suppression of ASI activity was likely due to its known role as a chemosensory neuron [13]. The time at which ASI reached a baseline level, about 60 sec prior to encounter, roughly corresponds to the time at which animals begin to change their locomotor rate as they near a patch of food (whether decelerating, in the case of wild-type animals, or accelerating, in the case of *daf-7* and *tph-1* mutants). To illustrate the relationship between the time-course of ASI activation and other chemosensory respones, we overlaid the traces of ADF and NSM fluoresence activity that we previously reported (see Fig. 4 in [97]). ADF activity, which we showed to play a role in preemptive slowing, begins to increase just as ASI activity reaches its suppressed baseline; NSM activity rises upon encounter and likely mediates the abrupt slowdown.

3.3.6 Mechanosensation plays a minor role in responses to encounter with food.

Because mechanosensory roperties were identified in *daf-7*-expressing ADE [71] and OLQ [120] neurons, we sought to determine the extent to which mechanosensation contributes to slowing responses upon food encounter. To address this we compared responses to food with responses to inedible polystyrene microspheres ("beads"), similar in diameter to OP50 bacteria and therefore a plausible approximation of the mechanical, but not chemical or nutritive, stimulus provided by food (see Methods). Wild type animals exhibited abrupt by minor slowdowns upon encounter with beads (Fig. 3.8A), suggesting that a mechanical stimulus alone was insufficient to elicit the response observed when animals encounter food. When we replaced the liquid in the beads solution with OP50-conditioned medium (see Methods), thereby partially reintroducing the diffusible molecule-based chemical stimulus inherent in food, wild-type slowing responses upon encounter were more profound than responses to beads along but still minor compared to responses to food. No preemptive slowing was exhibited as wild-type animals approached beads or beads in medium (Fig. 3.10, top row). Taken together, these results suggest that (1) volatile, not diffusable, molecules released by OP50 underlie the chemosensory component of responses to food (preemptive and upon encounter), and (2) chemosensation, not mechanosensation, primarily mediates for the behavioral response.

To identify the neurons that mediate the mechanosensation-based partial response of wild-type animals to encounter with a patch of beads, we assayed *mec-10::deg-3(u662)* transgenics in which the mechanosensory neurons that innervate the body wall are degenerated by a constitutively active nicotinic acetylcholine receptor channel subunit [90]. These trangenics were generally slow but exhibited roughly normal responses to food and mild responses to beads and beads in medium, mirroring the behavior of wild-type animals (Fig. 3.8B). Thus, we determined that the mechanosensory component of slowing responses to food is not mediated by *mec-10*-expressing neurons along the body wall; rather, it may be mediated

by the *daf-7*-expressing mechanosensory neurons of the head, ADE and OLQ.

3.3.7 The contribution of daf-7 *to slowdown is primarily chemosensory and may be required for proper priming.*

Having determined that wild-type responses to encounter with food depend primarily upon chemosensation rather than mechanosensation, we next aimed to elucidate the mechanism by which *daf-7* contributes to slowdown. We considered two (not mutually exclusive) hypotheses: (1) consistent with the fact that *daf-7* is expressed in mechanosensory neurons, *daf-7* contributes to mechansensory responses to food encounter, and (2) consistent with the massive preemptive acceleration exhibited by *daf-7* mutants, *daf-7* functions to "prime" animals for food encounter. To clarify each of these hypotheses, we assayed responses of *daf-7*, *tph-1*, and double mutants to encounters with beads and beads in OP50-conditioned medium.

Upon encounter with beads, *daf-7* mutants exhibited some slowing, but these responses were more mild than those displayed by wild-type animals (Fig. 3.9A). Responses of *tph-1* mutants were similar to wild-type. Taken together, these results suggest that *daf-7*, but not *tph-1*, functions at least partly in mechanosensation. Consistent with this idea was the fact that *tph-1*; *daf-7* double mutants we no more defective than *daf-7* single mutants; if *tph-1* plays no role in mechanosensation, the addition of a *tph-1* mutation should not exacerbate the phenotype exhibited by *daf-7* mutants.

Assaying these strains in the context of beads in OP50-conditioned medium illuminated the function of *daf-7* in chemosensation. When encountering beads in medium, *daf-7* and *tph-1* mutants were clearly defective relative to wild-type animals, exhibited a greatly reduced slowdown (Fig. 3.9B). Thus, both *daf-7* and *tph-1* contribute to chemosensory aspects of responses to food encounter, given the chemical stimulus present in the medium. However, daf-7ok3125 mutants did not exhibit preemptive acceleration as they approached the patch of beads in medium (Fig. 3.10). On the other hand, *daf-7(e1372)* mutants exhibited

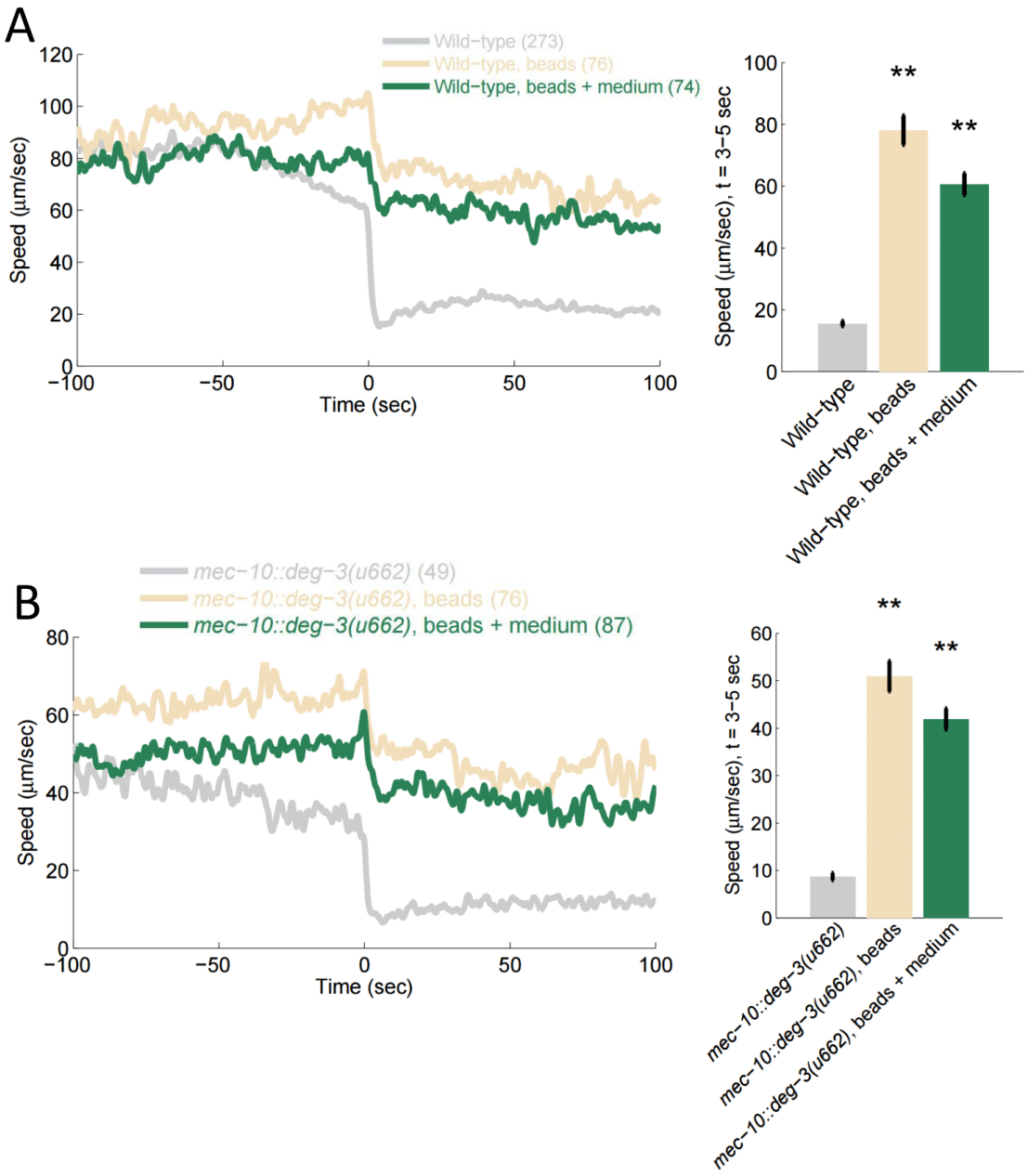

Figure 3.8: **Mechanosensation plays a minor role in responses to encounter with food. A** Left: the mean speeds of wild-type animals around the time of encounter with the edge of a large patch of food, beads, or beads in OP50-conditioned medium (shown without standard errors as a guide to the eye; see summary statistics in adjacent plot). Right: The speeds of the groups shown to the left shortly after the encounter. **B** The same comparisons made in panel (**A**) with mechanosensation-defective *mec-10::deg-3* transgenics. Bars and error bars (right side) depict mean ± s.e.m and the number of animals assayed for each group is noted in parentheses (left side). Mean velocities were compared to encounter with food using a t-test and corrected post hoc for multiple comparisons with a Bonferroni correction. Double asterisks denote a significant difference from encounter with food ($p<0.01$).

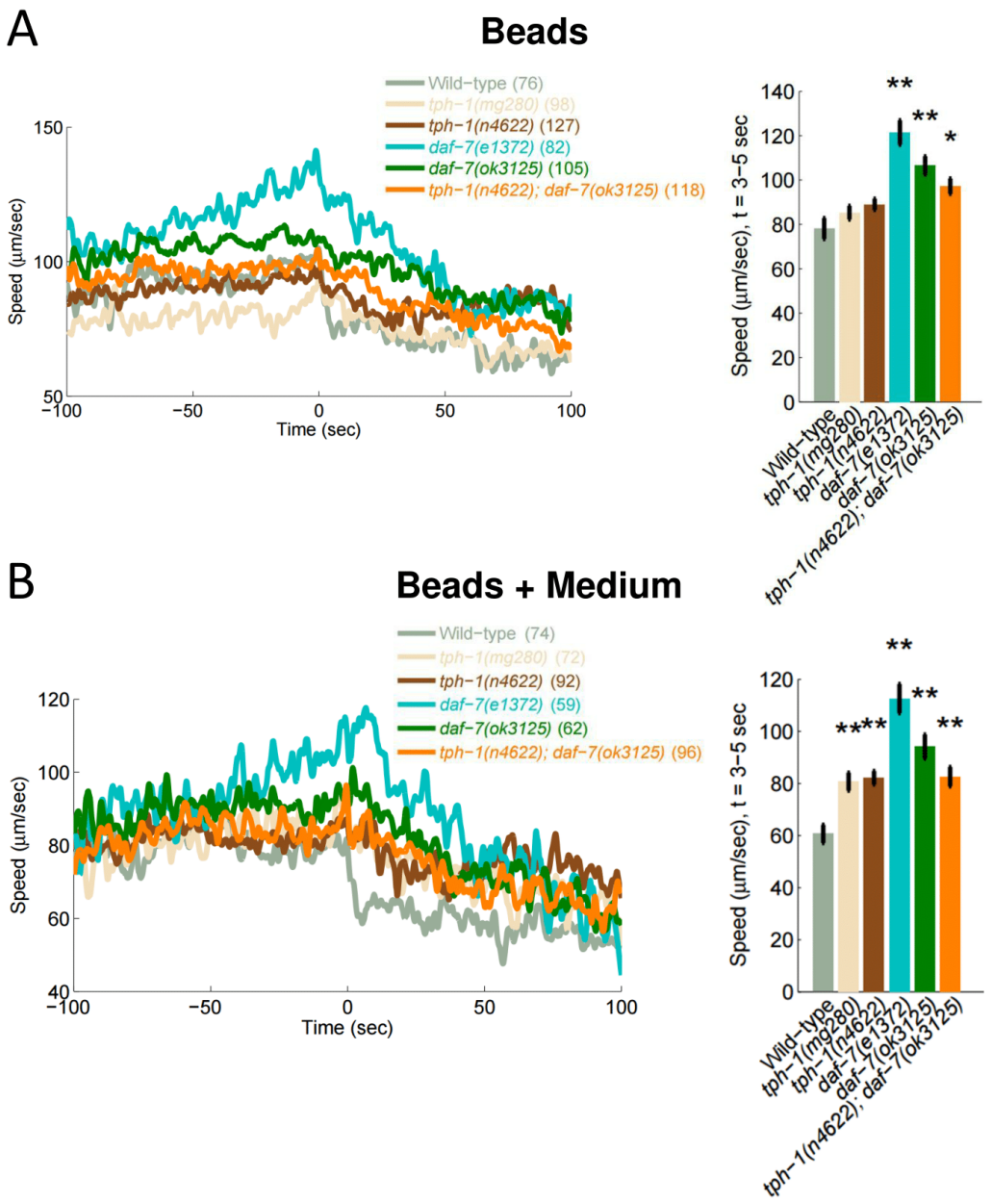

Figure 3.9: ***daf-7* contributes to slowdown primarily through chemosensory functions.** **A** Left: the mean speeds of wild-type animals, *tph-1* mutants, *daf-7* mutants, and double mutants around the time of encounter with the edge of a large patch beads (shown without standard errors as a guide to the eye; see summary statistics in adjacent plot). Right: The speeds of the strains shown to the left shortly after the encounter. **B** The same comparisons made in panel (**A**) for encounter with a large patch of beads in OP50-conditioned medium. Bars and error bars (right side) depict mean ± s.e.m and the number of animals assayed for each strain is noted in parentheses (left side). Mean velocities were compared to wild-type using a t-test and corrected post hoc for multiple comparisons with a Bonferroni correction. Single and double asterisks denote a significant difference from wild-type ($p<0.05$ and $p<0.01$, respectively).

a preemptive acceleration as they approached a patch of beads (with or without medium). This suggests that some attractant chemical may have been present in the beads solution, perhaps due to contamination.

Importantly, the beads experiments demonstrate that slowdown upon encounter is not passive (i.e., due only to a physical constraint on movement) because some strains, including *tph-1; daf-7* double mutants, exhibited no slowdown at all upon encounter with beads.

The role of chemosensation in responses to food could be prominent at any or all of three phases: (1) prior to encounter (i.e., priming), (2) upon encounter (i.e., edge detection), and (3) after encounter (i.e., sensing of new environment). Our calcium imaging and beads experiments suggest that *daf-7* contributes to slowdown primarily through the function of chemosensory ASI neurons and that this contribution may be most significant during the priming phase.

Taken together, these results suggest *daf-7* plays a role in both mechnosensory and chemosensory aspects of response to encounter with food, with the chemosensory function predominant and likely contributing to both preemptive priming and post-encounter slowing.

3.4 Discussion

Signaling in nervous systems occurs on timescales that range from milliseconds to years [136]. Timescales of operation can vary widely within a given signaling pathway; for example, when the activity of dorsal raphe neurons was recorded in behaving mice that predicted and responded to rewards and punishment, serotonergic neurons signaled on short (hundreds of milliseconds) and long (minutes) timescales [36].

We have shown that in *C. elegans* TGF-β signaling, in conjunction with 5-HT signaling, primes animals for encounter with novel food and accelerates the attenuation of locomotion upon encounter. Whereas TGF-β signaling was previously implicated in developmental processes that occur on the timescale of tens of hours, we have shown that TGF-β also functions in acute responses to environmental stimuli on the timescale of seconds.

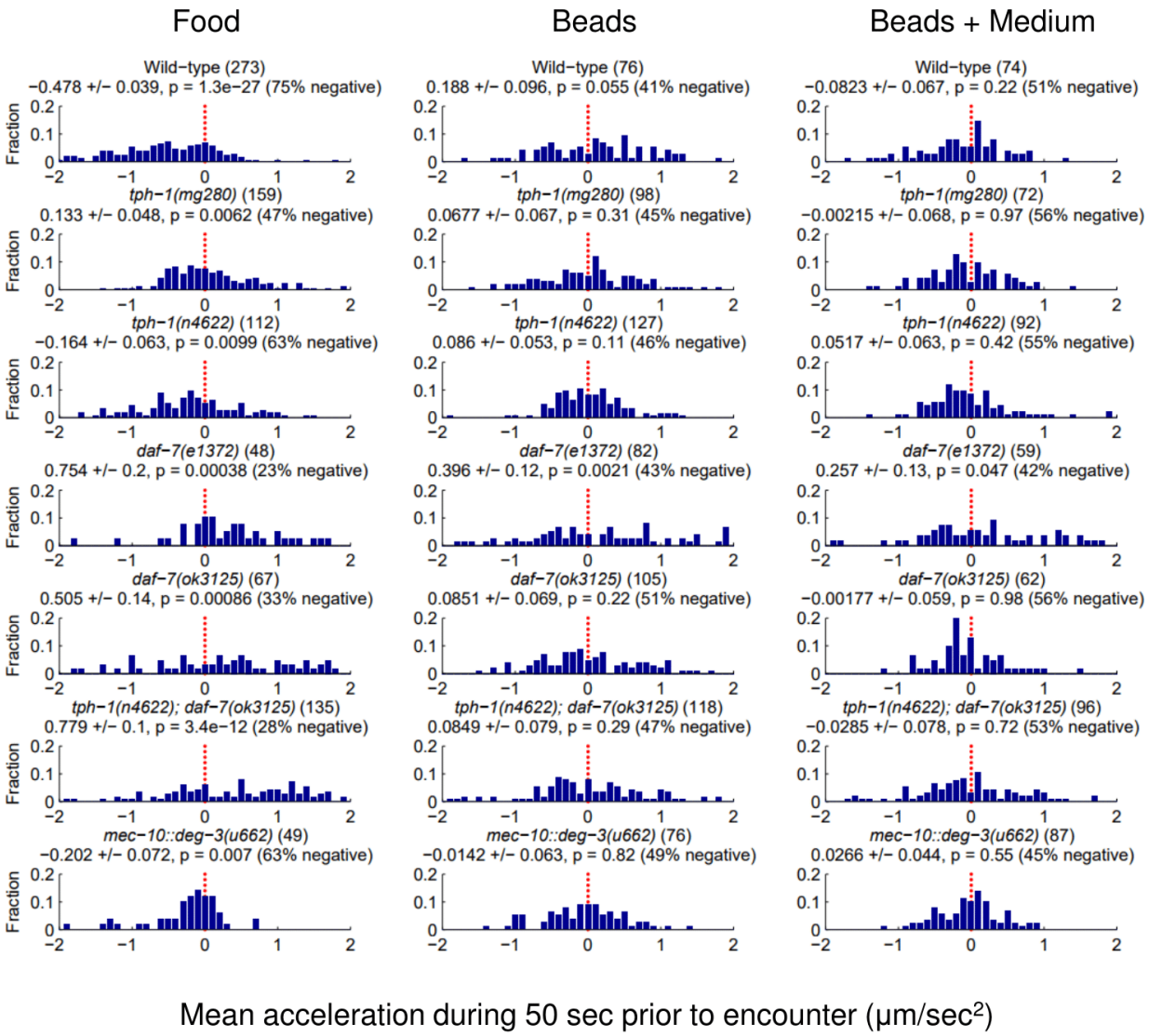

Figure 3.10: **Preemptive responses to encounters with patches.** For key strains of this study, histograms of preemptive slopes measured in individual animals during the 50 sec prior to encountering a large patch of bacterial food (left), beads (middle), or beads in bacteria-conditioned medium (right). The number of animals assayed is noted in parentheses for each strain-condition combination. Errors denote ± s.e.m and p values denote the probability that the measured distribution of slopes was obtained from a distribution with zero mean (red dotted line), as determined by a t-test.

Genotype	Description	Notes	Ref.
daf-2(e1368)	Insulin/insulin growth factor (IGF) receptor		[60]
daf-2(e1370)	See above		[103]
daf-11(m47)	Transmembrane guanylate cyclase		[70]
daf-16(mu86)	Transcription factor for insulin/IGF signaling	Generally slow	[113]
daf-16(mgdf50)	See above	Generally slow	[138]
daf-28(sa191)	Insulin		[119]
dbl-1(nk3)	TGF-β ligand	Generally slow	[126]
dbl-1(wk70)	See above	Generally slow	[185]
egl-4(ad450)	Cyclic GMP-dependent protein kinase	Generally slow	[149]
egl-4(n479)	See above		[43]
ocr-2(ak47)	Ion channel for sensory transduction	No preemptive slowing	[192]
ocr-2(yz5)	See above	No preemptive slowing	[209]
ocr-4(vs137)	Ion channel expressed in OLQ		[100]
ocr-4(vs137); ocr-2(ak47)	See above	No preemptive slowing	[100]
ocr-4(vs137); ocr-1(ok132)	See above; ocr-1 is an ion channel		[192]
ocr-4(vs137); ocr-2(ak47); ocr-1(ok132)	See above	No preemptive slowing	[192]
osm-9(ky10)	Ion channel for sensory transduction		[38]
osm-9(ok1677)	See above	Generally slow	[96]
sox-3(ok510)	Transcription factor	Generally slow	[198]
tig-2(ok3336)	TGF-β ligand		[185]
tig-2(ok3516)	See above		[185]
unc-129(ev554)	TGF-β ligand		[37]
unc-129(ev557)	See above		[37]

Table 3.2: Mutants of TGF-β pathway genes, mutants of genes related to the expression profile of *daf-7*, and mutants of other genes implicated in dauer formation that did not exhibit defective responses to encounter with food. Mutants of *ocr-2* displayed a lack of preemptive slowing, consistent with its role in chemosensation [192, 209].

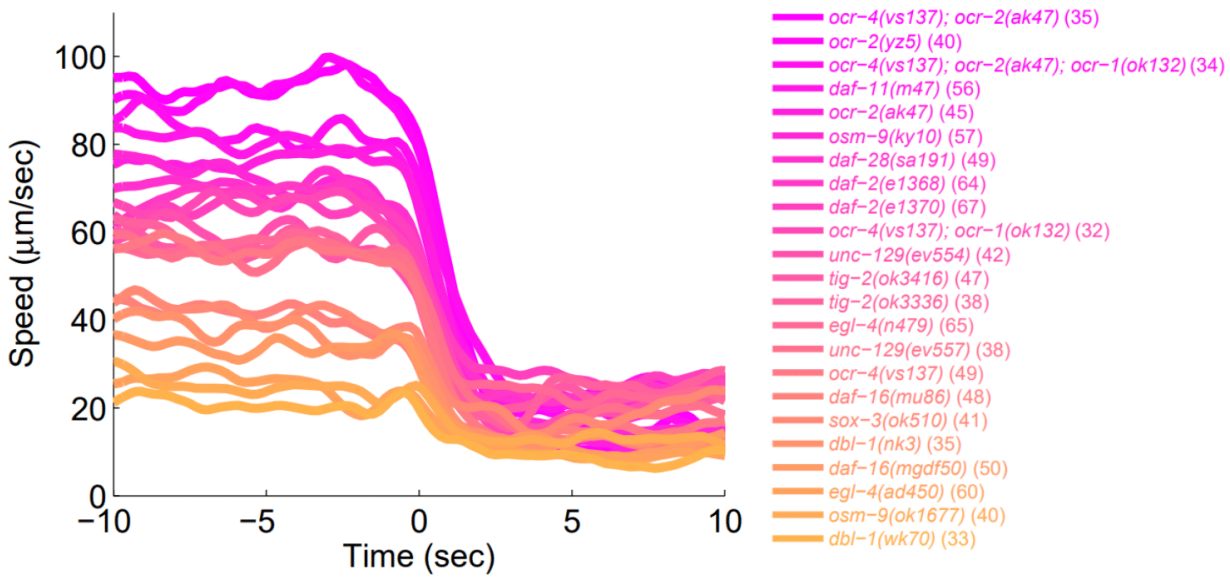

Figure 3.11: **Slowdown dynamics of non-defective mutants.** The mean speeds of non-defective (with respect to slowing response) mutants around the time of encounter with the edge of a large bacterial lawn. The number of animals assayed for each strain is noted in parentheses. Color map corresponds to pre-encounter speed. Strains presented here are mutants of TGF-β pathway genes, mutants of genes related to the expression profile of *daf-7*, or mutants of other genes implicated in dauer formation.

Mutants defective in TGF-β signaling exhibited dramatic acceleration as they approached a patch of bacterial food, in contrast to the preemptive slowing observed in wild-type animals. Upon reaching the edge of the lawn, TGF-β pathway mutants displayed incomplete abrupt or gradual slowdowns, similar to *tph-1* mutants.

We focused our investigation on the gene that encodes the TGF-β ligand, *daf-7*. Double mutants of *daf-7* and *tph-1* displayed exaggerated defects relative to single mutants in pre-emptive acceleration and slowdown upon encounter, suggesting that the two genes operate in parallel.

We formulated two hypotheses regarding the role of *daf-7* in responses to food encounter: (1) given its expression in the mechanosensory neuron types ADE and OLQ, *daf-7* contributes to slowing responses through mechanical interaction with food (i.e., upon encounter); and (2) given its expression in chemosensory ASI neurons, *daf-7* plays a role in priming the animal to respond as it approaches food, through detection of volatile or soluble particles

released by bacteria.

To test hypothesis (1), we replaced the food with inedible beads similar in size to bacteria; if *daf-7* functions in mechanosensation then we expected mutants to display a defect upon encounter with beads. Indeed, *daf-7* mutants exhibited milder slowdowns than wild-type animals upon reaching the beads. Furthermore, transgenic animals lacking the function of MEC-10 mechanoreceptors, the primary transducers of gentle touch sensation along the body wall, exhibited wild-type responses to beads. This suggested that mechanosensory neurons that do not express *mec-10*, such as *daf-7*-expressing ADE and OLQ neurons, may be the primary mediators of the mechanosensory component of slowdown. We hoped to further address this possibility by genetically silencing ADE and OLQ. Transgenics in which all dopaminergic neurons, including ADE, were silenced, displayed incomplete slowdowns; however, because neurons other than ADE were affected, we cannot attribute the defect to silencing of ADE specifically. Silencing OLQ neurons remains an important experiment to perform in order to assess the contribution of that cell type.

To test hypothesis (2), we suspended the inedible beads in bacteria-conditioned medium such that the chemical component of the food was partially recreated; if *daf-7* functions in chemosensation, then we expected the difference between mutants and wild-type animals upon encounter with beads to be exacerbated by the presence of the conditioned medium. Indeed, the addition of conditioned medium increased the magnitude of slowdown uopn encounter of wild-type animals but not *daf-7* mutants. That is, whereas beads in medium elicited a more food-like response from wild-type animals than beads alone, *daf-7* responded similarly to beads and beads in medium. This suggests that the defective slowdown exhibited by *daf-7* upon encounter with food is partially due to a failure of chemosensation. Consistent with this finding was the dramatic preemptive acceleration of *daf-7* mutants approaching food (in contrast to preemptive slowing in wild-type animals), a clear indication of a chemosensory defect. We also found that *daf-7*-expressing ASI neurons showed a suppression of activity as the animal approached food. This provided further evidence of the

role *daf-7* in chemosensory responses to food, perhaps through a priming process.

Mechanosensation does not seem to be the primary mediator of slowdown, as shown by the very mild response of wild-type animals to encounter with beads. That observation, along with the experiments recapitulated above, suggests that the contribution of *daf-7* to responses to food is primarily chemosensory. This complements our previous work which implicated 5-HT in both preemptive detection of food via chemosensory ADF neurons [97].

Our calcium imaging experiments suggested that *daf-7*-expressing ASI neurons play a role in priming the animal for encounter with food. Suppression of activity in ASI occurred as animals approached food. This phenomenon was observed in approximately one third of animals assayed and was rather variable, with the decline in activity beginning 90 to 120 sec prior to encounter and occurring over a period of 30 to 60 sec. Interestingly, transgenics in which ASI neurons were genetically silenced showed only a minor defect in slowdown upon encounter and no abnormality in preemptive slowing. If ASI's contribution to priming is mediated by suppression of its own activity then it is logical that silencing of ASI elicits no defect. To further clarify, it would be possible to optically activate ASI during the relevant time period. If such activation results in preemptive acceleration rather than preemptive slowing, that would suggest that suppression of ASI activity contributes to priming.

Due to technical limitations we failed to assess the contribution of OLQ mechanosensory neurons to slowdown behavior. The role of these neurons needs to be probed, as well as the sufficiency of combinations of ASI, ADE, and OLQ to mediate wild-type responses.

Future experiments should also examine of dauer-defective genes *daf-3* and *daf-5*. Given that mutants of these genes fail to undergo dauer arrest under harsh conditions[109], whereas dauer-constitutive mutants such as *daf-7* become dauers in favorable environments, might *daf-3* and *daf-5* show a different food-encounter phenotype altogether?

In cases in which two genes regulate a physiological process, if one gene functions upstream of the other then double mutants will display the same phenotype as single mutants of the upstream gene. Our observation that *daf-7*; *tph-1* double mutants exhibit exagger-

ated defects relative to single mutants in preemptive and upon-encounter responses to food supports the hypothesis that TGF-β and 5-HT signal in parallel rather than in series. Further evidence of this parallel organization comes from studies of *tph-1* and *daf-7* expression levels in the context of food-dependent lifespan changes. In *C. elegans*, lifespan increases then decreases then increases again as food concentration is reduced from a high level; the longest lifespans occur when food is absent once animals reach adulthood [51]. Entchev et al. found that loss of *tph-1* or *daf-7* lowers the accuracy of food level representation and reduces the dynamic range of lifespan responses [51]. Furthermore, they demonstrated that *tph-1* and *daf-7* mutants exhibit additive phenotypes in both gene-expression responses and predictive accuracy of lifespan. Because predictive accuracy is a function of the quantity of information conveyed, the additive defect of double mutants indicates that *daf-7* and *tph-1* carry non-redundant information about food abundance. That is, 5-HT and TGF-β signal in parallel, not sequentially.

In mammals, TGF-β is involved in processes as varied as wound healing [4], tumor growth and metastasis [25], and diabetes [5]. Therefore, elucidating TGF-β signaling pathways that govern behavior in a simple model organism is crucial for enhancing our understanding of human neuroendocrine processes. Our results show that TGF-β signaling functions similarly to bioamine neuromodulators to tune behavioral responses. However, it is unclear whether TGF-β mediates behavior by functioning as an acute signal or as a modulator of synaptic connections [55]. Optically stimulating neurons that express *daf-7* could help differentiate between these possibilities; if such stimulation evokes behavioral responses, that would provide evidence of acute TGF-β signaling.

Dauer formation occurs in the absence of food [27]. Thus, dauer formation should be thought of as part of the same set of behaviors to which slowdown responses belong: an array of behavioral or physiological responses that result from changes in food availability. In that sense, it is logical that interactions between genes involved in acute sensation of food (i.e., *tph-1*) interact with pathways involved in responses to food on longer timescales, such

as TGF-β and insulin signaling [194].

3.5 Conclusions

This study suggests that TGF-β pathway genes contribute to both gradual preemptive slowing as animals approach food and abrupt slowing upon encounter. Our observation that double mutants of both *daf-7* and *tph-1* exhibited exaggerated defects relative to single mutants supported the hypothesis that TGF-β and 5-HT function in parallel rather than in series. Finally, this study implicates both mechanosensory and chemosensory transduction in mediating responses to food encounter, with *daf-7* primarily involved in chemosensation.

3.6 Methods

3.6.1 Strains

C. elegans strains were maintained and grown according to standard protocols [21]. The following strains were used: wild type strain N2, MT15434 *tph-1(mg280)*, QL101 *tph-1(n4622)*, DR40 *daf-1(m40)*, DR609 *daf-1(m213)*, DR960 *daf-1(m402)*, DR62 *daf-7(m62)*, CB1372 *daf-7(e1372)*, QL282 *daf-7(ok3125)*, CB1393 *daf-8(e1393)*, DR77 *daf-14(m77)*, RB2620 *daf-14(ok3647)*, QL300 *tph-1(n4622); daf-7(ok3125)*, AB16 *Is[mec-10::deg-3(u662)]*, IV205 *ueEx122 [str-3::TeTx::GFP; elt-2::sl2GFP]*, INV33005 *Ex[dat-1::TeTx::mCherry]*, LX950 *ocr-4(vs137)*, LX980 *ocr-4(vs137); ocr-1(ok132)*, LX981 *ocr-4(vs137); ocr-2(ak47)*, LX982 *ocr-4(vs137); ocr-2(ak47); ocr-1(ok132)*, CX4544 *ocr-2(ak47)*, JY243 *ocr-2(yz5)*, LT121 *dbl-1(wk70)*, NU3 *dbl-1(nk3)*, NW987 *unc-129(ev554)*, NW990 *unc-129(ev557)*, RB2430 *tig-2(ok3336)*, RB2476 *tig-2(ok3416)*, MT1074 *egl-4(n479)*, DA521 *egl-4(ad450)*, GR1307 *daf-16(mgdf50)*, CF1038 *daf-16(mu86)*, DR47 *daf-11(m47)*, CX10 *osm-9(ky10)*, VC1262 *osm-9(ok1677)*, VC266 *sox-3(ok510)*, JT191 *daf-28(sa191)*, DR1572 *daf-2(e1368)*, CB1370 *daf-2(e1370)*. CX10979 *kyEx2865 [sra-6::gcamp3; ofm-1::gfp]*, SN03 *Ex[dat-1::gcamp3]*. The QL101, QL282, and QL300 strains were a gift from QueeLim Ch'ng's laboratory (King's

College London). The CX10979 strain was a gift from Cornelia Bargmann's laboratory (Rockefeller University). The IV205 strain was a gift from Sreekanth Chalasani's laboratory (Salk Institute for Biological Studies).

3.6.2 Behavioral assays: large bacterial lawn

To assay re-feeding on a large bacterial lawn, 72-96 hour old adults were washed twice in a drop of M9 buffer and transferred to unseeded NGM plates for 1-2 hours. Animals were assayed on 60 mm NGM plates seeded with a 25 μl drop of 3X concentrated overnight culture of OP50 *E. coli* bacteria. The bacteria were spread in an oval shape of area 100-150 mm^2 on one side of the plate and assay plates were kept at 4 °C prior to the assay. In each assay, 10-30 animals were transferred to M9 droplets on the empty side of the assay plate and started to crawl once the droplets were absorbed. Unless stated otherwise, animals that reached the bacterial lawn in less than 150 sec (<20% of the total number of animals) were not scored in order to minimize the effect of the transfer on the data. Images were captured using a cooled CCD camera (Photometrics Cool- SNAP HQ2, Tucson, AZ), an Olympus SZX16 stereo- microscope equipped with an SDF PLAPO 1XPF objective (Olympus America Inc., Center Valley, PA), and the Micro-manager open source software. Imaging was performed at 5 frames per sec, using a magnification of 0.7X and 4x4 binning. Under these conditions, the area of a single animal was 40-45 pixels. The centers of mass of the animal bodies were tracked using custom Matlab scripts. Center of mass velocities were computed using a temporal resolution of 1 sec. Each genotype was assayed at least on 3 different days and control animals were recorded each day. In our hands, day to day variability was typically small. To assess whether preemptive responses were statistically significant, a linear function was fitted to the speeds of individual animals during the 50 sec prior to encountering food using the Matlab curve fitting toolbox. Experiments were performed on at least three independent days and day-to-day inconsistencies were not identified.

For data shown in Fig. 3.4, wild-type or *daf-1(m213)* animals were grown on agar plates

in a 15 °C incubator until they reached L4, the last larval stage before adulthood. L4 larvae were picked and transferred to agar plates held at 20 °C until adulthood, about 24 hours later, and then assayed as described above (at 20 °C). At 15 °C animals take approximately twice as long to reach L4 relative to development at 15 °C [23]; thus, the animals in this condition were about twice as old as animals assayed under standard growth protocol.

3.6.3 Behavioral assays: bead patches

To assay responses to inedible substances, 72-96 hour old adults were washed twice in a drop of M9 buffer and transferred to unseeded NGM plates for 1-2 hours. Animals were assayed on 60 mm NGM plates seeded with a 25 μl drop of either 1% 1 μm diameter polystyrene microspheres (Polybeads, Polysciences, Niles, IL; "beads") in M9 or 1% beads in OP50 conditioned medium. To obtain conditioned medium, overnight cultured OP50 were centrifuged and the supernatant was extracted and filtered through a 0.45 μm membrane filter. The beads or beads + medium solution was spread in an oval shape of area 100-150 mm^2 on one side of the plate and assay plates were kept at 4 °C prior to the assay. In each assay, 30-60 animals were transferred to M9 droplets on the empty side of the assay plate and started to crawl once the droplets were absorbed. Unless stated otherwise, animals that reached the bead patch in less than 150 sec (<20% of the total number of animals) were not scored in order to minimize the effect of the transfer on the data. Images were captured using a cooled CCD camera (Photometrics Cool- SNAP HQ2, Tucson, AZ), an Olympus SZX16 stereo- microscope equipped with an SDF PLAPO 1XPF objective (Olympus America Inc., Center Valley, PA), and the Micro-manager open source software. Imaging was performed at 5 frames per sec, using a magnification of 0.7X and 4x4 binning. Under these conditions, the area of a single animal was 40-45 pixels. The centers of mass of the animal bodies were tracked using custom Matlab scripts. Center of mass velocities were computed using a temporal resolution of 1 sec. Each genotype was assayed at least on 3 different days and control animals were recorded each day. In our hands, day to day variability was typically small.

To assess whether preemptive responses were statistically significant, a linear function was fitted to the speeds of individual animals during the 50 sec prior to encountering food using the Matlab curve fitting toolbox. Experiments were performed on at least three independent days and day-to-day inconsistencies were not identified.

3.6.4 Calcium imaging

Calcium imaging was performed on freely behaving animals on large bacterial lawn, 60 mm diameter, assay plates. Here, 50 μl overnight bacterial culture was seeded in a ring and incubated overnight at 37 °C. The transgenic strains assayed expressed the calcium indicator GCaMP3 in the target neuron(s) (see strain list). Food deprivation was performed as described above, several animals were initially placed at the center of the ring, and a single animal approaching the inner diameter of the ring was continuously imaged. The analysis of neuronal calcium transients was performed similarly to the previously described procedure in [163]. Data shown in Fig. 3.7 was acquired using the setup described above for large bacterial lawn assays. Imaging was performed at 5 frames per second at a magnification of 10X for up to 25 minutes. In our hands, bacterial lawns had clearly visible sharp edges. First-day adults were transferred to assay plate and allowed several minutes to equilibrate. Animals were tracked manually until they were approximately 15 body lengths from the edge of the food patch, at which point the assay plate remained in place.

3.6.5 Statistical analysis

Data analysis was performed using custom Matlab (Mathworks Inc., Natick, MA) scripts. Individual statistical tests are detailed in the corresponding figure legends.

CHAPTER 4

EXPERIMENTAL AND COMPUTATIONAL METHODS FOR BEHAVIORAL AND PHYSIOLOGICAL PHENOTYPING

Adam Brown[1], Stanislav Nagy[2], Shachar Iwanir[2], Celia Cook[3], Laura Manning[4], Janet Richmond[4], and David Biron[2,3]

AB contributed to the conception and design of the study, performed, analyzed, and interpreted behavioral and physiological assays, and contributed analysis tools. SN contributed to the conception and design of the study, generated transgenic animals, performed, analyzed, and interpreted behavioral and physiological assays, and contributed analysis tools. SI contributed to the conception and design of the study, performed, analyzed, and interpreted behavioral assays, and contributed analysis tools. CC analyzed behavioral assays and contributed analysis tools. LM contributed to the conception and design of the study and contributed reagents/materials. JR contributed to the conception and design of the study and contributed reagents/materials. DB contributed to the conception and design of the study and helped analyze and interpret the data.

4.1 Abstract

Novel assays were developed in the course of the work reported in this dissertation and related projects. Accordingly, we also developed novel analysis tools and applied previously established tools in novel ways. Nearly all measurements reported here derive from continuous video recordings of behaving nematodes. We primarily quantified behavioral responses to

1. Committee on Computational Neuroscience, The University of Chicago, Chicago, IL 60637, USA.

2. The Institute of Biophysical Dynamics, The University of Chicago, Chicago, IL 60637, USA.

3. Department of Physics and the James Franck Institute, The University of Chicago, Chicago, IL 60637, USA.

4. Department of Biological Sciences, University of Illinois at Chicago, Chicago, IL60607, USA.

food and other stimuli, using image processing tools to extract information about movement. We used similar tools to quantify physiological responses, such as changes in the fluorescence of a calcium indicator expressed in a subset of neurons. This chapter summarizes the protocols of our novel assays and describes the computational tools we used to quantify behavioral and physiological phenotypes. The final section of this chapter reports on a study in which we applied some of our most computationally intensive and mathematically interesting tools to explore phenotypes resulting from mutations of Gα_s signaling pathway genes.

4.2 Introduction

The study of animal behavior is perhaps best thought of as taking place along a spectrum. At one end of the spectrum are experiments in which animals are subjected to highly-constrained conditions and made to select one of a few discrete behavioral responses. Early psychophysical experiments and foundational studies of classical and operant conditioning are found at this end [72, 75, 175]. At the other end of the spectrum are observational studies of animals behaving in their natural habitats, an approach termed ethology [20, 191]. Relatively simple model organisms such as *C. elegans* provide an opportunity to find middle ground along this spectrum such that complex and somewhat naturalistic behaviors can be quantified in concise ways.

Although agar plates and microfluidic chambers are hardly a faithful recreation of a nematode's natural habitat (a rotting apple, for example), these artificial environments do allow for unconstrained movements. Furthermore, it is possible to construct foraging environments (i.e., arrangements of patches of food) on the surface of agar plates that worms can freely interact with. In the studies reported in this dissertation, video recordings of worms in such semi-naturalistic environments yielded plenty of insight into neurobiology and behavior. Two primary challenges were inherent in these studies: (1) designing and producing foraging environments suitable for addressing research questions and (2) creating and applying computational tools to extract behavioral data from video recordings. Addressing each of these

challenges required the development of novel experimental assays and analysis frameworks.

Numerous studies have established foraging assays [45, 148]) and/or tools for automated quantification of worm behavior [54, 122, 186, 199]. Nevertheless, our research questions led us to develop our own approaches, detailed in this chapter. The utility of the tools we established extends well beyond the specific aims of our foraging studies; indeed, our techniques can be applied to study nearly any aspect of *C. elegans* behavior, particularly locomotor behavior. Furthermore, whereas genetic studies of *C. elegans* neurobiology often make do with qualitative or rudimentary quantitative descriptions of behavior (e.g., manual counting of body bends [106]), our tools can be used to establish detailed quantitative phenotypes. One such application, an exploration of the role of cyclic AMP (cAMP) signaling in muscle contraction, is reported at the end of this chapter.

4.3 Methods

4.3.1 Patch experiments

Large patch: Multi-worm tracking

To assay re-feeding on a large bacterial lawn, 72-96 hour old adults were washed twice in a drop of M9 buffer and transferred to unseeded NGM plates for 1-2 hours. Animals were assayed on 35 mm or 60 mm NGM plates seeded with a 25 μl drop of 3X concentrated overnight culture of OP50 bacteria. The bacteria were spread in an oval shape of area 100-150 mm^2 on one side of the plate and assay plates were kept at 4 °C prior to the assay. In each assay, 10-30 animals were transferred to M9 droplets on the empty side of the assay plate and started to crawl once the droplets were absorbed. The number of animals transferred and the distance they were placed from the patch depended on the locomotor phenotype of the strain. In general, starting distance and number of animals were scaled together to reduce crowding (which prevented tracking of individuals). Furthermore, strains that crawled slowly were placed nearer to the patch and strains that exhibited hyperactive

locomotion were placed farther away. Starting distances were typically in the range of 1-2 cm. Adjusting the starting distance increased the throughput such that most animals arrived at the patch after 150 sec; unless stated otherwise, animals that reached the bacterial lawn in less than 150 sec (<20% of the total number of animals) were not scored in order to minimize the effect of the transfer on the data.

Images were captured using a cooled CCD camera (Photometrics Cool- SNAP HQ2, Tucson, AZ), an Olympus SZX16 stereo- microscope equipped with an SDF PLAPO 1XPF objective (Olympus America Inc., Center Valley, PA), and the Micro-manager open source software. Imaging was performed at 5 frames per sec, using a magnification of 0.7X and 4x4 binning. Under these conditions, the area of a single animal was 40-45 pixels. The centers of mass of the animal bodies were tracked using custom Matlab scripts. Center of mass velocities were computed using a temporal resolution of 1 sec. Each genotype was assayed at least on 3 different days and control animals were recorded each day. In our hands, day to day variability was typically small. To assess whether the preemptive slowdown was statistically significant, a linear function was fitted to the speeds of individual animals during the 50 sec prior to encountering food using the Matlab curve fitting toolbox. Post-encounter decay constants (τ) were based on a single exponential fit of the 0-150 sec data. The goodness of fit (R^2) was higher than 0.9 in all cases. Experiments were performed on at least three independent days and day-to-day inconsistencies were not identified.

For data shown in Figs. 3.8 and 3.9, animals were assayed on 60 mm NGM plates seeded with a 25 μl drop of either 1% 1 μm diameter polystyrene microspheres (Polybeads, Polysciences, Niles, IL; "beads") in M9 or 1% beads in OP50 conditioned medium. To obtain conditioned medium, overnight cultured OP50 were centrifuged and the supernatant was extracted and filtered through a 0.45 μm membrane filter. As with the OP50 patch experiments described above, the beads solution was spread in an oval shape of area 100-150 mm^2 on one side of the plate. Assay plates were kept at 4 °C prior to the assay. In each assay, 30-60 animals were transferred to M9 droplets on the empty side of the assay plate

and started to crawl once the droplets were absorbed; compared to OP50 patch experiments, larger numbers of animals were used in the beads experiments to maintain high throughput in light of the animals' lack of attraction to the patch. As explained above, the number of animals transferred and the distance they were placed from the patch were adjusted according to the locomotor phenotype of the strain.

Large patch: Single worm locomotion studies

Note: The following description refers to experiments reported in the last section of this chapter (see Fig. 4.7).

Young adult nematodes were washed in M9 buffer and transferred to a small droplet of M9 adjacent to a roughly oblong 7.5 mm x 15 mm patch of OP50 bacteria on an otherwise unseeded 35 mm NGM plate. These plates were made by placing a 25 μl droplet of overnight cultured OP50 in the center of the plate and tilting the plate to create the oblong shape. Plates were kept in a 4 °C incubator overnight and removed from the incubator before the experiment, allowing enough time for the plates to reach room temperature (20 °C). After the M9 droplet evaporated and the worm began crawling on the plate, 30 minutes elapsed before starting a one hour recording. Most worms remained in the field of view, and typically on the bacterial patch, for the full one hour movie. The patch was angled at a diagonal across the square field of view, occupying approximately 1/3 of all pixels.

In some experiments *acy-1;[myo-3::acy-1(+)]* animals were directly placed on the patch itself because individuals of this strain that were placed in an adjacent droplet often never reached the patch during the 90 minute assay period due to severe locomotion defects.

A single animal per plate was imaged at 5 frames per second using a 5MP scientific CCD camera (Prosilica GC2450, Allied Vision Technologies, Stadtroda, Germany) at a magnification of 0.65X. Under these conditions a worm body typically occupied about 1000 pixels. Custom LabView (National Instruments Inc., Austin TX) and Matlab (Mathworks Inc., Natick, MA) scripts were used for image acquisition and data analysis. Images were analyzed

using the posture-based method as described previously [133] and below. Patch outlines were traced manually for each experiment, and frames where the nose-tip of the worm was within 5% of the body-length from a patch were labeled "on food".

Micro-patch "arenas"

For long-term assays in a complex environment, patches contained OP50 bacteria at a concentration of $OD_{600} = 2.5$. Assay plates were freshly seeded prior to the experiment. Individual food patches were seeded by gently touching preloaded thin gel loading tips to a standard agar plate, typically resulting in a patch diameter of 0.8-1 mm. Unless stated otherwise, the bacteria mix was supplemented with 10X kanamycin to prevent growth. Prolonged experiments (5-10 hours, Fig. 2.5) were performed on a 7x7 square lattice. Shorter experiments (2.5 hours, Fig. 2.13) were performed on a 5x5 hexagonal lattice. In both cases the distance between nearest neighbors was 2 mm. Printed templates were affixed to the bottom of the agar plate as a guide for patch seeding (Fig. **??**) and removed prior to the experiment. Food deprivation was performed as described above.

A single animal per plate was imaged at 5 frames per second using a 5MP scientific CCD camera (Prosilica GC2450, Allied Vision Technologies, Stadtroda, Germany) at magnifications of 0.33-0.65X. Under these conditions a worm body typically occupied 500-1000 pixels. A 3D printed square frame (18 mm inner and 24 mm outer diameter) lined with copper tape was used to contain the animal in the field of view. Custom LabView (National Instruments Inc., Austin TX) and Matlab (Mathworks Inc., Natick, MA) scripts were used for image acquisition and data analysis.

Images were analyzed using the posture-based method as described previously [133]. Patch outlines were traced manually for each experiment, and frames where the nose-tip of the worm was within 5% of the body-length from a patch were labeled "encounter". If, during an encounter, the mean velocity of the animal was at the lowest 15th percentile of measured roaming velocities then the frames of the encounter were labeled "exploitation".

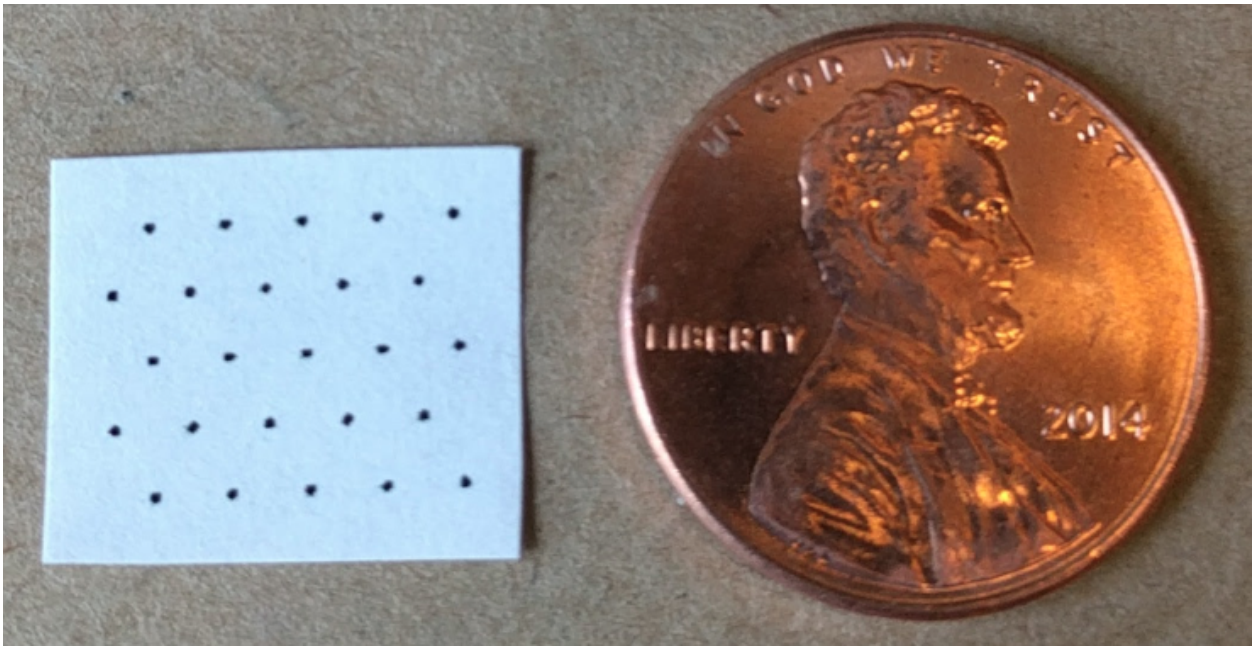

Figure 4.1: **Template for micro-patch arena construction.** A printed template for a 5x5 hexagonal grid of patches with 2 mm distance between nearest neighbors. Diameter of actual patches was 2-3X greater than the dots on the template. Penny shown for scale.

Brief (exploratory or accidental) excursions out of the patch, in which the distance between the edge and the nose-tip was no greater than 20% of the body-length, were consolidated. Thus, motion on the order of 100 μm beyond the patch edge did not fractionate a continuous event. Patch coverage was quantified by determining the area occupied during each exploitation event. Experiments were performed on at least three independent days and day-to-day inconsistencies were not identified. Examples of tracked locomotion in this assay are presented in Fig. 4.2.

4.3.2 Calcium imaging: particle tracking and brightness quantification

Calcium imaging was performed on freely behaving animals on large bacterial lawn, 60 mm diameter, assay plates. Here, 50 μl overnight bacterial culture was seeded in a ring and incubated overnight at 37 °C. The transgenic strains assayed expressed the calcium indicator GCaMP3 in the target neuron on a *lite-1* mutant background [50, 201] (see strain list). Food deprivation was performed as described above, several animals were initially

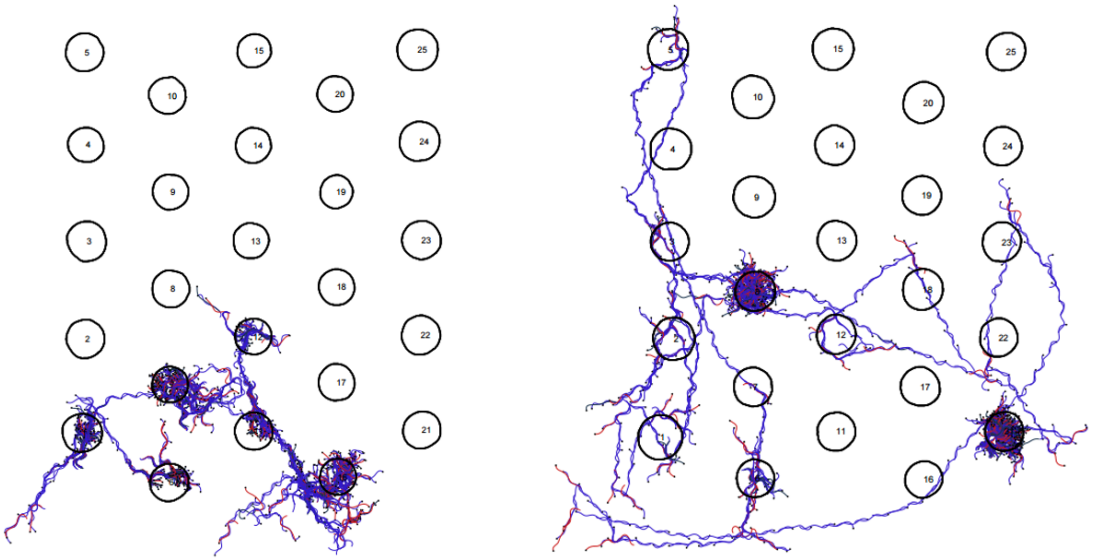

Figure 4.2: **Micro-patch assay locomotion tracks.** Single animal locomotion tracking during 2.5 hour micro-patch experiments. Left: wild-type. Right: *tph-1*. Large open black circles depict bacterial patches. Blue and red curves depict forward and reverse locomotion, respectively. Small closed black circles depict head position. Postures are extracted from video via PyCelegans (see below) and are plotted at 4 sec intervals.

placed at the center of the ring, and a single animal approaching the inner diameter of the ring was continuously imaged. To image NSM during evoked pauses (Fig. 2.7, left inset), a standard platinum pick was manually placed near the anterior of a forward moving animal such that it gently touched it due to its own motion.

The analysis of neuronal calcium transients was performed similarly to the previously described procedure in [163]. Data shown in Figs. 2.7A and 2.8 was acquired using the setup described above for large bacterial lawn assays. Imaging was performed at 5 frames per second at a magnification of 10X for up to 25 minutes. In our hands, bacterial lawns had clearly visible sharp edges. First-day adults were transferred to assay plate and allowed several minutes to equilibrate. Animals were tracked manually until they were approximately 15 body lengths from the edge of the food patch, at which point the assay plate remained in place. For reverse patch imaging (Fig. 2.8A), assay plates were prepared with 2 ml agar; the resulting thickness was 2-3 mm. Prior to the assay, the agar was carefully flipped such that the animals crawled on the agar surface opposite to the lawn. The minimal possible

distance of the animal from the bacteria was thus 2-3 mm.

Data shown in Fig. 2.7B-C, imaging was acquired at a frame rate of 11 frames per second. Images were captured using a cooled EMCCD camera (Evolve 512, Photometrics, Tucson AZ), an Olympus 83X inverted microscope equipped with a UPLSAPO 10X objective (Olympus America Inc., Center Valley, PA), and the Micro-Manager open source microscopy software. Animals were tracked automatically using a custom worm tracker (coded in Matlab).

Image analysis was performed using custom MATLAB scripts (Mathworks, Inc. Natick, MA) which identified the fluorescent neuron (the only bright particle in the head), measured the background fluorescence in its vicinity, and calculated the background subtracted mean fluorescence intensity of the identified particle. Velocities in Fig. 2.7B were calculated based on the displacement of the imaged cell. Experiments were performed on at least three independent days and day-to-day inconsistencies were not identified.

4.3.3 Optogenetics

Set-up

For data shown in Figs. 2.12 and 4.9:

Optogenetic assays were performed in 1.1x1.1 mm microfluidic "artificial dirt" chambers in which young adult animals could move freely; a chip contained up to 24 chambers and a single animal was placed in each chamber (Fig. 4.9) The chambers contained 1 mM all trans-retinal (ATR) in NGM. Blue light illumination ($\lambda = 475\pm15$ nm) was supplied by a Luxeon Star 7-LED assembly with a diffused optic array driven by a 700 mA FlexBlock driver. The LED assembly was mounted to the scopes approximately 7 cm from the sample location. Prior to the experiment animals were grown on NGM plates seeded with 1 μl 100 mM ATR in 250 μl OP50 bacteria in LB.

For data shown in Fig. 2.12:

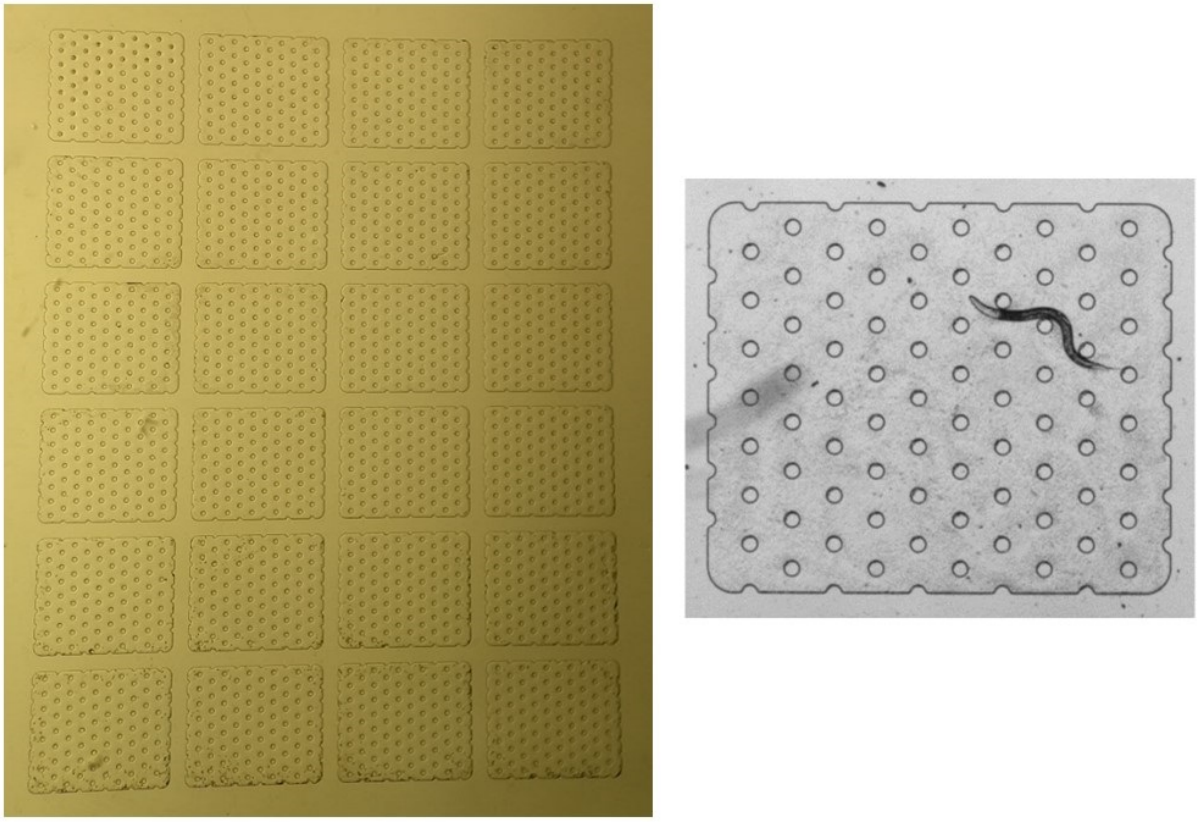

Figure 4.3: **"Artificial dirt" microfluidic chambers.** Left: a microfluidic chip with 24 individual chambers (no animals present). Right: a single nematode crawling in one of the 1.1x1.1 mm microfluidic chambers. The circular features are columns that span the height of the chamber (i.e., the dimension not visible in this top-down view). This individual is not an adult but an L4, the last larval stage before adulthood.

Light intensity at the location of the animals was set to 0.8 mW/mm^2. Transgenic animals expressing the light-gated ion channel channelrhodopsin (ChR2) in all serotonergic neurons on a *lite-1* mutant background (see Chapter 2 Methods) were illuminated for 30 sec in the presence of 1 mM ATR. Control animals were assayed in the absence of ChR2 and presence of ATR. Experimental animals were grown on ATR-seeded NGM plates.

For data shown in Fig. 4.9:

Light intensity at the location of the animals was set to 1.25 mW/mm^2. Transgenic animals expressing the light-gated ion channel channelrhodopsin (ChR2) in all cholinergic neurons were illuminated for 20 sec in the presence of 1 mM ATR. Control animals were assayed in the absence of ATR.

Frame subtraction analysis of motion

For data shown in Fig. 2.12:

The level of activity of the animals was assayed using the frame subtraction method as described below. Frame subtraction data was obtained from the raw images using custom Matlab script (Mathworks Inc., Natick MA) that utilized the Matlab image processing toolbox. In order to vary the interval of frame subtraction, the images were acquired at 10 frames per second and down-sampled appropriately.

The frame subtraction method is essentially the beam crossing principle applied at the level of a single pixel. Pairs of temporally adjacent video images are subtracted. Gray-scale pixel values change if there is any movement between the two images. The timescale, Δt, is therefore set by the frame rate of image acquisition and typically varies between 0.5-10 sec, depending on the image magnification and type of camera. The frame subtraction method is therefore a beam-crossing method with one pixel resolution (corresponding to approximately 10 μm in our setup) for movement detection. Due to electronic noise inherent in digital cameras, pixel brightness fluctuates slightly; accordingly, a threshold must be applied to differentiate between true animal motion and mere noise. However, this threshold need not

be finely tuned if the imaging set up is optimized to yield a strong contrast between the animal and background. Lastly, animal size can vary by genotype, so properly quantifying movement requires normalization of the number of pixels moved to the average total number of pixels that comprise the animal's body.

In order to obtain the timescales of slowdown and recovery, as described in the text, a single exponential function was fitted to each dataset using the Matlab curve fitting toolbox. The goodness of fit (R^2) was higher than 0.9 in all cases except for the recovery of the faster recovering *lite-1; Ex[Ptph-1::ChR2]* line (shown in orange), where $R^2 = 0.73$. Experiments were performed on three independent days and day-to-day inconsistencies were not identified.

Body length quantification

Data shown in Fig. 4.9 were obtained from images acquired at a rate of 5 frames per second and analyzed using the posture-based method as described previously [133] and below.

To quantify post-stimulus recovery, we computed the latency between stimulus offset and the time body length returned to 98% of the pre-stimulus value, a threshold chosen to reduce the influence of outliers.

4.3.4 PyCelegans: high performance image analysis tool

This section describes a custom suite of tools, called PyCelegans, for image analysis on high performance parallel computing resources. PyCelegans allows for automated identification of a single worm's posture in each frame of a video recording. In brief, PyCelegans identifies the midline and the edges of the body of the animal in each frame, as well as the positions of the head and the tail. In the experiments reported in this dissertation, PyCelegans was use to track single animals; however, the modular design of PyCelegans could accommodate multi-animal tracking with appropriate modification.

Rate of data capture for recording hours-long behavior at a sufficiently high temporal resolution can exceed 100,000 images per experiment. For a dataset of this magnitude,

the required post-processing is the rate-limiting step of the experiment. Using PyCelegans, the rate-limiting component of the analysis scaled linearly with the number of available processing-cores. By using 256 cores we achieved a speed-up of two orders of magnitude relative to previous implementations. For proof of principle, analyses have been run on up to 1024 processors. The number of processors that could be utilized, for example, from publically available clusters, is in the tens of thousands for a single dataset.

The objective of the image-processing portion of PyCelegans is to identify the head, tail, and body of the animal and to compute secondary properties based on this identification (e.g., the body midline, perimeter, and orientation). Tertiary properties can then be computed from the resulting raw data.

Midline identification

PyCelegans identifies the body of the animal in each frame and calculates the coordinates of 100 points along its midline, ordered from head to tail. The rate of segmentation failure, where the animals could not be properly identified, was typically 5% of all frames. Frames in which the animal was not identified were excluded from datasets, but their timing was accounted for when time-stamping subsequent frames.

Some fundamental properties of animal shape and behavior are easily computed once the midline is identified. The first of these is the length of the animal, which is simply the cumulative Euclidian distances between pairs of adjacent points that comprise the midline. Body length is an appropriate correlate of optically induced muscle contraction (see Fig. 4.9) and is also a useful measurement in developmental studies (see [132, 133]). Another extractable feature is the center-of-mass (COM) velocity of the animal. The COM is defined as the center of the smallest rectangle that can contain the midline. To compute instantaneous velocity, a sliding window (with a temporal resolution of 1 sec, for example) can be applied; that is, the distance between the COM coordinates of a pair of frames (e.g., at t = 1 sec and t = 2 sec) is divided by the temporal interval between them; the computed velocity is

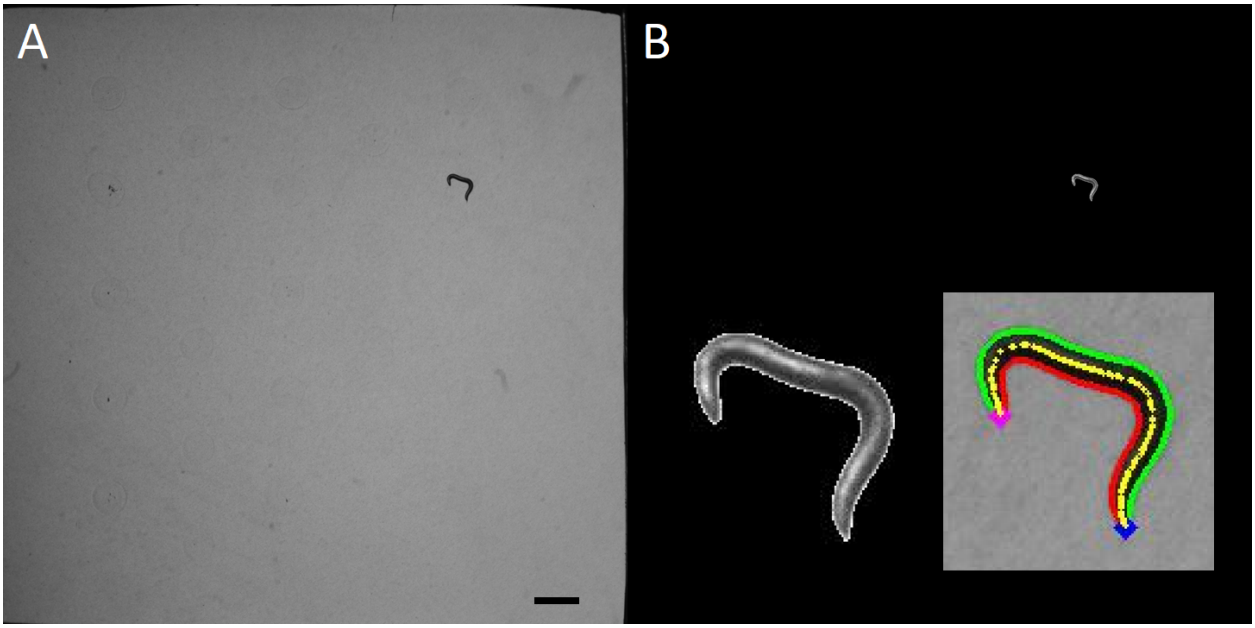

Figure 4.4: **Worm body midline identification.** Based on method described in [133].**A** Original image of worm crawling on the surface of an agar plate. Scale bar = 1 mm. **B** Background subtracted image with enlarged detail (lower left) and processed image (lower right). Yellow dots denote the midline; red and green curves denote the perimeter; pink and blue diamonds denote the head and tail, respectively.

assigned to the average of the two frames' time-stamps (in this example, t = 1.5 sec).

Body bend wave identification and behavioral state categorization

Our analysis of posture and locomotion was based on dividing the midline of the body of each animal into 20 segments and measuring the local angles between them (Fig. 4.5A). The raw angle dynamics data was typically smoothed with a Gaussian filter with a width of 5 frames (1 sec). This method extended previous analyses based on body curvature as a function of time and body-coordinate [52, 199]: we tagged individual body-bends, followed them from initiation to eventual demise, and recorded their origin, velocity, amplitude, and life-time. The identification of the midlines and individual body-bends enabled measurements of local properties as a function of the body-coordinate (e.g., quiescence of individual body-segments), as well as global behavioral patterns such as mean curvature, growth rate, or modes of locomotion.

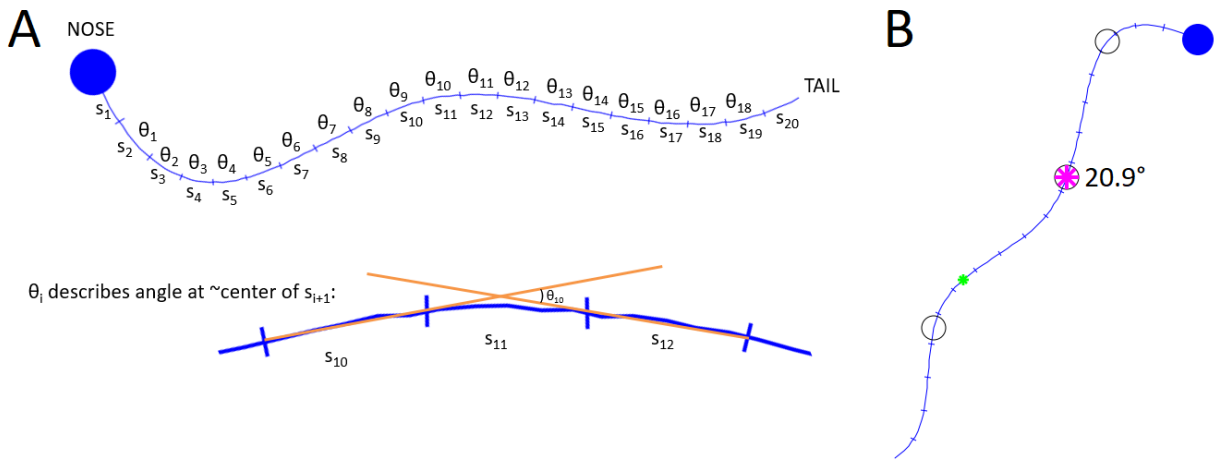

Figure 4.5: **Body angle schematic for orientation-agnostic representation of posture.** Based on method described in [133]. **A** The worm midline is divided into 20 segments (s_1 to s_{20}) and the local angle between segments is computed, where θ_i corresponds to the angle at the approximate center of segment s_{i+1}. **B** Sample posture with curvature peaks identified. Filled blue circle: nose. Open circles: fixed reference points at anterior, medial, and posterior body segments. Magenta star: peak curvature at reference segment with angle magnitude. Filled green circle: peak curvature at non-reference segment.

Body-bends were defined as positions of local spatial maxima or minima of the angles (Fig. 4.5B). The position of each bend was tracked from the time of its initiation until it decayed (typically at the head or the tail) or was interrupted by 10 consecutive missing frames. Forward locomotion was defined by the propagation of bends in the anterior-posterior direction that persisted for at least three consecutive midline segments. Backward locomotion was defined analogously. Quiescence of an individual segment was defined as an interval in which the rate of change of the corresponding angle did not exceed a threshold of 0.01 radians/sec.

At each time point, the whole-animal behavior was classified as forward, backward or dwelling by applying a majority rule to the dynamics of the individual body-bends. Dwelling occurred when the number of bends propagating in both directions was equal (typically zero). Whole-animal quiescence was defined as the state where the most anterior angle (between the head and neck segments) and at least 16 of the remaining 17 angles were quiescent. The fraction of time spent in each behavior was calculated with a running-average window of 10

min (see Fig. 4.7).

Static posture statistical analysis ("eigenworms")

Note: The following description refers to experiments reported in the last section of this chapter.

The set of angles derived from the midline of a worm as extracted by PyCelegans (see above) provides an adequate representation of an animal's movements. The following method, established by [182], applies dimensionality reduction to characterize worm postures in a simple coordinate space. Dimensionality reduction has proved to be a useful tool for the characterization of motor patterns in other animals, such as smooth pursuit eye movements in primates [142]. It is also a feature of some machine-vision algorithms for facial recognition [195].

Although nematodes lack discrete joints, the dimensionality of a worm's shape is effectively limited by the elasticity of its body wall and its finite number of muscles [64, 182]. A suitable low dimensional space may simply be a Euclidean projection of the high dimensional space (in our case, the set of 18 angles ($i = 1$ to $i = 18$) between midline segements). If such a projection is possible, the covariance matrix of body angles, $C(i, i') = \langle(\theta(i)-\langle\theta\rangle)(\theta(i')-\langle\theta\rangle)\rangle$ will have only a small number of nonzero eigenvalues. A shown in Fig. 4.8, for a set of worm postures collected from images of wild-type worms crawling on agar plates more than 93% of the total variance in angle along the body is accounted for by just four eigenvalues. Associated with each of the eigenvalues λ_μ is an eigenvector $u_\mu(i)$, also called a "principal component" of the function $\theta(i)$. Because only $K = 4$ eigenvalues are significant, the shape of the worm can be approximated by a superposition of "eigenworm" shapes,

$$\theta(i) \approx \sum_{\mu=1}^{K} a_\mu u_\mu(i),$$

where the variables $\{a_\mu\}$ correspond to a given posture's projected amplitudes onto the var-

ious principal components. Taking this idea further, it is possible to approximate (more roughly) the worm's shape by its projections onto just the first two principal components. In this way, the representation of the worm's posture is simplified from the original 100-dimensional midline vector (see above), to an 18-dimensional angle vector, to a two-dimensional coordinate in the space defined by the first two principal components. In Fig. 4.8, note that the first two principal components are approximately sinusoidal and thus correspond to oscillations of the body shape; different combinations of these two modes correspond to the propagation of a wave of contraction along the body.

The following section demonstrates how the "eigenworms" analysis, in conjunction with several of the other techniques described above, can be used to establish rigorous quantitative phenotypes associated with various disruptions of neurobiology in *C. elegans*.

4.4 Application: Adenylyl cyclase signaling in neurons and muscles

4.4.1 Background

The preceding chapters of this dissertation addressed foraging behavior. Foraging depends, of course, on locomotion. As many questions remain about locomotion per se, it is attractive to use the tools described above to probe the genetic basis of locomotion.

Hundreds of genes are known to impact locomotion in *C. elegans* [10]. Computational tools can be applied to extract detailed quantitative information from a video recording of a crawling nematode and thereby illuminate non-obvious phenotypes. Well-defined quantitative phenotypes can yield novel insights into gene function and help establish mechanistic descriptions of nervous system function and behavior.

Among the genes involved in locomotion are dozens that encode the machinery of the neuromuscular junction (NMJ), the chemical synapse between a motor neuron and a muscle cell [155]. At the NMJ, a motor neuron releases synaptic vesicles containing acetylcholine

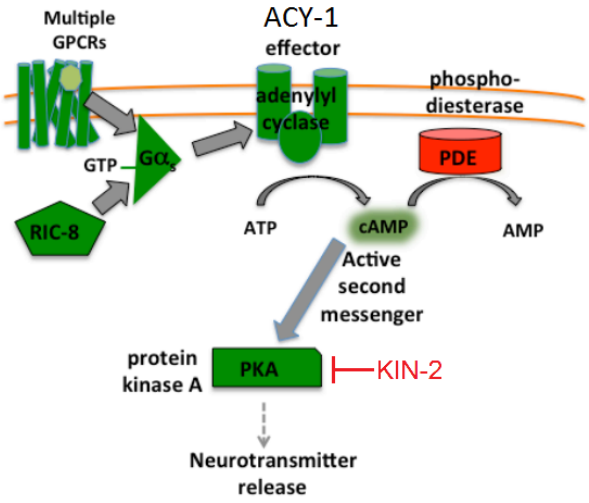

Figure 4.6: **Gα_s signaling in motor neurons.** Adapted from [105]. Solid grey arrows indicate direct physical interactions. Dashed arrow indicates a poorly understood effect. Green, proteins that promote Gα_s signaling; red, proteins that inhibit Gα_s signaling.

(ACh). Binding of ACh to receptors on the muscle cell activates cation channels embedded in the muscle membrane, resulting in depolarization of the muscle cell and, subsequently, muscle contraction [156]. *C. elegans* locomotion is a roughly sinusoidal undulation in which a wave of muscle contraction propagates along the anterior-posterior axis of the body [135, 203]. Thus, locomotion depends upon coordinated muscle contractions, which in turn depend upon proper functioning of the NMJ.

Numerous genes expressed in motor neurons regulate stages of synaptic vesicle release including trafficking, docking, priming, and fusion [155]. Genes expressed in muscle cells regulate ion flow and the propagation of depolarization and contraction [159]. Many genes that are hypothesized to play a role in the functioning of the NMJ are expressed in both neurons and muscle cells [155]. Accordingly, it is important identify the site of action of these genes insofar as they contribute to muscle contraction and, therefore, to locomotion. One such gene is *acy-1*, which encodes an adenylyl cyclase (ACY) and is part of the Gα_s pathway that regulates synaptic vesicle release [14, 165]. Illustrated in Fig. 4.6, the Gα_s pathway can summarized as follows: binding of certain ligands to Gα_s protein-coupled receptors

activates ACY; ACY converts ATP to the second messenger cAMP; cAMP activates protein kinase A (PKA); PKA phosphorylates components of synaptic vesicle release machinery, thereby altering the synaptic strength of the NMJ [105]. Through this pathway, *acy-1* may contribute to synaptic strength by affecting the "readily releasable" (i.e., primed) pool of synaptic vesicles [31, 32, 184]. However, because *acy-1* is expressed in both neurons and muscles, it is unclear whether *acy-1* acts in both or just one cell type to modulate muscle contraction.

To clarify the role of *acy-1* in muscle contraction, we compared the locomotion of freely behaving wild-type animals to that of *acy-1* mutants and other related strains. Applying machine-vision tools for posture analysis to video recordings of crawling nematodes, we determined that loss of *acy-1* in either neurons or muscles impairs locomotion, with greater defects associated with loss of *acy-1* in neurons. We extended this analysis by optically activating cholinergic motor neurons and quantifying the resulting body contraction in wild-type animals, *acy-1* mutants, and related strains. The optogenetics experiments indicated that sustained contractions require appropriate cAMP levels in body wall muscles whereas acute responses require appropriate cAMP/PKA signaling in cholinergic neurons.

4.4.2 Results

Loss of *acy-1* in neurons or muscles causes multiple locomotion defects.

To explore locomotion phenotypes of *acy-1* mutants and related strains, we simply made video recordings of individual animals crawling on agar plates for a period of one hour. In each experiment the agar plate included a patch of bacterial food; thus, we were able to obtain locomotion for animals both on and off food. The analyses described below address primarily data obtained while the animal was on the food patch; differences in behavior between on- and off-food periods are outside the scope of this methods chapter, but the data are presented for the curious reader (see Fig. 4.7)

Genotype	Description	Designation in text	Ref.
acy-1(ce2)	Gain-of-function	*acy-1(gf)*	[162]
kin-2(ce179)	Null mutation of a regulatory subunit of PKA	*kin-2*	[165]
acy-1(nu329)	Partial loss-of-function	*acy-1(lf)*	[16]
acy-1(pk1279); Ex67[myo-3::acy-1(+)]	Tissue-specific rescue of wild-type *acy-1* in body wall muscles on a null *acy-1* background	*acy-1;[myo-3::acy-1(+)]*	[154]
acy-1(pk1279); Ex87[myo-3::acy-1(ce2)]	Tissue-specific rescue of gain-of-function *acy-1* in body wall muscles on a null *acy-1* background	*acy-1;[myo-3::acy-1(gf)]*	[154]
acy-1(pk1279); Ex165[rab-3::acy-1(+)]	Tissue-specific rescue of wild-type *acy-1* in neurons on a null *acy-1* background	*acy-1;[rab-3::acy-1(+)]*	[154]

Table 4.1: Strains used for locomotion assays.

As described in the Methods section above, we used the PyCelegans tool to characterize locomotion. The genotypes of strains compared to wild-type animals in this study are summarized in Table 4.1.

Relative to wild-type animals, *acy-1(gf)* and *kin-2* mutants displayed more movement overall, faster crawling during forward locomotion, and faster propagation of body waves during forward locomotion (Fig. 4.7A-C). Note that because *kin-2* encodes a negative regulator of PKA, it is logical that *kin-2* and *acy-1(gf)* mutants are phenotypically similar; upregulation of *acy-1* or its downstream targets causes hyperactivity. In contrast, *acy-1(lf)* mutants, *acy-1;[myo-3::acy-1(+)]* animals, and *acy-1;[myo-3::acy-1(gf)]* animals all displayed reductions in these features of locomotion. Note that in these two rescue strains, *acy-1* is present in muscles but absent in neurons. Therefore, it is apparent that loss of *acy-1* in neurons is detrimental to locomotion. Additionally, we found that *acy-1;[rab-3::acy-1(+)]* animals, in

which *acy-1* is present in neurons but absent in muscles, display similar locomotion defects. Thus, disruption of *acy-1* in muscles also adversely impacts locomotion. The importance of *acy-1* levels in both neurons and muscles was further underscored by two control strains, in which only the *acy-1(+))* rescue transgene was present in either tissue type; both of these strains displayed locomotion defects as well, presumably from overexpression of *acy-1(+)*. Note that in all strains, defects relative to wild-type with respect to propagation velocity of body waves tended to be more mild than defects in overall movement or forward crawling speed. This difference is explored further below.

We next asked whether *acy-1* mutants and related strains displayed different behavioral state frequencies than wild-type animals. As described in the Methods section above, we used patterns in body angle fluctuations, such as the propagation of waves of curvature, to label portions of video recordings with any of four behavioral states: forward crawling, reverse crawling, dwelling, and quiescence. The behavioral state frequencies of the two hyperactive mutants, *kin-2* and *acy-1(gf)*, were similar to wild-type (Fig. 4.7D; see also Fig. 7A in [133]). However, all other strains assayed displayed decreases in forward crawling and increases in dwelling and, in some cases, quiescence. Thus, not only do these animals crawl more slowly than wild-type, they also spend less time crawling at all. This suggests that *acy-1* may function in muscles and neurons to promote wild-type behavior patterns, rather than merely affecting locomotion speed.

Loss of *acy-1* in neurons or muscles is detrimental to proper posture regulation required for forward crawling.

We noted that while *acy-1* defective mutants showed considerable deficits in crawling speed, the velocity of body bend propagation in these animals was only slightly slower than in wild-type. If not a difference of body bend propagation, why might explain the slow crawling of *acy-1* defective mutants? To answer these question, we performed the principal component analysis of postures established by [182] and detailed in the Methods section above. This

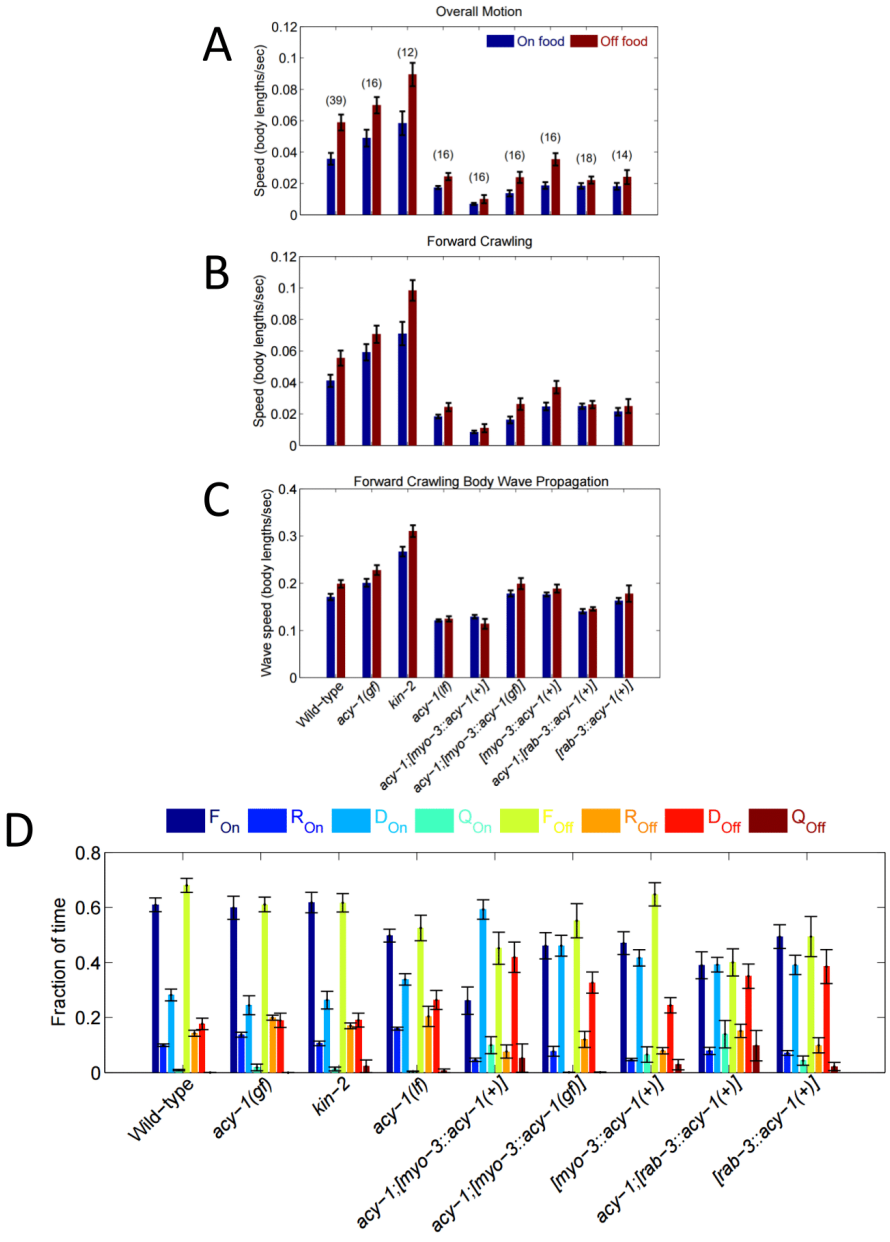

Figure 4.7: **Loss of *acy-1* in neurons or muscles reduces overall motion, forward crawling speed, propagation velocity of body bends, and fraction of time spent on forward crawling.** **A** Mean center-of-mass speeds throughout full video recordings. **B** Mean center-of-mass speeds during forward crawling subsets of recordings (see Methods and panel (**D**)). **C** Mean body wave propagation speeds during forward crawling subsets of recordings (see Methods and panel (**D**)). **D** Mean fractions of time spent in each of four behavioral states (F = forward; R = reverse; D = dwelling; Q = quiescence) (see Methods). "On" and "Off" denote subsets of recordings during which animals were on or off the food patch, respectively. Bars and error bars depict mean ± s.e.m, respectively. In panel (**A**), the number of animals assayed is noted in parentheses for each strain (same data set for all panels).

method takes advantage of the fact that all points along a worm's body do not vary independently; rather, its muscles contract in a coordinated manner such that dimensionality of its shape during crawling is limited. In brief, we used tens of thousands of frames categorized as forward crawling in wild-type animals to compute a covariance matrix of body angles $C(i, i')$, where i refers to the segmentation of the worm as described above. We then computed the eigenvalues of $C(i, i')$ and then σ_K^2, the fraction of the total variance captured by K modes, determining that just four modes captured 93% of the variance (Fig. 4.8A). Corresponding to each mode is an eigenvector describing angle versus position along the worm; these are referred to as the the eigenworms $u_\mu(i)$ (Fig. 4.8B). Note that the first two modes are roughly sinusoidal (and out of phase) and therefore could themselves form an adequate basis for describing postures during forward crawling. Accordingly, considering the full sets of forward locomotion postures (i.e., frames labeled as parts of forward locomotion bouts) from wild-type and all other strains presented in Fig. 4.7, we computed the joint probability densities of projections of these postures onto the first two eigenworms (Fig. 4.8C). The two-dimensional coordinate space is defined by a given posture's projected amplitudes on $u_1(i)$ and $u_2(i)$, denoted a_1 and a_2, respectively. Note that strains that exhibited wild-type, the hyperactive mutants *acy-1(gf)* and *kin-2*, and some other strains each show two peaks in their projection distributions, whereas the strains with the most defective locomotion such as *acy-1;[myo-3::acy-1(+)]* and *acy-1;[myo-3::acy-1(gf)]* each show a single peak near the origin. As illustrated in Fig. 4.8D, if "postures" are reconstructed using the coordinates at these peaks, wild-types animals show properly sinusoidal patterns whereas defective mutants show nearly straight conformations (note that these "postures" are in fact vectors of body angles which, while similar to the true postures they correspond to, are slightly different; see Methods). That is, defective strains typically fail to generate the sinusoidal postures required for proper locomotion. The extreme defect in posture regulation demonstrated by *acy-1;[myo-3::acy-1(+)]* and *acy-1;[myo-3::acy-1(gf)]* animals supports the conclusion that loss of *acy-1* in neurons severely impacts locomotion.

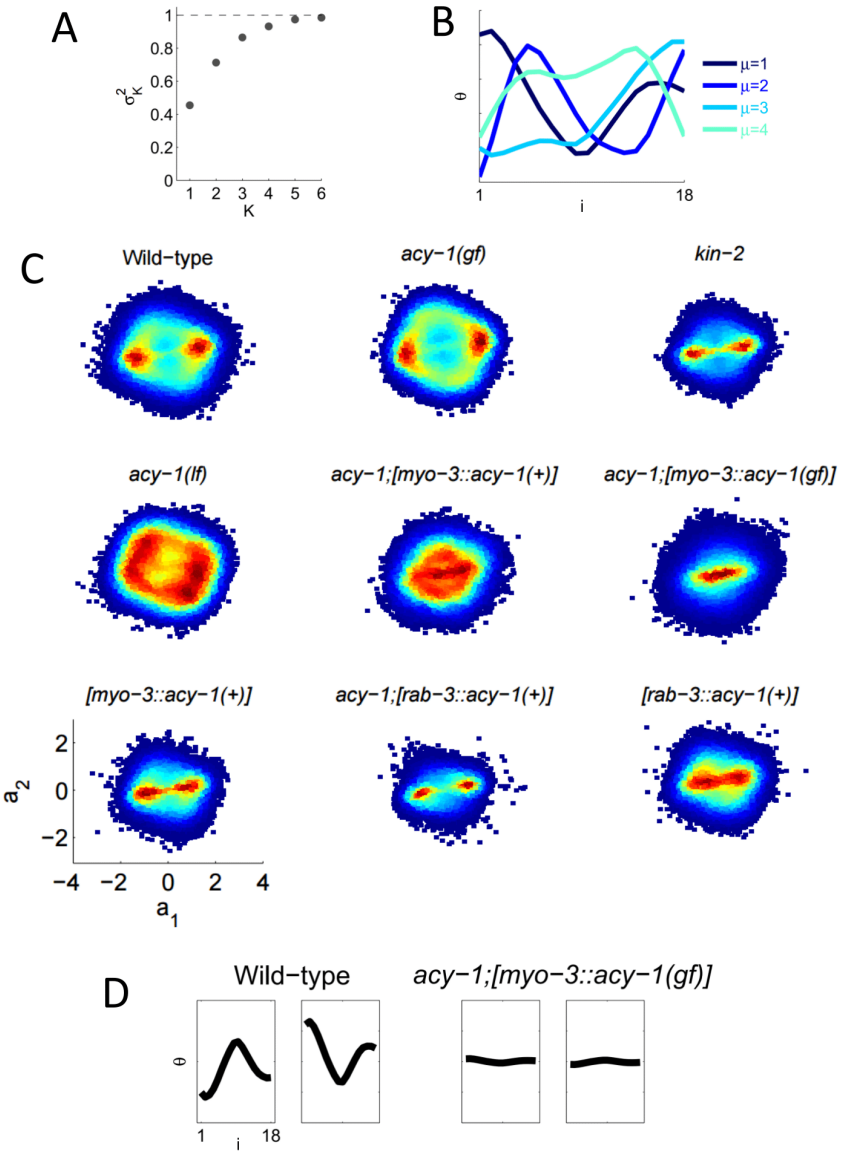

Figure 4.8: **Loss of *acy-1* in neurons or muscles is detrimental to proper posture regulation required for forward crawling.** The covariance matrix of body angles $C(i, i')$ was computed from tens of thousands of images across 39 wild-type animals. **A** After finding the eigenvalues of $C(i, i')$, we computed σ_K^2, the fraction of the total variance captured by K modes (see Methods); 93% of the variance was captured by the first four modes. **B** Corresponding to each mode is an eigenvector describing angle versus position along the worm; these are referred to as the the eigenworms $u_\mu(i)$. **C** Joint probability densities of projections of forward crawling postures onto the first two eigenworms. The two-dimensional coordinate space is defined by a given posture's projected amplitudes on $u_1(i)$ and $u_2(i)$, denoted a_1 and a_2, respectively. Red areas indicate highest density; blue areas indicate lowest density. Tens of thousands of postures from each genotype were analyzed. **D** Sample "postures" (see text) reconstructed from peaks of the distributions in **(C)** of wild-type (left) and *acy-1;[myo-3::acy-1(gf)]* (right) animals; peaks around the origin (as in the latter case) reflect defective non-sinuous postures.

Wild-type sustained contractions require appropriate cAMP levels in body wall muscles whereas acute responses require appropriate cAMP/PKA signaling in cholinergic neurons.

Having quantified locomotion defects associated with loss of *acy-1* signaling, we next asked whether related defects could be measured in the magnitude of muscle contractions induced by optical stimulation. At the NMJ, ACh released from motor neurons binds to receptors on the muscle cell and initiates muscle contraction. In freely moving animals, we optically stimulated cholinergic neurons that innervate body wall muscles and quantified the resulting muscle contraction dynamics; an animal's length serves as an appropriate correlate of muscle contraction because its body shortens when all body wall muscles contract simultaneously [112].

When we optically stimulated cholinergic neurons in otherwise wild-type animals expressing the transgene *zxIs6* (see Methods) for 20 sec, animals showed sustained body contraction (averaged over the stimulus period) to 94.1 ± 0.5% of initial body length (Fig. 4.9A). The magnitude of sustained contraction in *acy-1;[myo-3::acy-1(+)]* animals (also expressing the transgene *zxIs6*) was similar to wild-type. However, *acy-1(lf)*, *acy-1(gf)*, and *kin-2* mutants expressing the transgene *zxIs6* all displayed more minor sustained contractions (i.e, the reduction in body length during the stimulation period was smaller) (Fig. 4.9A). For example, *acy-1(gf)* mutants contracted only to 95.9 ± 0.4% of initial body length. Transgenic *zxIs6* worms grown without all-trans retinal did not contract during illumination (Fig. 4.9A). Because levels of cAMP in body wall muscles are approximately normal in *acy-1;[myo-3::acy-1(+)]* animals but are abnormal in *acy-1(lf)*, *acy-1(gf)*, and *kin-2* mutants, we concluded that wild-type sustained contractions require appropriate cAMP levels in body wall muscles.

Note: in subsequent text and in Fig. 4.9, it is implied that all animals described express the zxIs6 *transgene; for simplicity, animals are denoted by "background" genotype.*

Responses sustained over a 20 sec stimulus period may not be very physiologically rel-

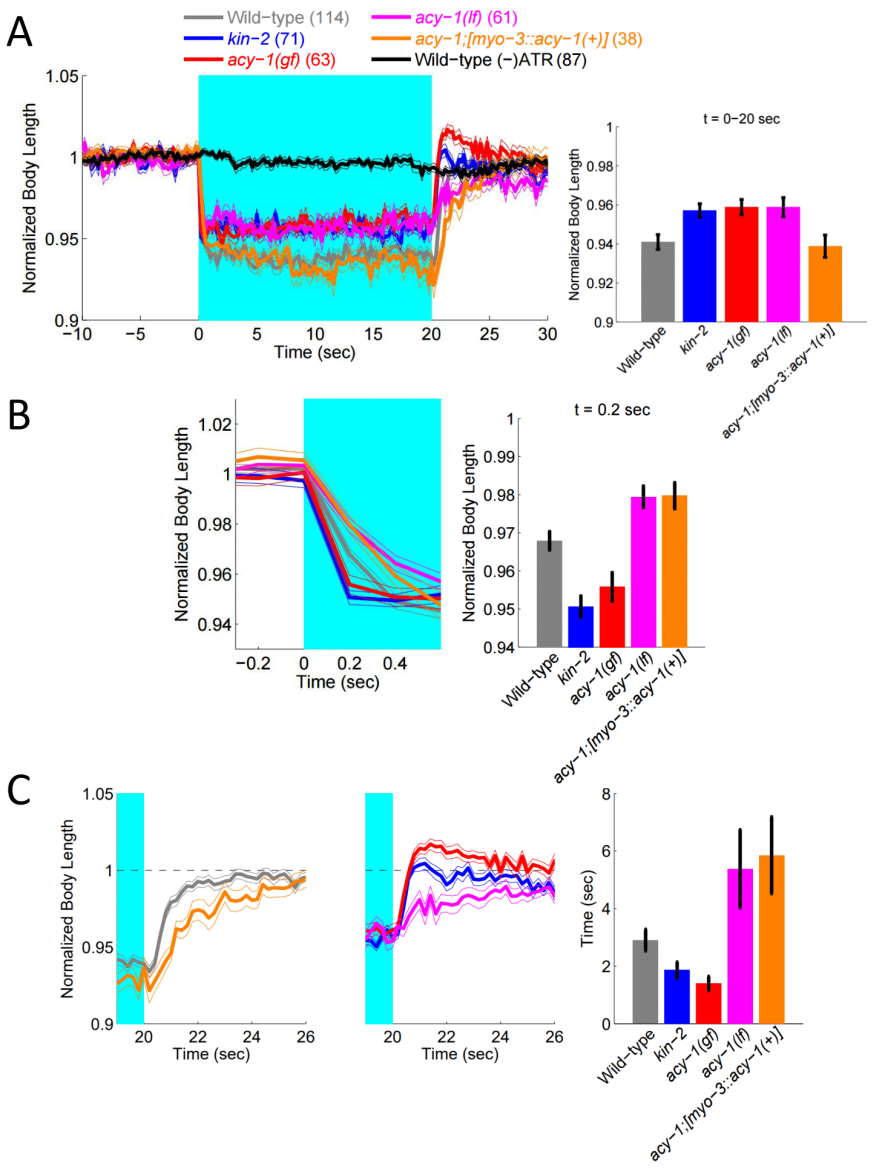

Figure 4.9: **Wild-type sustained contractions require appropriate cAMP levels in body wall muscles whereas acute responses require appropriate cAMP/PKA signaling in cholinergic neurons. A** left: body length in the peri-stimulus period; right: mean body-length during the stimulus. **B** left: body length immediately before and after stimulus onset; right: mean body-length immediately after stimulus onset. **C** left and middle: body length immediately before and after stimulus offset - traces are split into two plots so that genotypes with similar starting points (i.e., body lengths at the time of stimulus offset) can be easily compared; right: mean time to recover to 98% of pre-stimulus body length. The shaded area depicts the period in which the blue light was on. Thick and thin lines or bars and error bars depict mean ± s.e.m, respectively. In panel (**A**), the number of trials (approximately 5 per animal assayed) performed is noted in parentheses for each strain (same data set for all panels). Control animals were assayed in the absence of ATR.

evant as muscle contractions involved in locomotion occur on much finer timescales [131]. We therefore next considered responses immediately following stimulus onset. In images captured just 0.2 sec after stimulus onset, we found that wild-type animals showed acute body contraction to 96.8 ± 0.2% of initial body length (Fig. 4.9B). In contrast, immediate post-onset contraction was greater in *acy-1(gf)* and *kin-2* mutants, to 95.6 ± 0.35% and 95.1 ± 0.3% of initial body length, respectively (Fig. 4.9B). Displaying the opposite phenotype, *acy-1(lf)* mutants and *acy-1;[myo-3::acy-1(+)]* animals exhibited less contraction immediately following stimulus onset, to 97.9 ± 0.3% and 98.0 ± 0.3% of initial body length, respectively (Fig. 4.9B).

At the time of stimulus offset, muscles relax and the animals return to their resting body length. However, this relaxation is not instantaneous. We therefore examined the time course of relaxation. For each individual animal, we quantified the latency between stimulus offset and the time body length returned to 98% of the pre-stimulus value, a threshold chosen to reduce the influence of outliers. In Fig. 4.9C, body length traces for the five genotypes presented are split into two plots so that animals with similar starting points (i.e., body lengths at the time of stimulus offset) can be more easily compared. We found that wild-type animals relaxed on a timescale of 2.9 ± 0.3 sec (Fig. 4.9C, left and right). In contrast, *acy-1(gf)* and *kin-2* mutants relaxed more quickly, on timescales of 1.4 ± 0.25 sec and 1.85 ± 0.3 sec, respectively (Fig. 4.9C, middle and right). The rapid relaxation at stimulus offset displayed by these mutants is consistent with their enhanced contraction immediately following stimulus onset; in both cases, these acute responses are exaggerated relative to wild-type. The opposite effect is displayed by *acy-1(lf)* mutants and *acy-1;[myo-3::acy-1(+)]* animals: in these animals, relaxation occurs on timescales of 5.4 ± 1.0 sec and 5.85 ± 1.3 sec, respectively (Fig. 4.9C, left, middle, and right). Again, these protracted relaxation phenotypes are consistent with the strains' reduced (relative to wild-type) contractions immediately following stimulus onset.

Levels of cAMP/PKA in neurons are reduced in *acy-1(lf)* mutants and *acy-1;[myo-3::acy-*

1(+)] animals and elevated in *acy-1(gf)* and *kin-2* mutants. Accordingly, contractions immediately following stimulus onset and relaxation time courses after stimulus offset indicate that acute responses to stimulation require appropriate cAMP/PKA signaling in cholinergic neurons. Crucially, because *acy-1;[myo-3::acy-1(+)]* animals have approximately normal levels of cAMP/PKA in muscles but not in neurons, the acute response defects associated with this strain can be ascribed to the disruption of *acy-1* function in neurons specifically. This suggests that *acy-1* acts primarily in neurons to regulate muscle contraction and, consequently, locomotion.

Note: all data presented in Fig. 4.9 correspond to experiments in which the blue light stimulation intensity was 1.25 mW/mm^2; we also performed experiments with stimulation intensity of 2.5 mW/mm^2 but, because of apparent saturation effects, those data are not shown here.

4.4.3 Strains

C. elegans strains were maintained and grown according to standard protocols [21]. The following strains were used: wild type strain N2, KG518 *acy-1(ce2gf)*, KG532 *kin-2(ce179)*, KP1182 *acy-1(nu329)*, JER1249 *acy-1(pk1279); Ex67[myo-3::acy-1(+)]*, JER1327 *acy-1(pk1279); Ex77[myo-3::acy-1(ce2gf)]*, INV49000 *Ex67[myo-3::acy-1(+)]*, KG1040 *acy-1(pk1279); Ex165[rab-3::acy-1(+)]*, INV49001 *Ex165[rab-3::acy-1(+)]*, JER893 *zxIs6[unc-17::ChR2::YFP+lin-15(+)]*, JER1469 *zxIs6[unc-17::ChR2::YFP+lin-15(+)]; kin-2(ce179)*, JER1470 *zxIs6[unc-17::ChR2::YFP+lin-15(+)]; acy-1(ce2gf)*, JER1472 *zxIs6[unc-17::ChR2::YFP+lin-15(+)]; acy-1(+)*, JER1480 *zxIs6[unc-17::ChR2::YFP+lin-15(+)]; acy-1(nu329)*. The KG1040 strain was a gift from Kenneth Miller's laboratory (Oklahoma Medical Research Foundation).

4.5 Discussion

Note: this discussion addresses the study of adenylyl cyclase signaling and muscle contraction presented in the preceding section.

We have shown that in *C. elegans* the function of adenylyl cyclase in neurons and muscles is required for wild-type locomotion patterns. Loss of *acy-1* in neurons resulted in more severe defects than did loss of *acy-1* in muscles. Optically evoked muscle contractions revealed that sustained contractions depend upon appropriate cAMP levels in body wall muscles whereas acute responses (i.e., initiation of contraction and relaxation) require appropriate cAMP/PKA signaling in cholinergic neurons.

In strains with loss of *acy-1* in neurons or muscles, defects in propagation velocity of body waves tended to be more mild than defects in overall movement or forward crawling speed. We argued that this discrepancy resulted from the failure of these strains to generate proper postures for locomotion. Another possibility exists that we did not fully explore: though body waves propagated at near normal speeds, they perhaps did not survive as long in time or space. That is, it may be that waves of contraction generated by defective strains failed to propagate along the full length of the body. These statistics can be extracted from our existing data sets.

Our optical simulations of muscle contraction provided insight into the function of *acy-1* in neurons. Technical limitations prevented us from performing the same experiments with transgenic animals in which *acy-1* was rescued neurons but not muscles. As these transgenics exhibited defects in locomotion in our other experiments, it is likely that they would yield interesting phenotypes in optogenetic assays as well. We would expect these trangenics to exhibit roughly normal acute respones but defective sustained respones, the opposite of the phenotype displayed by transgenics in which *acy-1* was rescued in muscles but not neurons.

Electrophysiological and electron microscopy studies would complement the results summarized in this chapter. We obtained preliminary data (Richmond lab; data not shown) suggesting that evoked currents in muscles require appropriate cAMP/PKA signaling in

cholinergic neurons and that cAMP-defective strains exhibit altered profiles of vesicle localization in cholinergic neuron axon terminals. Taken together, these results implicate *acy-1* and its downstream effectors in mediation of muscle contraction, perhaps through regulation of synaptic vesicle priming.

CHAPTER 5

CONCLUSIONS AND DISCUSSION

In a spatially and temporally dynamic environment, animals must forage efficiently in order to thrive. Although foraging is studied extensively in a wide range of species both experimentally and theoretically, the biological substrates of foraging remain poorly understood. To approach a mechanistic understanding of foraging, I used continuous video recordings of *C. elegans* nematodes in patchy landscapes. Comparing quantitative behavioral phenotypes of wild-type animals and mutants, I probed the genetic basis of foraging. Using physiological imaging and optical stimulation of neurons, I also characterized cellular mediation of foraging.

In this dissertation, I provide evidence that a key role of serotonergic signaling in *C. elegans* is to accelerate decision-making and promote efficient exploitation of resources in complex environments. My work primarily implicates the serotonergic neuron type NSM, the serotonin-gated chloride channel MOD-1, and the ortholog of mammalian 5-HT1 metabotropic serotonin receptors SER-4 in mediating this process. In addition, I demonstrate how different cells can use a common modulator to affect locomotion in complementary manners.

I further show that, like 5-HT, TGF-β pathway genes contribute to both gradual preemptive slowing as animals approach food and abrupt slowing upon encounter. My observation that double mutants of both *daf-7* and *tph-1* exhibit exaggerated defects relative to single mutants supports the hypothesis that TGF-β and 5-HT function in parallel rather than in series. Finally, my work implicates both mechanosensory and chemosensory transduction in mediating responses to food encounter, with *daf-7* primarily involved in chemosensation.

Taken together, the findings described above demonstrate how multiple signaling pathways play overlapping roles in regulating behavioral responses. Moreover, my work indicates that molecules implicated in mediation of developmental processes can also function on acute timescales to tune behavior.

In this chapter, I outline possible extensions of my foraging studies, discuss the evolutionary context of *C. elegans*, and speculate about the future of comparative genetic neuroethology.

5.1 Future directions for the study of foraging

In this dissertation, I elucidated cellular and molecular mechanisms of responses to encounter with food and foraging in a patchy landscape. My studies could be extended in several ways. One possible direction is the identification of additional signaling pathways that contribute to foraging behavior. This is essentially the motivation underlying the progression from Chapter 2 to Chapter 3; I characterized the role of TGF-β signaling in foraging behavior and explored how it complements 5-HT signaling. As the logic of investigating new pathways is already thoroughly discussed in this dissertation, I will address here other avenues for the extension of my work.

5.1.1 More complex environments

The study of the role of 5-HT and TGF-β in regulation of foraging behavior could be extended through the consideration of more complex environments. For example, *C. elegans* is able to distinguish between numerous varieties of bacterial food, showing preference for familiar over unfamiliar food and seeking out more nutritious food [173, 178]. *C. elegans* also displays experience-dependent avoidance of pathogenic bacteria. *C. elegans* initially prefers *Pseuodomonas aeruginosa* over the standard diet of *E. coli* (OP50); however, *P. aeruginosa* causes intestinal infection and, after a few hours, nematodes leave the pathogenic food and return to their standard lawn [210]. Accordingly, one could construct an "advanced arena" of micro-patches in which the quality of food varies from patch to patch. Thus, while feeding at a given patch there is a certain cost associated with dwelling rather than exploring, inversely related to the quality of the current patch. Investigating behavior in such an environment

could connect my work to the field of neuroeconomics, the study of how animals assign value to objects in the environment and select between competing alternatives [26].

Characterizing the behavior of wild-type animals in arenas of varying food qualities would itself be an extensive endeavor, as numerous arrangements are possible. A natural next step would be to examine how perturbations of 5-HT or TGF-β signaling affect the dynamics of foraging in these environments. One could also ask whether defects in chemosensory neurons required for differentiation between food types interact with foraging decisions on acute and long timescales.

5.1.2 Foraging theory

As referenced above and in Chapter 1, studies of *C. elegans* behavior in patchy environments could also be examined within a theoretical framework. In 1976, Eric Charnov posited the Marginal Value Theorem (MVT), which states that animals should spend more time in and extract more resources from patches when travel times are long (i.e., when distances between patches are large), because an understaying forager loses opportunities associated with exploiting the current patch; conversely, when travel times are short a forager loses future opportunities by overstaying [33, 180]. The relationship between time and energy extracted from a patch is described by a gain function such that the rate-maximizing patch exploitation time matches the energy intake rate in a uniform environment of the same average density (Fig. 5.1).

The micro-patch "arena" experiments reported in Chapter 2 provide an opportunity to test optimal foraging theory. Travel time could be manipulated by altering the spacing between patches. If the MVT applies, increasing travel time should be associated with longer give-up times (i.e., longer bouts of foraging at individual patches) in wild-type animals. Furthermore, comparisons between wild-type animals and 5-HT signaling mutants (or TGF-β signaling mutants, though we did not perform arena assays with those) could be insightful. The foraging defect exhibited by 5-HT (i.e., the deficit relative to wild-type in fraction of

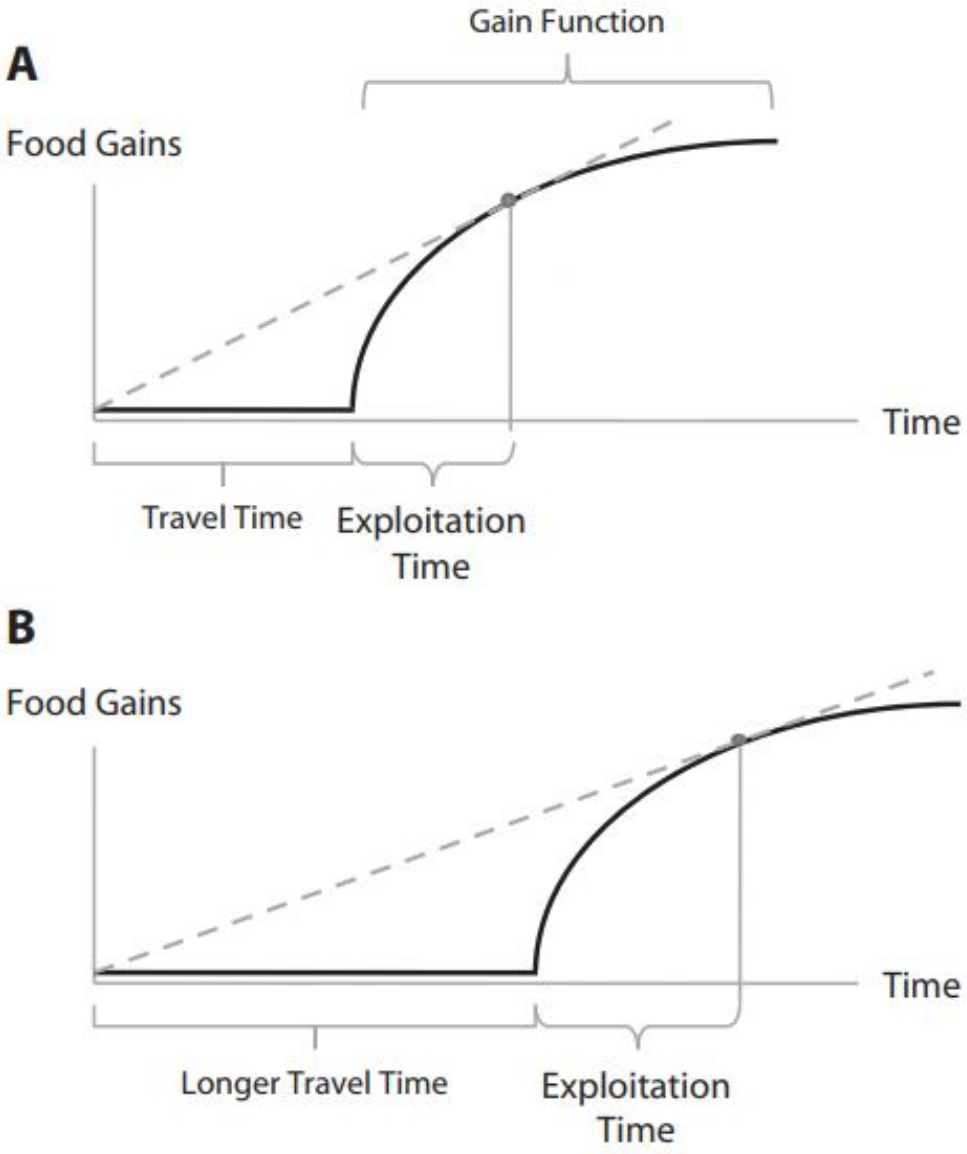

Figure 5.1: **Graphical model of patch exploitation.** Each plot shows the relationship between time and the amount of energy extracted from a patch. The forager gains no energy while it is traveling to the patch, so we show a flat line of height 0 during the travel phase of a patch exploitation cycle. The forager begins to obtain resources when it enters a patch, and we characterize this gain process by a decelerating but increasing curve. This gain function bends down because the resources in the patch are finite, so the rate of extraction must ultimately slow down. To find the patch exploitation time that gives the highest intake rate, we construct a straight line from the origin to the gain curve, so that this line is just tangential to the gain curve. The slope of this line is the intake rate (gains/total time), and the rate-maximizing patch exploitation time corresponds to the point of tangency (where the dashed line touches the curve). Panel (**A**) shows a short travel time (rich habitat), and panel (**B**) shows a long travel time (poor habitat). One can see that this tangent construction model predicts longer exploitation times in poorer habitats. Reproduced from [180].

total time spent on food or exploiting) signaling mutants may be exacerbated when travel times are longer, as the cost of failing to exploit a given patch scales with patch spacing. Conversely, when inter-patch spacing is small, mutants may exhibit a more mild defect. Consider that as inter-patch spacing is reduced to zero the arena landscape converges to the large patch landscape; in the large patch assay, mutants exhibited gradual rather then abrupt slowdown upon encounter but were nevertheless just as successful as wild-type animals in exploiting. Thus, a theoretical perspective and systematic manipulation of travel time could provide an additional test of the role of 5-HT (and other pathways) in foraging.

5.2 The *scala naturae* fallacy and *C. elegans*

Originating from Plato and fundamental to Christian theology in the Middle Ages, the concept of *scala naturae* (Latin for "ladder of being") states that all life is arranged along a hierarchy from most complex and god-like to most simple and profane [123]. Of course, our modern understanding of evolution and phylogenetics firmly refutes the existence of such a hierarchy in any meaningful biological sense. Yet, *scale natuae*-like thinking persists even amongst biologists when it comes to the relationship between humans and two preeminent model organisms, "the worm" (*C. elegans*) and "the fly" (*Drosophila melanogaster*).

Over the course of my dissertation work I have noticed that many in the scientific community are rather wedded to a conceptual hierarchy which states that *C. elegans* < *Drosophila* < human, in terms of complexity. The most obvious justification for this hierarchy comes from the composition of these animals' nervous systems: 302 neurons $< 10^5$ neurons $< 10^{11}$ neurons. Given these figures, it is not surprising that *Drosophila* and humans share many traits which are absent in *C. elegans* (e.g., elaborate sensory organs, action potentials in neurons, limbs, circadian sleep cycles, etc.) because *Drosophila* is perceived as being closer to humans than is *C. elegans*.

However, this way of thinking becomes problematic upon considering the overwhelming evidence that *C. elegans Drosophila* (both protostomes) are more closely related to each

other than they are to humans (deuterostomes). The phylogenetic relationship between these three animals paints a rather different picture with respect to the traits shared by *Drosophila* and humans but lacking in *C. elegans*. In light of the relevant phylogenetics, there are two evolutionary histories that can explain a given trait's status: either (a) the trait was present in the protostome-deuterostome common ancestor and was secondarily lost in *C. elegans* but retained in the other two animals, or (b) the trait was absent in the prostostome-deuterostome common ancestor and evolved independently in *Drosophila* and humans but never in *C. elegans*.

I have found that many biologists, including some of my close colleagues, are very resistant to this way of thinking. It seems obvious to them that *Drosophila* is closer to humans than is *C. elegans* due to the abundance of morphological traits that support this schema. The allure of this conceptual hierarchy is so powerful that some, even as they concede that humans are the outgroup among these three species, still insist that *Drosophila* is somehow closer to humans, a logical fallacy. In my view, the real problem is that without appreciating the actual phylogenetic relationships, one misses out on two essential aspects of the story of metazoan evolution: (1) convergence upon complex morphological traits and (2) secondary simplification.

Convergence refers to independent evolution of particular traits in separate lineages. Organisms that occupy similar ecological niches often display convergence of gross morphological traits (e.g., the body shapes of sharks and dolphins) [65]. Convergence provides evidence that evolution results in optimal solutions to biomechanical problems, for example [204]. As stated above, it is possible that some traits present in *Drosophila* and humans but not in *C. elegans* are due to convergent evolution in arthropods and chordates. However, stronger evidence exists that *C. elegans* lacks traits found in the other two species because of secondary simplification.

To examine the possible role of secondary simplification in the evolution of *C. elegans*, let us consider the fact that *Drosophila* and humans possess a complex brain and central

nervous system but *C. elegans* does not. Monophyly of the brain (i.e., the claim that protostome-deuterostome common ancestor had a brain) is partially corroborated by functional equivalence of a character identity gene: the *ems* (a gene required for head formation in *Drosophila*) homolog *ceh-2*[1] of *C. elegans* is able to rescue *ems* mutant brain defects in *Drosophila* [7, 84]. This provides limited evidence that *C. elegans* secondarily lost the character "tripartite brain" and perhaps a complex central nervous system as well. The same conclusion could be drawn for any other brainless bilaterian, including invertebrate chordates such as sea squirts and lancelets.

The fact that secondary simplification may explain the limited nature of the *C. elegans* nervous system has important implications for how we conceptualize *C. elegans* as a model organism. Instead of viewing *C. elegans* as a highly primitive relic of early metazoan evolution, we should recognize that *C. elegans* may be something like an optimization, a remarkable case in which the maximum repertoire of behaviors can be performed with the minimum number of neurons. With respect to this dissertation, consider for example our finding that bioamine signaling mediates a form of decision-making in *C. elegans*. As the role of bioamine signaling in decision-making is well-studied in arthropods (for examples, see [28, 63, 94]), it would be wrong to claim that our work shows the phenomenon to be more evolutionarily ancient than previously demonstrated. Rather, our work shows how bioamine signaling can mediate decision-making in a nervous system of only 302 neurons. The focus should be on the simplicity of the system (and, accordingly, the level of detail at which it can be studied) rather than the evolutionary implications which are already apparent from studies with *Drosophila*, for example.

1. Interestingly, *ceh-2* is a gene expressed only in the serotonergic NSM neurons which are discussed extensively in Chapter 2.

5.3 Comparative genetic neuroethology

The cost of DNA sequencing has been decaying exponentially for decades. In the last ten years, sequencing costs fell even faster than predicted by Moore's law, which states that the cost should drop by half every two years. In fact, sequencing is so inexpensive that it is now the cost of data storage that constitutes the bottleneck [128]. One important implication of advances in sequencing capabilities for the field of behavioral neuroscience is the feasibility of comparative studies.

C. elegans is one of approximately 30,000 identified species of nematodes; the total number of living species is hypothesized to be as high as 10 million [166]. The closest relatives of nematodes are the rest of the ecdysozoans (animals that undergo periodic molting of an exoskeleton or cuticle), including horsehair worms (Nematomorpha), panarthropods (including arthropods, tardigrades, and onychophorans) and a few other phyla (Fig. 5.2). As discussed above, the nervous systems of ecdysozoans vary widely from the minimalist structures of nematodes such as *C. elegans* to the elaborate and cephalized nervous systems of social insects such as honeybees. Among a large group of nematodes relatively closely related to *C. elegans* (but still separated by perhaps 500 million years of evolution), striking similarity in nervous system composition exists between species despite dramatic differences in size and ecological niche. For example, nematodes of genus *Ascaris* parasitize humans and pigs, can grow to 40 cm in length and possess 50,000 body muscle cells (whereas *C. elegans* has only 79). Yet, the number and identity (in terms of morphology, connectivity, and neurotransmitter usage) of motor neurons that innervate body muscles in *Ascaris* and *C. elegans* is nearly identical [183]. The *Ascaris suum* genome was recently sequenced and the genomes of numerous other nematodes are now being analyzed. Once genetic tools can be applied in these species, the potential to generalize or clarify principles of nervous system function elucidated from the study of *C. elegans* is limitless. Such studies may initially focus on neuroanatomy and molecular identity of signaling pathways but it will be possible to investigate behavioral questions as well. Given the diversity of lifestyles among nematodes, it will be

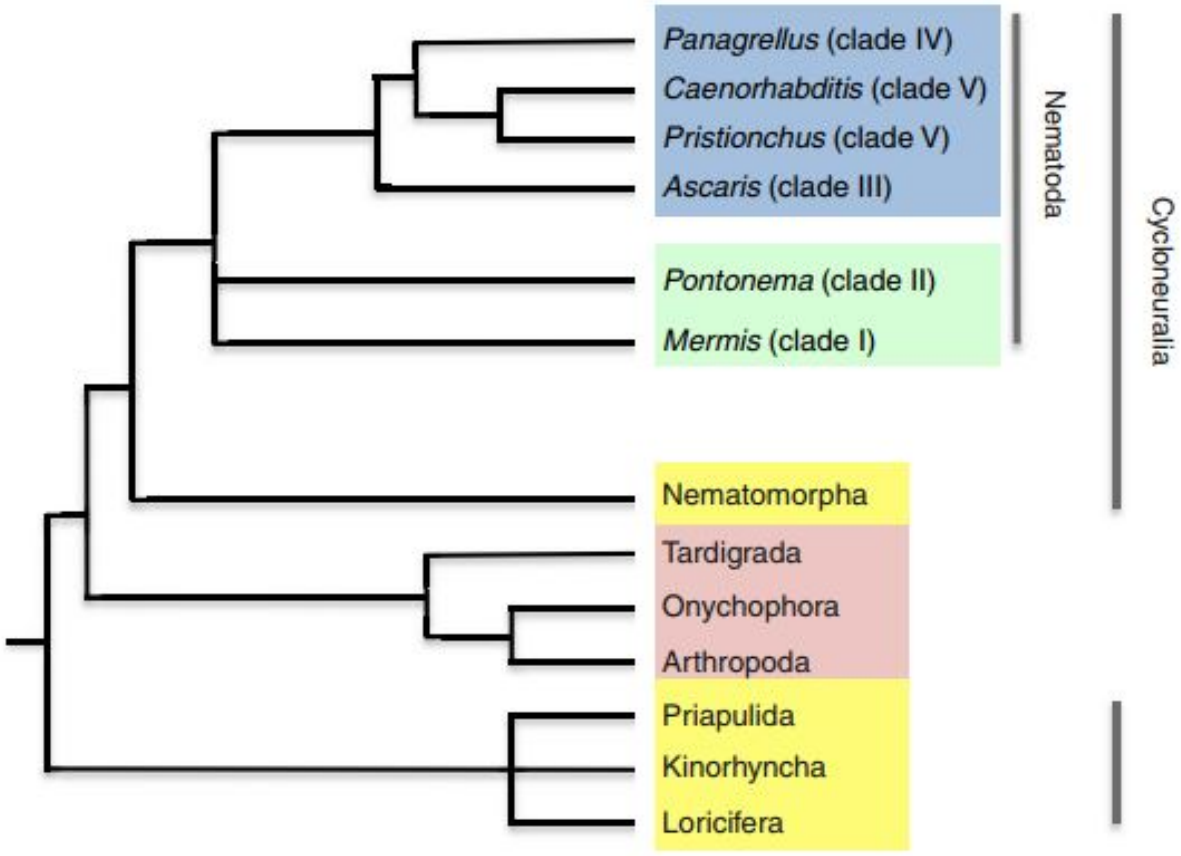

Figure 5.2: **Phylogeny of nematodes and related groups.** Species highlighted in blue represent crown clade nematodes with simple, invariant nervous systems and those highlighted in green are basally branching species with larger nervous systems. Phyla highlighted in yellow are ecdysozoans with circumoral brains and no cephalic ganglia (Cycloneuralia). Phyla in red are ecdysozoan phyla with more complex brains. Phylogeny based on [87] and [121]. Branch lengths are arbitrary. Reproduced from [166].

very illuminating to compare behavioral circuits in, for example, free-living versus parasitic species.

Interestingly, a number of nematode groups more distantly related to *C. elegans* possess more complex nervous systems (see clades highlighted in green in Fig. 5.2). For example, marine nematodes such as *Pontonema* have several thousand neurons, many of which make up the lateral plexus, a complex circuit that innervates somatosensory bristle-like structures termed setae [118]. Since the setae vary in number and position, the number of neurons in the nervous system is also variable (in contrast to the invariant composition of the *C.*

elegans nervous system). Another nematode, the insect parasite *Mermis* has an estimated 1,000 neurons in its ventral nerve cord alone, enabling complex motor behavior [59]. Along with the sophisticated brains of arthropods, the presence of complex nervous systems in some nematodes provides some limited evidence for secondary simplification of species such as *C. elegans*. Genetic manipulations and behavioral experiments in such "complex" nematodes could reveal much about how and to what extent behavioral repertoires are maintained even when the components are minimized, as in *C. elegans*. Investigation of neurobiological processes in "complex" nematodes, which occupy perhaps a middle ground between *C. elegans* and *Drosophila* in terms of sophistication of nervous systems, would contribute greatly to mechanistic understanding of behavior. Moreover, expanding the scope of invertebrate neuroethology would provide a more valuable complement to studies of mammals and other vertebrates.

REFERENCES

[1] Geoffrey K Adams, Karli K Watson, John Pearson, and Michael L Platt. Neuroethology of decision-making. *Current opinion in neurobiology*, 22(6):982–989, 2012.

[2] Michael Ailion and James H Thomas. Dauer formation induced by high temperatures in caenorhabditis elegans. *Genetics*, 156(3):1047–1067, 2000.

[3] Mark J Alkema, Melissa Hunter-Ensor, Niels Ringstad, and H Robert Horvitz. Tyramine functions independently of octopamine in the caenorhabditis elegans nervous system. *Neuron*, 46(2):247–260, 2005.

[4] Claudia Cristina Alves, Raquel Susana Torrinhas, Ricardo Giorgi, Maria Mitzi Brentani, Angela Flavia Logullo, and Dan Linetzky Waitzberg. Tgf-β1 expression in wound healing is acutely affected by experimental malnutrition and early enteral feeding. *International wound journal*, 11(5):533–539, 2014.

[5] Eliana P Araujo, Claudio T De Souza, and Licio A Velloso. Atypical transforming growth factor-[beta] signaling in the hypothalamus is linked to diabetes. *Nature medicine*, 20(9):985–987, 2014.

[6] Juliette Ben Arous, Sophie Laffont, and Didier Chatenay. Molecular and sensory basis of a food related two-state behavior in c. elegans. *PloS one*, 4(10):e7584, 2009.

[7] Gudrun Aspöck, Gary Ruvkun, and Thomas R Bürglin. The caenorhabditis elegans ems class homeobox gene ceh-2 is required for m3 pharynx motoneuron function. *Development*, 130(15):3369–3378, 2003.

[8] Claes Axäng, Manish Rauthan, David H Hall, and Marc Pilon. Developmental genetics of the c. elegans pharyngeal neurons nsml and nsmr. *BMC developmental biology*, 8(1):38, 2008.

[9] Mohammad A Abu Baker and Joel S Brown. Foraging in space and time structure an african small mammal community. *Oecologia*, 175(2):521–535, 2014.

[10] Cornelia I Bargmann. Neurobiology of the caenorhabditis elegans genome. *Science*, 282(5396):2028–2033, 1998.

[11] Cornelia I Bargmann. Chemosensation in c. elegans. 2006.

[12] Cornelia I Bargmann. Beyond the connectome: how neuromodulators shape neural circuits. *Bioessays*, 34(6):458–465, 2012.

[13] Cornelia I Bargmann and H Robert Horvitz. Chemosensory neurons with overlapping functions direct chemotaxis to multiple chemicals in c. elegans. *Neuron*, 7(5):729–742, 1991.

[14] Carol Bastiani and Jane Mendel. Heterotrimeric g proteins in c. elegans. 2006.

[15] Andres Bendesky, Makoto Tsunozaki, Matthew V Rockman, Leonid Kruglyak, and Cornelia I Bargmann. Catecholamine receptor polymorphisms affect decision-making in c. elegans. *Nature*, 472(7343):313–318, 2011.

[16] Allison J Berger, Anne C Hart, and Joshua M Kaplan. Gαs-induced neurodegeneration incaenorhabditis elegans. *Journal of Neuroscience*, 18(8):2871–2880, 1998.

[17] Paola Bertucci and Detlev Arendt. Somatic and visceral nervous systems-an ancient duality. *BMC biology*, 11(1):54, 2013.

[18] Matthew Beverly, Sriram Anbil, and Piali Sengupta. Degeneracy and neuromodulation among thermosensory neurons contribute to robust thermosensory behaviors in caenorhabditis elegans. *Journal of Neuroscience*, 31(32):11718–11727, 2011.

[19] Matthew A Birk and J Wilson White. Experimental determination of the spatial scale of a prey patch from the predators perspective. *Oecologia*, 174(3):723–729, 2014.

[20] Johan J Bolhuis and Luc-Alain Giraldeau. The study of animal behaviour. *The behaviour of animals: mechanisms, function, and evolution*, pages 1–9, 2005.

[21] Sydney Brenner. The genetics of caenorhabditis elegans. *Genetics*, 77(1):71–94, 1974.

[22] Graham E Budd and Sören Jensen. The origin of the animals and a savannahhypothesis for early bilaterian evolution. *Biological Reviews*, 92(1):446–473, 2017.

[23] L Byerly, RC Cassada, and RL Russell. The life cycle of the nematode caenorhabditis elegans: I. wild-type growth and reproduction. *Developmental biology*, 51(1):23–33, 1976.

[24] Adam J Calhoun, Ada Tong, Navin Pokala, James AJ Fitzpatrick, Tatyana O Sharpee, and Sreekanth H Chalasani. Neural mechanisms for evaluating environmental variability in caenorhabditis elegans. *Neuron*, 86(2):428–441, 2015.

[25] A Calon, DVF Tauriello, and E Batlle. Tgf-beta in caf-mediated tumor growth and metastasis. In *Seminars in cancer biology*, volume 25, pages 15–22. Elsevier, 2014.

[26] Colin Camerer, George Loewenstein, and Drazen Prelec. Neuroeconomics: How neuroscience can inform economics. *Journal of economic Literature*, 43(1):9–64, 2005.

[27] Randall C Cassada and Richard L Russell. The dauerlarva, a post-embryonic developmental variant of the nematode caenorhabditis elegans. *Developmental biology*, 46(2):326–342, 1975.

[28] Sarah J Certel, Adelaine Leung, Chih-Yung Lin, Philip Perez, Ann-Shyn Chiang, and Edward A Kravitz. Octopamine neuromodulatory effects on a social behavior decision-making network in drosophila males. *PLoS One*, 5(10):e13248, 2010.

[29] Sreekanth H Chalasani, Nikos Chronis, Makoto Tsunozaki, Jesse M Gray, Daniel Ramot, Miriam B Goodman, and Cornelia I Bargmann. Dissecting a circuit for olfactory behaviour in caenorhabditis elegans. *Nature*, 450(7166):63–70, 2007.

[30] Andy J Chang, Nikolas Chronis, David S Karow, Michael A Marletta, and Cornelia I Bargmann. A distributed chemosensory circuit for oxygen preference in c. elegans. *PLoS Biol*, 4(9):e274, 2006.

[31] Nicole K Charlie, Michael A Schade, Angela M Thomure, and Kenneth G Miller. Presynaptic unc-31 (caps) is required to activate the gα s pathway of the caenorhabditis elegans synaptic signaling network. *Genetics*, 172(2):943–961, 2006.

[32] Nicole K Charlie, Angela M Thomure, Michael A Schade, and Kenneth G Miller. The dunce camp phosphodiesterase pde-4 negatively regulates gα s-dependent and gα s-independent camp pools in the caenorhabditis elegans synaptic signaling network. *Genetics*, 173(1):111–130, 2006.

[33] Eric L Charnov. Optimal foraging, the marginal value theorem. *Theoretical population biology*, 9(2):129–136, 1976.

[34] Daniel L Chase and Michael R Koelle. Biogenic amine neurotransmitters in c. elegans. 2007.

[35] Lars Chittka, Peter Skorupski, and Nigel E Raine. Speed–accuracy tradeoffs in animal decision making. *Trends in ecology & evolution*, 24(7):400–407, 2009.

[36] Jeremiah Y Cohen, Mackenzie W Amoroso, and Naoshige Uchida. Serotonergic neurons signal reward and punishment on multiple timescales. *Elife*, 4:e06346, 2015.

[37] Antonio Colavita, Srikant Krishna, Hong Zheng, Richard W Padgett, and Joseph G Culotti. Pioneer axon guidance by unc-129, a c. elegans tgf-β. *Science*, 281(5377):706–709, 1998.

[38] Heather A Colbert, Tracy L Smith, and Cornelia I Bargmann. Osm-9, a novel protein with structural similarity to channels, is required for olfaction, mechanosensation, and olfactory adaptation incaenorhabditis elegans. *Journal of Neuroscience*, 17(21):8259–8269, 1997.

[39] Joan Collet, Caroline A Spike, Erik A Lundquist, Jocelyn E Shaw, and Robert K Herman. Analysis of osm-6, a gene that affects sensory cilium structure and sensory neuron function in caenorhabditis elegans. *Genetics*, 148(1):187–200, 1998.

[40] James E Cresswell and Juliet L Osborne. The effect of patch size and separation on bumblebee foraging in oilseed rape: implications for gene flow. *Journal of Applied Ecology*, 41(3):539–546, 2004.

[41] Katherine A Cunningham, Zhaolin Hua, Supriya Srinivasan, Jason Liu, Brian H Lee, Robert H Edwards, and Kaveh Ashrafi. Amp-activated kinase links serotonergic signaling to glutamate release for regulation of feeding behavior in c. elegans. *Cell metabolism*, 16(1):113–121, 2012.

[42] Sasha RX Dall, Luc-Alain Giraldeau, Ola Olsson, John M McNamara, and David W Stephens. Information and its use by animals in evolutionary ecology. *Trends in ecology & evolution*, 20(4):187–193, 2005.

[43] Susan A Daniels, Michael Ailion, James H Thomas, and Piali Sengupta. egl-4 acts through a transforming growth factor-β/smad pathway in caenorhabditis elegans to regulate multiple neuronal circuits in response to sensory cues. *Genetics*, 156(1):123–141, 2000.

[44] DL Davidson and DW Morris. Density-dependent foraging effort of deer mice (peromyscus maniculatus). *Functional Ecology*, 15(5):575–583, 2001.

[45] Mario De Bono and Cornelia I Bargmann. Natural variation in a neuropeptide y receptor homolog modifies social behavior and food response in c. elegans. *Cell*, 94(5):679–689, 1998.

[46] Serge Dernovici, Tanja Starc, Joseph A Dent, and Paula Ribeiro. The serotonin receptor ser-1 (5ht2ce) contributes to the regulation of locomotion in caenorhabditis elegans. *Developmental neurobiology*, 67(2):189–204, 2007.

[47] Giovanni Diana, Dhaval S Patel, Eugeni V Entchev, Mei Zhan, Hang Lu, and QueeLim Ch'ng. Genetic control of encoding strategy in a food-sensing neural circuit. *eLife*, 6:e24040, 2017.

[48] Gerard Driessen and Carlos Bernstein. Patch departure mechanisms and optimal host exploitation in an insect parasitoid. *Journal of Animal Ecology*, 68(3):445–459, 1999.

[49] William M Durham, Eric Climent, Michael Barry, Filippo De Lillo, Guido Boffetta, Massimo Cencini, and Roman Stocker. Turbulence drives microscale patches of motile phytoplankton. *Nature communications*, 4, 2013.

[50] Stacey L Edwards, Nicole K Charlie, Marie C Milfort, Brandon S Brown, Christen N Gravlin, Jamie E Knecht, and Kenneth G Miller. A novel molecular solution for ultraviolet light detection in caenorhabditis elegans. *PLoS Biol*, 6(8):e198, 2008.

[51] Eugeni V Entchev, Dhaval S Patel, Mei Zhan, Andrew J Steele, Hang Lu, and QueeLim Ch'ng. A gene-expression-based neural code for food abundance that modulates lifespan. *Elife*, 4:e06259, 2015.

[52] Christopher Fang-Yen, Matthieu Wyart, Julie Xie, Risa Kawai, Tom Kodger, Sway Chen, Quan Wen, and Aravinthan DT Samuel. Biomechanical analysis of gait adaptation in the nematode caenorhabditis elegans. *Proceedings of the National Academy of Sciences*, 107(47):20323–20328, 2010.

[53] Marie-Anne Félix and Christian Braendle. The natural history of caenorhabditis elegans. *Current Biology*, 20(22):R965–R969, 2010.

[54] Zhaoyang Feng, Christopher J Cronin, John H Wittig, Paul W Sternberg, and William R Schafer. An imaging system for standardized quantitative analysis of c. elegans behavior. *BMC bioinformatics*, 5(1):115, 2004.

[55] Nicole Fielenbach and Adam Antebi. C. elegans dauer formation and the molecular basis of plasticity. *Genes & development*, 22(16):2149–2165, 2008.

[56] John R Finnerty. Did internal transport, rather than directed locomotion, favor the evolution of bilateral symmetry in animals? *BioEssays*, 27(11):1174–1180, 2005.

[57] Steven W Flavell, Navin Pokala, Evan Z Macosko, Dirk R Albrecht, Johannes Larsch, and Cornelia I Bargmann. Serotonin and the neuropeptide pdf initiate and extend opposing behavioral states in c. elegans. *Cell*, 154(5):1023–1035, 2013.

[58] Thomas Gallagher, Theresa Bjorness, Robert Greene, Young-Jai You, and Leon Avery. The geometry of locomotive behavioral states in c. elegans. *PloS one*, 8(3):e59865, 2013.

[59] Carl Gans and AH Burr. Unique locomotory mechanism of mermis nigrescens, a large nematode that crawls over soil and climbs through vegetation. *Journal of Morphology*, 222(2):133–148, 1994.

[60] David Gems, Amy J Sutton, Mark L Sundermeyer, Patrice S Albert, Kevin V King, Mark L Edgley, Pamela L Larsen, and Donald L Riddle. Two pleiotropic classes of daf-2 mutation affect larval arrest, adult behavior, reproduction and longevity in caenorhabditis elegans. *Genetics*, 150(1):129–155, 1998.

[61] Laura L Georgi, Patrice S Albert, and Donald L Riddle. daf-1, a c. elegans gene controlling dauer larva development, encodes a novel receptor protein kinase. *Cell*, 61(4):635–645, 1990.

[62] Birgit Gerisch, Cindy Weitzel, Corinna Kober-Eisermann, Veerle Rottiers, and Adam Antebi. A hormonal signaling pathway influencing c. elegans metabolism, reproductive development, and life span. *Developmental cell*, 1(6):841–851, 2001.

[63] Tugrul Giray, Charles I Abramson, Ana Chicas-Mosier, Tiyi Brewster, Christine Hayes, Karianne Rivera-Vega, Maya Williams, and Harrington Wells. Effect of octopamine manipulation on honeybee decision making: Reward and cost differences associated with foraging. *Animal Behaviour*, 100:144–150, 2015.

[64] Julijana Gjorgjieva, David Biron, and Gal Haspel. Neurobiology of caenorhabditis elegans locomotion: where do we stand? *Bioscience*, 64(6):476–486, 2014.

[65] Adrian C Gleiss, Salvador J Jorgensen, Nikolai Liebsch, Juan E Sala, Brad Norman, Graeme C Hays, Flavio Quintana, Edward Grundy, Claudio Campagna, Andrew W Trites, et al. Convergent evolution in locomotory patterns of flying and swimming animals. *Nature communications*, 2:352, 2011.

[66] Andrea Gloria-Soria and Ricardo BR Azevedo. npr-1 regulates foraging and dispersal strategies in caenorhabditis elegans. *Current Biology*, 18(21):1694–1699, 2008.

[67] PD Gluckman and MA Hanson. Developmental and epigenetic pathways to obesity: an evolutionary-developmental perspective. *International journal of obesity*, 32:S62–S71, 2008.

[68] James W Golden and Donald L Riddle. A pheromone influences larval development in the nematode caenorhabditis elegans. *Science*, 218(4572):578–580, 1982.

[69] James W Golden and Donald L Riddle. The caenorhabditis elegans dauer larva: developmental effects of pheromone, food, and temperature. *Developmental biology*, 102(2):368–378, 1984.

[70] James W Golden and Donald L Riddle. A pheromone-induced developmental switch in caenorhabditis elegans: Temperature-sensitive mutants reveal a wild-type temperature-dependent process. *Proceedings of the National Academy of Sciences*, 81(3):819–823, 1984.

[71] Miriam B Goodman. Mechanosensation. *WormBook: the online review of C. elegans biology*, pages 1–14, 2006.

[72] I Gormezano and JW Moore. Classical conditioning. *Experimental methods and instrumentation in psychology*, 1:385–420, 1966.

[73] James Gray. *How animals move*. Cambridge University Press, 2013.

[74] Jesse M Gray, Joseph J Hill, and Cornelia I Bargmann. A circuit for navigation in caenorhabditis elegans. *Proceedings of the National Academy of Sciences of the United States of America*, 102(9):3184–3191, 2005.

[75] DM Green and JA Swets. Signal detection theory and psychophysics (rev. ed.). *Huntington, NY: RF Krieger*, 1974.

[76] Min Guo, Tai-Hong Wu, Yan-Xue Song, Ming-Hai Ge, Chun-Ming Su, Wei-Pin Niu, Lan-Lan Li, Zi-Jing Xu, Chang-Li Ge, Maha TH Al-Mhanawi, et al. Reciprocal inhibition between sensory ash and asi neurons modulates nociception and avoidance in caenorhabditis elegans. *Nature communications*, 6:5655, 2015.

[77] Güliz Gürel, Megan A Gustafson, Judy S Pepper, H Robert Horvitz, and Michael R Koelle. Receptors and other signaling proteins required for serotonin control of locomotion in caenorhabditis elegans. *Genetics*, 192(4):1359–1371, 2012.

[78] Vera Hapiak, Philip Summers, Amanda Ortega, Wen Jing Law, Andrew Stein, and Richard Komuniecki. Neuropeptides amplify and focus the monoaminergic inhibition of nociception in caenorhabditis elegans. *Journal of Neuroscience*, 33(35):14107–14116, 2013.

[79] Vera M Hapiak, Robert J Hobson, Lindsay Hughes, Katherine Smith, Gareth Harris, Christina Condon, Patricia Komuniecki, and Richard W Komuniecki. Dual excitatory and inhibitory serotonergic inputs modulate egg laying in caenorhabditis elegans. *Genetics*, 181(1):153–163, 2009.

[80] Jeffrey B Harborne. *Introduction to ecological biochemistry*. Academic press, 2014.

[81] Gareth Harris, Amanda Korchnak, Philip Summers, Vera Hapiak, Wen Jing Law, Andrew M Stein, Patricia Komuniecki, and Richard Komuniecki. Dissecting the serotonergic food signal stimulating sensory-mediated aversive behavior in c. elegans. *PLoS One*, 6(7):e21897, 2011.

[82] Gareth P Harris, Vera M Hapiak, Rachel T Wragg, Sarah B Miller, Lindsay J Hughes, Robert J Hobson, Robert Steven, Bruce Bamber, and Richard W Komuniecki. Three distinct amine receptors operating at different levels within the locomotory circuit are each essential for the serotonergic modulation of chemosensation in caenorhabditis elegans. *Journal of Neuroscience*, 29(5):1446–1456, 2009.

[83] Benjamin Y Hayden, John M Pearson, and Michael L Platt. Neuronal basis of sequential foraging decisions in a patchy environment. *Nature neuroscience*, 14(7):933–939, 2011.

[84] Frank Hirth. On the origin and evolution of the tripartite brain. *Brain, behavior and evolution*, 76(1):3–10, 2010.

[85] Frank Hirth, Lars Kammermeier, Erich Frei, Uwe Walldorf, Markus Noll, and Heinrich Reichert. An urbilaterian origin of the tripartite brain: developmental genetic insights from drosophila. *Development*, 130(11):2365–2373, 2003.

[86] Linda Z Holland, João E Carvalho, Hector Escriva, Vincent Laudet, Michael Schubert, Sebastian M Shimeld, and Jr-Kai Yu. Evolution of bilaterian central nervous systems: a single origin? *EvoDevo*, 4(1):27, 2013.

[87] Martijn Holterman, Andre van der Wurff, Sven van den Elsen, Hanny van Megen, Tom Bongers, Oleksandr Holovachov, Jaap Bakker, and Johannes Helder. Phylum-wide analysis of ssu rdna reveals deep phylogenetic relationships among nematodes and accelerated evolution toward crown clades. *Molecular biology and evolution*, 23(9):1792–1800, 2006.

[88] H Robert Horvitz, Martin Chalfie, Carol Trent, John E Sulston, and Peter D Evans. Serotonin and octopamine in the nematode caenorhabditis elegans. *Science*, 216(4549):1012–1014, 1982.

[89] Patrick J Hu. Dauer. *WormBook: the online review of C. elegans biology*, pages 1–19, 2007.

[90] Mingxia Huang and Martin Chalfie. Gene interactions affecting mechanosensory transduction in caenorhabditis elegans. *Nature*, 367(6462):467, 1994.

[91] Renate K Hukema, Suzanne Rademakers, Martijn PJ Dekkers, Jan Burghoorn, and Gert Jansen. Antagonistic sensory cues generate gustatory plasticity in caenorhabditis elegans. *The EMBO journal*, 25(2):312–322, 2006.

[92] Yuichi Iino and Kazushi Yoshida. Parallel use of two behavioral mechanisms for chemotaxis in caenorhabditis elegans. *Journal of Neuroscience*, 29(17):5370–5380, 2009.

[93] Auke Jan Ijspeert, Alessandro Crespi, Dimitri Ryczko, and Jean-Marie Cabelguen. From swimming to walking with a salamander robot driven by a spinal cord model. *science*, 315(5817):1416–1420, 2007.

[94] Konstantin G Iliadi. The genetic basis of emotional behavior: has the time come for a drosophila model? *Journal of neurogenetics*, 23(1-2):136–146, 2009.

[95] Hitoshi Inada, Hiroko Ito, John Satterlee, Piali Sengupta, Kunihiro Matsumoto, and Ikue Mori. Identification of guanylyl cyclases that function in thermosensory neurons of caenorhabditis elegans. *Genetics*, 172(4):2239–2252, 2006.

[96] Peter N Inglis, Oliver E Blacque, and Michel R Leroux. Functional genomics of intraflagellar transport-associated proteins in c. elegans. *Methods in cell biology*, 93:267–304, 2009.

[97] Shachar Iwanir, Adam S Brown, Stanislav Nagy, Dana Najjar, Alexander Kazakov, Kyung Suk Lee, Alon Zaslaver, Erel Levine, and David Biron. Serotonin promotes exploitation in complex environments by accelerating decision-making. *BMC biology*, 14(1):9, 2016.

[98] Gholamali Jafari, Yusu Xie, Andrey Kullyev, Bin Liang, and Ji Ying Sze. Regulation of extrasynaptic 5-ht by serotonin reuptake transporter function in 5-ht-absorbing neurons underscores adaptation behavior in caenorhabditis elegans. *Journal of Neuroscience*, 31(24):8948–8957, 2011.

[99] Kailiang Jia, Di Chen, and Donald L Riddle. The tor pathway interacts with the insulin signaling pathway to regulate c. elegans larval development, metabolism and life span. *Development*, 131(16):3897–3906, 2004.

[100] Antony M Jose, I Amy Bany, Daniel L Chase, and Michael R Koelle. A specific subset of transient receptor potential vanilloid-type channel subunits in caenorhabditis elegans endocrine cells function as mixed heteromers to promote neurotransmitter release. *Genetics*, 175(1):93–105, 2007.

[101] Alejandro Kacelnik and Ian A Todd. Psychological mechanisms and the marginal value theorem: effect of variability in travel time on patch exploitation. *Animal Behaviour*, 43(2):313–322, 1992.

[102] Joshua M Kaplan and H ROBERT HoRVITZ. A dual mechanosensory and chemosensory neuron in caenorhabditis elegans. *Proceedings of the National Academy of Sciences*, 90(6):2227–2231, 1993.

[103] Cynthia Kenyon, Jean Chang, Erin Gensch, Adam Rudner, and Ramon Tabtiang. A c. elegans mutant that lives twice as long as wild type. *Nature*, 366(6454):461–464, 1993.

[104] Michael Klass and David Hirsh. Non-ageing developmental variant of caenorhabditis elegans. *Nature*, 260(5551):523–525, 1976.

[105] Michael R Koelle. Neurotransmitter signaling through heterotrimeric g proteins: insights from studies in c. elegans. *wormbook*, pages 1–78, 2016.

[106] Michael R Koelle and H Robert Horvitz. Egl-10 regulates g protein signaling in the c. elegans nervous system and shares a conserved domain with many mammalian proteins. *Cell*, 84(1):115–125, 1996.

[107] John R Krebs and Nicholas B Davies. *Behavioural ecology: an evolutionary approach*. John Wiley & Sons, 2009.

[108] D Kvitsiani, S Ranade, B Hangya, H Taniguchi, JZ Huang, and A Kepecs. Distinct behavioural and network correlates of two interneuron types in prefrontal cortex. *Nature*, 498(7454):363–366, 2013.

[109] Pamela L Larsen, Patrice S Albert, and Donald L Riddle. Genes that regulate both development and longevity in caenorhabditis elegans. *Genetics*, 139(4):1567–1583, 1995.

[110] William C Lemon. Fitness consequences of foraging behaviour in the zebra finch. *Nature*, 352(6331):153, 1991.

[111] Zhaoyu Li, Yidong Li, Yalan Yi, Wenming Huang, Song Yang, Weipin Niu, Li Zhang, Zijing Xu, Anlian Qu, Zhengxing Wu, et al. Dissecting a central flip-flop circuit that integrates contradictory sensory cues in c. elegans feeding regulation. *Nature communications*, 3:776, 2012.

[112] Jana F Liewald, Martin Brauner, Greg J Stephens, Magali Bouhours, Christian Schultheis, Mei Zhen, and Alexander Gottschalk. Optogenetic analysis of synaptic function. *Nature methods*, 5(10):895–902, 2008.

[113] Kui Lin, Jennie B Dorman, Aylin Rodan, and Cynthia Kenyon. daf-16: An hnf-3/forkhead family member that can function to double the life-span of caenorhabditis elegans. *Science*, 278(5341):1319–1322, 1997.

[114] Michael A Lochrie, Jane E Mendel, Paul W Sternberg, and Melvin I Simon. Homologous and unique g protein alpha subunits in the nematode caenorhabditis elegans. *Cell regulation*, 2(2):135–154, 1991.

[115] Linjiao Luo, Damon A Clark, David Biron, L Mahadevan, and Aravinthan DT Samuel. Sensorimotor control during isothermal tracking in caenorhabditis elegans. *Journal of experimental biology*, 209(23):4652–4662, 2006.

[116] Evan Z Macosko, Navin Pokala, Evan H Feinberg, Sreekanth H Chalasani, Rebecca A Butcher, Jon Clardy, and Cornelia I Bargmann. A hub-and-spoke circuit drives pheromone attraction and social behaviour in c. elegans. *Nature*, 458(7242):1171–1175, 2009.

[117] Sean M Maguire, Christopher M Clark, John Nunnari, Jennifer K Pirri, and Mark J Alkema. The c. elegans touch response facilitates escape from predacious fungi. *Current Biology*, 21(15):1326–1330, 2011.

[118] VV Malakhov. The structure of the nervous system of the cephalic end of the free-living marine nematode pontonema vulgare. *Zoologicheskii zhurnal*, 57:645–52, 1978.

[119] Elizabeth A Malone and James H Thomas. A screen for nonconditional dauer-constitutive mutations in caenorhabditis elegans. *Genetics*, 136(3):879–886, 1994.

[120] Andres V Maricq, Erin Peckol, Monica Driscoll, and Carnelia I Bargmann. Mechanosensory signalling in c. elegans mediated by the glr-1 glutamate receptor. *Nature*, 378(6552):78, 1995.

[121] Christine Martin and Georg Mayer. Neuronal tracing of oral nerves in a velvet worm-implications for the evolution of the ecdysozoan brain. *Frontiers in neuroanatomy*, 8, 2014.

[122] Mark D Mathew, Neal D Mathew, and Paul R Ebert. Wormscan: a technique for high-throughput phenotypic analysis of caenorhabditis elegans. *PloS one*, 7(3):e33483, 2012.

[123] Ernst Mayr. Classification and phylogeny. *American Zoologist*, pages 165–174, 1965.

[124] Kevin S McCann, JB Rasmussen, and James Umbanhowar. The dynamics of spatially coupled food webs. *Ecology Letters*, 8(5):513–523, 2005.

[125] Kate Milward, Karl Emanuel Busch, Robin Joseph Murphy, Mario de Bono, and Birgitta Olofsson. Neuronal and molecular substrates for optimal foraging in caenorhabditis elegans. *Proceedings of the National Academy of Sciences*, 108(51):20672–20677, 2011.

[126] Kiyokazu Morita, Anthony J Flemming, Yukiko Sugihara, Makoto Mochii, Yo Suzuki, Satoru Yoshida, William B Wood, Yuji Kohara, Armand M Leroi, and Naoto Ueno. A caenorhabditis elegans tgf-β, dbl-1, controls the expression of lon-1, a pr-related protein, that regulates polyploidization and body length. *The EMBO journal*, 21(5):1063–1073, 2002.

[127] Kiyokazu Morita, Miho Shimizu, Hiroshi Shibuya, and Naoto Ueno. A daf-1-binding protein bra-1 is a negative regulator of daf-7 tgf-β signaling. *Proceedings of the National Academy of Sciences*, 98(11):6284–6288, 2001.

[128] Paul Muir, Shantao Li, Shaoke Lou, Daifeng Wang, Daniel J Spakowicz, Leonidas Salichos, Jing Zhang, George M Weinstock, Farren Isaacs, Joel Rozowsky, et al. The real cost of sequencing: scaling computation to keep pace with data generation. *Genome biology*, 17(1):53, 2016.

[129] Eadweard Muybridge. *The Attitudes of Animals in Motion Illustrated With the Zoopraxiscope*, volume 1. Library of Alexandria, 1882.

[130] Eadweard Muybridge. *Animals in motion*. Courier Corporation, 2012.

[131] Georg Nagel, Martin Brauner, Jana F Liewald, Nona Adeishvili, Ernst Bamberg, and Alexander Gottschalk. Light activation of channelrhodopsin-2 in excitable cells of caenorhabditis elegans triggers rapid behavioral responses. *Current Biology*, 15(24):2279–2284, 2005.

[132] Stanislav Nagy, David M Raizen, and David Biron. Measurements of behavioral quiescence in caenorhabditis elegans. *Methods*, 68(3):500–507, 2014.

[133] Stanislav Nagy, Charles Wright, Nora Tramm, Nicholas Labello, Stanislav Burov, and David Biron. A longitudinal study of caenorhabditis elegans larvae reveals a novel locomotion switch, regulated by gαs signaling. *Elife*, 2:e00782, 2013.

[134] Erica KO Namigai, Nathan J Kenny, and Sebastian M Shimeld. Right across the tree of life: The evolution of left–right asymmetry in the bilateria. *Genesis*, 52(6):458–470, 2014.

[135] Ernst Niebur and Paul Erdös. Theory of the locomotion of nematodes: dynamics of undulatory progression on a surface. *Biophysical journal*, 60(5):1132–1146, 1991.

[136] Jeremy E Niven and Lars Chittka. Evolving understanding of nervous system evolution, 2016.

[137] Akira Ogawa, Adrian Streit, Adam Antebi, and Ralf J Sommer. A conserved endocrine mechanism controls the formation of dauer and infective larvae in nematodes. *Current Biology*, 19(1):67–71, 2009.

[138] Scott Ogg, Suzanne Paradis, Shoshanna Gottlieb, Garth I Patterson, et al. The fork head transcription factor daf-16 transduces insulin-like metabolic and longevity signals in c. elegans. *Nature*, 389(6654):994, 1997.

[139] Bjorn Olde and W Richard McCombie. Molecular cloning and functional expression of a serotonin receptor from caenorhabditis elegans. *Journal of Molecular Neuroscience*, 8(1):53–62, 1997.

[140] Daniel T Omura, Damon A Clark, Aravinthan DT Samuel, and H Robert Horvitz. Dopamine signaling is essential for precise rates of locomotion by c. elegans. *PLoS One*, 7(6):e38649, 2012.

[141] Daniel Togo Omura. *C. elegans integrates food, stress, and hunger signals to coordinate motor activity*. PhD thesis, Massachusetts Institute of Technology, 2008.

[142] Leslie C Osborne, Stephen G Lisberger, and William Bialek. A sensory source for motor variation. *Nature*, 437(7057):412–416, 2005.

[143] Garth I Patterson and Richard W Padgett. Tgfβ-related pathways: roles in caenorhabditis elegans development. *Trends in genetics*, 16(1):27–33, 2000.

[144] John M Pearson, Karli K Watson, and Michael L Platt. Decision making: the neuroethological turn. *Neuron*, 82(5):950–965, 2014.

[145] Lizabeth A Perkins, Edward M Hedgecock, J Nichol Thomson, and Joseph G Culotti. Mutant sensory cilia in the nematode caenorhabditis elegans. *Developmental biology*, 117(2):456–487, 1986.

[146] Jonathan T Pierce-Shimomura, Thomas M Morse, and Shawn R Lockery. The fundamental role of pirouettes in caenorhabditis elegans chemotaxis. *Journal of Neuroscience*, 19(21):9557–9569, 1999.

[147] Roger Pocock and Oliver Hobert. Hypoxia activates a latent circuit for processing gustatory information in c. elegans. *Nature neuroscience*, 13(5):610–614, 2010.

[148] Jianhua Qin and Aaron R Wheeler. Maze exploration and learning in c. elegans. *Lab on a Chip*, 7(2):186–192, 2007.

[149] David M Raizen, Kevin M Cullison, Allan I Pack, and Meera V Sundaram. A novel gain-of-function mutant of the cyclic gmp-dependent protein kinase egl-4 affects multiple physiological processes in caenorhabditis elegans. *Genetics*, 173(1):177–187, 2006.

[150] Rajesh Ranganathan, Stephen C Cannon, and H Robert Horvitz. Mod-1 is a serotonin-gated chloride channel that modulates locomotory behaviour in c. elegans. *Nature*, 408(6811):470–475, 2000.

[151] Rajesh Ranganathan, Elizabeth R Sawin, Carol Trent, and H Robert Horvitz. Mutations in the caenorhabditis elegans serotonin reuptake transporter mod-5 reveal serotonin-dependent and-independent activities of fluoxetine. *Journal of Neuroscience*, 21(16):5871–5884, 2001.

[152] Heinrich Reichert. A tripartite organization of the urbilaterian brain: developmental genetic evidence from drosophila. *Brain research bulletin*, 66(4):491–494, 2005.

[153] Peifeng Ren, Chang-Su Lim, Robert Johnsen, Patrice S Albert, David Pilgrim, and Donald L Riddle. Control of c. elegans larval development by neuronal expression of a tgf-β homolog. *Science*, pages 1389–1391, 1996.

[154] Nicole K Reynolds, Michael A Schade, and Kenneth G Miller. Convergent, ric-8-dependent gα signaling pathways in the caenorhabditis elegans synaptic signaling network. *Genetics*, 169(2):651–670, 2005.

[155] Janet Richmond. Synaptic function. 2005.

[156] Janet E Richmond and Erik M Jorgensen. One gaba and two acetylcholine receptors function at the c. elegans neuromuscular junction. *Nature neuroscience*, 2(9):791–797, 1999.

[157] Donald L Riddle, Margaret M Swanson, and Patrice S Albert. Interacting genes in nematode dauer larva formation. *Nature*, 290(5808):668–671, 1981.

[158] Craig AL Riedl, Scott J Neal, Alain Robichon, J Timothy Westwood, and Marla B Sokolowski. Drosophila soluble guanylyl cyclase mutants exhibit increased foraging locomotion: behavioral and genomic investigations. *Behavior genetics*, 35(3):231–244, 2005.

[159] Merrilee Robatzek and James H Thomas. Calcium/calmodulin-dependent protein kinase ii regulates caenorhabditis elegans locomotion in concert with a g o/g q signaling network. *Genetics*, 156(3):1069–1082, 2000.

[160] Sarah H Roy, David V Tobin, Nadin Memar, Eleanor Beltz, Jenna Holmen, Joseph E Clayton, Daniel J Chiu, Laura D Young, Travis H Green, Isabella Lubin, et al. A complex regulatory network coordinating cell cycles during c. elegans development is revealed by a genome-wide rnai screen. *G3: Genes— Genomes— Genetics*, 4(5):795–804, 2014.

[161] William S Ryu and Aravinthan DT Samuel. Thermotaxis in caenorhabditis elegans analyzed by measuring responses to defined thermal stimuli. *Journal of Neuroscience*, 22(13):5727–5733, 2002.

[162] Owais Saifee, Laura B Metz, Michael L Nonet, and C Michael Crowder. A gain-of-function mutation in adenylate cyclase confers isoflurane resistance in caenorhabditis elegans. *The Journal of the American Society of Anesthesiologists*, 115(6):1162–1171, 2011.

[163] Jarred Sanders, Stanislav Nagy, Graham Fetterman, Charles Wright, Millet Treinin, and David Biron. The caenorhabditis elegans interneuron ala is (also) a high-threshold mechanosensor. *BMC neuroscience*, 14(1):156, 2013.

[164] Elizabeth R Sawin, Rajesh Ranganathan, and H Robert Horvitz. C. elegans locomotory rate is modulated by the environment through a dopaminergic pathway and by experience through a serotonergic pathway. *Neuron*, 26(3):619–631, 2000.

[165] Michael A Schade, Nicole K Reynolds, Claudia M Dollins, and Kenneth G Miller. Mutations that rescue the paralysis of caenorhabditis elegans ric-8 (synembryn) mutants activate the gα s pathway and define a third major branch of the synaptic signaling network. *Genetics*, 169(2):631–649, 2005.

[166] William Schafer. Nematode nervous systems. *Current Biology*, 26(20):R955–R959, 2016.

[167] Giampietro G Schiavo, Fabio Benfenati, Bernard Poulain, Ornella Rossetto, Patrizia Polverino de Laureto, Bibhuti R DasGupta, and Cesare Montecucco. Tetanus and botulinum-b neurotoxins block neurotransmitter release by proteolytic cleavage of synaptobrevin. *Nature*, 359(6398):832–835, 1992.

[168] Laurent Segalat, Daniel A Elkes, and Joshua M Kaplan. Modulation of serotonin-controlled behaviors by go in caenorhabditis elegans. *Science*, 267(5204):1648, 1995.

[169] RL Senft, MB Coughenour, DW Bailey, LR Rittenhouse, OE Sala, and DM Swift. Large herbivore foraging and ecological hierarchies. *BioScience*, 37(11):789–799, 1987.

[170] Christopher A Shaffer. Spatial foraging in free ranging bearded sakis: Traveling salesmen or lévy walkers? *American journal of primatology*, 76(5):472–484, 2014.

[171] Michael M Shen and Jonathan Hodgkin. mab-3, a gene required for sex-specific yolk protein expression and a male-specific lineage in c. elegans. *Cell*, 54(7):1019–1031, 1988.

[172] Yigong Shi and Joan Massagué. Mechanisms of tgf-β signaling from cell membrane to the nucleus. *Cell*, 113(6):685–700, 2003.

[173] Boris Borisovich Shtonda and Leon Avery. Dietary choice behavior in caenorhabditis elegans. *Journal of experimental biology*, 209(1):89–102, 2006.

[174] David W Sims, Emily J Southall, Nicolas E Humphries, Graeme C Hays, Corey JA Bradshaw, Jonathan W Pitchford, Alex James, Mohammed Z Ahmed, Andrew S Brierley, Mark A Hindell, et al. Scaling laws of marine predator search behaviour. *Nature*, 451(7182):1098–1102, 2008.

[175] Burrhus F Skinner. Operant behavior. *American Psychologist*, 18(8):503, 1963.

[176] Rebecca Solnit. *River of shadows: Eadweard Muybridge and the technological wild west*. Penguin, 2004.

[177] Bo-mi Song and Leon Avery. Serotonin activates overall feeding by activating two separate neural pathways in caenorhabditis elegans. *Journal of Neuroscience*, 32(6):1920–1931, 2012.

[178] Bo-mi Song, Serge Faumont, Shawn Lockery, and Leon Avery. Recognition of familiar food activates feeding via an endocrine serotonin signal in caenorhabditis elegans. *Elife*, 2:e00329, 2013.

[179] Supriya Srinivasan, Leila Sadegh, Ida C Elle, Anne GL Christensen, Nils J Faergeman, and Kaveh Ashrafi. Serotonin regulates c. elegans fat and feeding through independent molecular mechanisms. *Cell metabolism*, 7(6):533–544, 2008.

[180] David W Stephens. Decision ecology: foraging and the ecology of animal decision making. *Cognitive, Affective, & Behavioral Neuroscience*, 8(4):475–484, 2008.

[181] David W Stephens and John R Krebs. *Foraging theory*. Princeton University Press, 1986.

[182] Greg J Stephens, Bethany Johnson-Kerner, William Bialek, and William S Ryu. Dimensionality and dynamics in the behavior of c. elegans. *PLoS Comput Biol*, 4(4):e1000028, 2008.

[183] Antony Stretton, Judith Donmoyer, Ralph Davis, Jeffrey Meade, Cynthia Cowden, and Paisarn Sithigorngul. Motor behavior and motor nervous system function in the nematode ascaris suum. *The Journal of parasitology*, pages 206–214, 1992.

[184] Thomas C Südhof. The synaptic vesicle cycle revisited. *Neuron*, 28(2):317–320, 2000.

[185] Yo Suzuki, Mark D Yandell, Peter J Roy, Srikant Krishna, Cathy Savage-Dunn, Robert M Ross, Richard W Padgett, and William B Wood. A bmp homolog acts as a dose-dependent regulator of body size and male tail patterning in caenorhabditis elegans. *Development*, 126(2):241–250, 1999.

[186] Nicholas A Swierczek, Andrew C Giles, Catharine H Rankin, and Rex A Kerr. High-throughput behavioral analysis in c. elegans. *Nature methods*, 8(7):592–598, 2011.

[187] Ji Ying Sze, Martin Victor, Curtis Loer, Yang Shi, and Gary Ruvkun. Food and metabolic signalling defects in a caenorhabditis elegans serotonin-synthesis mutant. *Nature*, 403(6769):560–564, 2000.

[188] Tod R Thiele, Serge Faumont, and Shawn R Lockery. The neural network for chemotaxis to tastants in caenorhabditis elegans is specialized for temporal differentiation. *Journal of Neuroscience*, 29(38):11904–11911, 2009.

[189] Lin Tian, S Andrew Hires, and Loren L Looger. Imaging neuronal activity with genetically encoded calcium indicators. *Cold Spring Harbor Protocols*, 2012(6):pdb–top069609, 2012.

[190] Lin Tian, S Andrew Hires, Tianyi Mao, Daniel Huber, M Eugenia Chiappe, Sreekanth H Chalasani, Leopoldo Petreanu, Jasper Akerboom, Sean A McKinney, Eric R Schreiter, et al. Imaging neural activity in worms, flies and mice with improved gcamp calcium indicators. *Nature methods*, 6(12):875–881, 2009.

[191] Niko Tinbergen. On aims and methods of ethology. *Ethology*, 20(4):410–433, 1963.

[192] David M Tobin, David M Madsen, Amanda Kahn-Kirby, Erin L Peckol, Gary Moulder, Robert Barstead, Andres V Maricq, and Cornelia I Bargmann. Combinatorial expression of trpv channel proteins defines their sensory functions and subcellular localization in c. elegans neurons. *Neuron*, 35(2):307–318, 2002.

[193] Carol Trent, Nancy Tsung, and H Robert Horvitz. Egg-laying defective mutants of the nematode caenorhabditis elegans. *Genetics*, 104(4):619–647, 1983.

[194] Jennifer MA Tullet, Caroline Araiz, Matthew J Sanders, Catherine Au, Alexandre Benedetto, Irene Papatheodorou, Emily Clark, Kathrin Schmeisser, Daniel Jones, Eugene F Schuster, et al. Daf-16/foxo directly regulates an atypical amp-activated protein kinase gamma isoform to mediate the effects of insulin/igf-1 signaling on aging in caenorhabditis elegans. *PLoS genetics*, 10(2):e1004109, 2014.

[195] Matthew Turk and Alex Pentland. Eigenfaces for recognition. *Journal of cognitive neuroscience*, 3(1):71–86, 1991.

[196] Sarah M Tweedt and Douglas H Erwin. Origin of metazoan developmental toolkits and their expression in the fossil record. In *Evolutionary transitions to multicellular life*, pages 47–77. Springer, 2015.

[197] Massimo Vergassola, Emmanuel Villermaux, and Boris I Shraiman. infotaxis as a strategy for searching without gradients. *Nature*, 445(7126):406–409, 2007.

[198] Berta Vidal, Anthony Santella, Esther Serrano-Saiz, Zhirong Bao, Chiou-Fen Chuang, and Oliver Hobert. C. elegans soxb genes are dispensable for embryonic neurogenesis but required for terminal differentiation of specific neuron types. *Development*, 142(14):2464–2477, 2015.

[199] Andrés Vidal-Gadea, Stephen Topper, Layla Young, Ashley Crisp, Leah Kressin, Erin Elbel, Thomas Maples, Martin Brauner, Karen Erbguth, Abram Axelrod, et al. Caenorhabditis elegans selects distinct crawling and swimming gaits via dopamine and serotonin. *Proceedings of the National Academy of Sciences*, 108(42):17504–17509, 2011.

[200] Andrés Vidal-Gadea, Kristi Ward, Celia Beron, Navid Ghorashian, Sertan Gokce, Joshua Russell, Nicholas Truong, Adhishri Parikh, Otilia Gadea, Adela Ben-Yakar, et al. Magnetosensitive neurons mediate geomagnetic orientation in caenorhabditis elegans. *Elife*, 4:e07493, 2015.

[201] Alex Ward, Jie Liu, Zhaoyang Feng, and XZ Shawn Xu. Light-sensitive neurons and channels mediate phototaxis in c. elegans. *Nature neuroscience*, 11(8):916–922, 2008.

[202] PW Webb. Body form, locomotion and foraging in aquatic vertebrates. *American Zoologist*, 24(1):107–120, 1984.

[203] Quan Wen, Michelle D Po, Elizabeth Hulme, Sway Chen, Xinyu Liu, Sen Wai Kwok, Marc Gershow, Andrew M Leifer, Victoria Butler, Christopher Fang-Yen, et al. Proprioceptive coupling within motor neurons drives c. elegans forward locomotion. *Neuron*, 76(4):750–761, 2012.

[204] Mark W Westneat. Evolution of levers and linkages in the feeding mechanisms of fishes. *Integrative and Comparative Biology*, 44(5):378–389, 2004.

[205] John G White, Eileen Southgate, J Nichol Thomson, and Sydney Brenner. The structure of the nervous system of the nematode caenorhabditis elegans. *Philos Trans R Soc Lond B Biol Sci*, 314(1165):1–340, 1986.

[206] C Wolkow and DH Hall. Introduction to the dauer larva, overview. *WormAtlas*, 2015.

[207] Nilay Yapici, Manuel Zimmer, and Ana I Domingos. Cellular and molecular basis of decision-making. *EMBO reports*, page e201438993, 2014.

[208] Alon Zaslaver, Idan Liani, Oshrat Shtangel, Shira Ginzburg, Lisa Yee, and Paul W Sternberg. Hierarchical sparse coding in the sensory system of caenorhabditis elegans. *Proceedings of the National Academy of Sciences*, 112(4):1185–1189, 2015.

[209] Shenyuan Zhang, Irina Sokolchik, Gabriela Blanco, and Ji Ying Sze. Caenorhabditis elegans trpv ion channel regulates 5ht biosynthesis in chemosensory neurons. *Development*, 131(7):1629–1638, 2004.

[210] Yun Zhang, Hang Lu, and Cornelia I Bargmann. Pathogenic bacteria induce aversive olfactory learning in caenorhabditis elegans. *Nature*, 438(7065):179, 2005.

[211] Zejun Zhang, Xiangjiang Zhan, Li Yan, Ming Li, Jinchu Hu, and Fuwen Wei. What determines selection and abandonment of a foraging patch by wild giant pandas (ailuropoda melanoleuca) in winter? *Environmental Science and Pollution Research*, 16(1):79–84, 2009.